

Copyright
By
Megan A. Tolnai
2005

**Analytical Simulation of Vehicular Impact on
Retrofit Bridge Barriers**

by

Megan A. Tolnai, B.S.

Thesis

Presented to the Faculty of the Graduate School of

The University of Texas at Austin

in Partial Fulfillment

of the Requirements

for the Degree of

Masters of Science in Engineering

The University of Texas at Austin

May 2005

**Analytical Simulation of Vehicular Impact on
Retrofit Bridge Barriers**

**APPROVED BY
SUPERVISING COMMITTEE:**

Richard E. Klingner

Eric B. Williamson

Dedication

I would like to dedicate this thesis to my family, who has always encouraged me to follow my dreams, to my friends for their support, and to Mark for his love and encouragement.

Acknowledgements

I would like to take this opportunity to thank The University of Texas at Austin for allowing me to become a part of such a wonderful structural engineering program. I would also like to sincerely thank Dr. Richard Klingner and Dr. Eric Williamson for all of their support, guidance, and wisdom given to me throughout this research endeavor. I also thank Geoffrey Mitchell, my research partner, for his dedication and encouragement. I would also like to thank all of the staff at Ferguson Lab and the civil engineering department for helping me with all of my questions. This research project would not have been possible without the support of TxDOT, and so I would like to extend my thanks to them.

I would like to thank all of the professors at UT for giving me such a valuable education. Finally, I would like to thank Dr. Andrea Schokker and The Pennsylvania State University for a wonderful undergraduate education and for encouraging me to attend graduate school.

May 6, 2005

Analytical Simulation of Vehicular Impact on Retrofit Bridge Barriers

Megan A. Tolnai, M. S. E.

The University of Texas at Austin, 2005

SUPERVISORS: Richard Klingner and Eric Williamson

This is one of two theses addressing the first phase of TxDOT Study 4823, whose goal is to develop a retrofit design for existing cast-in-place vehicular impact barriers. To ensure structural integrity and acceptability, such barriers must be subjected to both static and dynamic testing, as specified by the Federal Highway Administration (FHWA) requirements, which require that bridge rails conform to the testing standards and performance requirements outlined in the National Highway Cooperative Research Program (NCHRP) *Report 350*. In this project, finite element analyses and pendulum tests are used to evaluate the behavior of the cast-in-place T203 deformable barrier and the retrofit design for that same barrier. Working in conjunction with the experimental tests and

NCHRP guidelines, good finite element models have been developed for studying vehicular impact and designing retrofit barriers. These models include the cast-in-place and retrofit barriers, the laboratory pendulum and associated crush package, and the use of pre-existing vehicle models. Experimental tests using a real laboratory pendulum impacting a rigid barrier, and analytical verifications of those pendulum tests, also show that the laboratory pendulum satisfies NCHRP standards based upon impact energy and the area under the force-time histories for the impact tests. The proposed testing procedure, including a refined crush package, should be implemented for crash tests. The response of the cast-in-place and the retrofit barriers to pendulum impact should be tested experimentally and simulated analytically. The retrofit design should be modified appropriately based on those test results. Finally, more advanced crash simulations can be created for the selected retrofit design to explore various initial impact conditions and vehicle responses such as snagging and rollover. After suitable retrofit bridge rail designs are developed as recommended above, they should be presented to TxDOT for implementation.

Table of Contents

CHAPTER 1 INTRODUCTION, PURPOSE, AND SCOPE.....	1
1.1 Introduction	1
1.2 Objectives of Project	2
1.3 Objectives of Thesis	2
1.4 Scope of Project	3
1.5 Scope of Thesis	5
CHAPTER 2 BACKGROUND.....	6
2.1 Performance Testing of Bridge Rails	6
2.1.1 NCHRP Report 350 Guidelines	7
2.1.2 Laboratory Pendulum Testing in Study 4823	8
2.2 Analytical Simulation using Finite Element Software	10
2.2.1 Crashworthiness Studies using Finite Element Analysis	10
2.2.2 Using LS-DYNA for Crash Simulations.....	11
2.2.3 Modeling of Crush Packages with LS-DYNA	12
CHAPTER 3 USING LS-DYNA FOR ANALYSIS	13
3.1 Finite Element Computer Programs	13
3.2 Selection of LS-DYNA for Use in this Study	14
3.3 LS-DYNA Program Manager	14
3.3.1 Pre-processing	15
3.3.2 Post-Processing	17
3.3.3 Graph Processing.....	18

3.4	Before Beginning to Use LS-DYNA	19
3.5	Overview of Major Steps involved in Using LS-DYNA	19
3.6	Create a File and Folder for the Model	20
3.7	Define Each <i>PART</i> Comprising the Model	21
3.8	Create Nodes and Lines for Each <i>PART</i>	22
	3.8.1 Create Nodes for Each <i>PART</i>	23
	3.8.2 Create Lines for Each <i>PART</i>	23
3.9	Create Elements and a Mesh for Each <i>PART</i>	25
3.10	Define Element Properties for Each <i>PART</i>	27
3.11	Select and Modify Materials for Each <i>Part</i>	29
3.12	Set Up Initial Conditions and Boundary Conditions.....	31
	3.12.1 Create a Node Set for Initial Conditions or Boundary Conditions	31
	3.12.2 Apply Initial Conditions.....	32
	3.12.3 Apply Boundary Conditions.....	35
3.13	Create Contact Surfaces	36
3.14	Select Information for Output	39
3.15	Run the Defined LS-DYNA Model	42
	CHAPTER 4 DEVELOPING LS-DYNA MODELS FOR STUDY 4823	46
4.1	Overview of Project 4823 Models	46
4.2	Development of LS-DYNA Model for Cast-in-Place Barrier	46
	4.2.1 Geometry of Cast-in-Place Barrier.....	48
	4.2.2 Develop Each <i>PART</i>	50
	4.2.3 Create the Mesh.....	50
	4.2.4 Select the Concrete Material Model.....	51

4.2.5	Treatment of Steel Reinforcement	53
4.3	Analytical Modeling of Retrofit Barrier.....	54
4.3.1	Modify the Cast-in-Place Barrier	56
4.3.2	Create Hollow Ducts for Retrofit Reinforcement or Anchors	56
4.3.3	Create Elements for Anchorage of Reinforcement	57
4.3.4	Treatment of Post-Installed Reinforcing Bars.....	59
4.4	Overall Considerations in Modeling Barriers	63
4.4.1	Modeling of Finite-Length versus Infinitely Long Barriers.....	63
4.4.2	Modeling of Infinitely Long Barriers.....	63
4.4.3	Analytical Model of Reinforced Concrete Bridge Deck.....	66
4.5	Development of Analytical Model for Impact Pendulum.....	66
4.5.1	Geometry of Pendulum Mass	67
4.5.2	Creation of Finite Element Mesh for Laboratory Pendulum Mass	67
4.5.3	Mesh for Simplified DYNA Model of Pendulum Mass	69
4.5.4	Material Model for Laboratory Pendulum Mass.....	70
4.6	Design of Crush Package	70
4.6.1	Overview of Preliminary Design of Crush Package	71
4.6.2	Creation and Connection of Layers for Model of Preliminary Crush Package	72
4.6.3	Material Model for Preliminary Crush Package.....	73
4.6.4	Input of Load Curve	76
4.7	Incorporation of FHWA Vehicle Models into LS-DYNA Models.....	78
4.7.1	Spatial Location and Orientation of Imported Vehicle Model.....	78
4.7.2	Initial Conditions for Pre-defined Vehicle Models	78
4.7.3	Contact Surfaces for Pre-defined Vehicle Models.....	79

4.8	Output Considerations for LS-DYNA Impact Simulations	79
CHAPTER 5 DESIGN OF CRUSH PACKAGE, VALIDATION OF TEST METHODS, AND SIGNIFICANCE OF RESULTS		80
5.1	Preliminary Design of Crush Package for Impact Pendulum	80
5.1.1	Select Material for Crush Package	81
5.1.2	Establish Geometry of Crush Package	83
5.2	Testing and Simulation of Preliminary Design of Crush Package.....	84
5.2.1	Results of Experimental Verification using Pendulum Testing	85
5.2.2	Results from LS-DYNA Simulation using Preliminary Design of Crush Package	86
5.2.3	Modifications to Preliminary Design of Crush Package.....	88
5.3	Modified Design of Crush Package for Laboratory Pendulum.....	91
5.3.1	Geometry of Modified Crush Package.....	92
5.3.2	Experimental Results from Pendulum Testing with Modified Design of Crush Package	93
5.3.3	Results of LS-DYNA Simulation of Pendulum Testing using Modified Design for Crush Package	94
5.3.4	Recommendations for Refined Design of Pendulum Crush Package .	96
5.4	Validity of Testing Methods and Significance of Results.....	98
5.5	Recommended Refinements to Current LS-DYNA Models.....	100
5.5.1	Evaluation of Material Models.....	101
5.5.2	Evaluate Boundary Conditions for Barrier Segments and Infinitely Long Barriers.....	101
5.5.3	Develop Analytical Models for the Bridge Deck.....	101
5.6	Recommendations for Overall Project Plan	102
5.6.1	Finish Design of the Crush Package	102
5.6.2	Test Cast-in-Place and Retrofit Barrier Designs	102
5.6.3	Modify Crash Characteristics using LS-DYNA Simulations	103

CHAPTER 6 SUMMARY, CONCLUSIONS, AND RECOMMENDATIONS.....	104
6.1 Summary	104
6.2 Conclusions	104
6.3 Recommendations	105
6.3.1 Recommendations for Analytical Simulation	105
6.3.2 Recommendations for Future Testing for Project 4823	106
6.3.3 Recommendations for Future Implementation for Project 4823.....	106
APPENDIX A EXAMPLE OF A .DYN FILE	107
REFERENCES	122
VITA.....	124

List of Tables

Table 4.1 – Dimensions (mm) of Cast-in-place T203 barrier	50
Table 4.2 – CARD 1 for concrete, modeled as Isotropic Elastic Failure Material	52
Table 4.3 – CARD 2 for concrete, modeled as Isotropic Elastic Failure Material	52
Table 4.4 – CARD 1 for Reinforcing Bars, modeled as Elastic Spring Material	.54
Table 4.5 – CARD 1 for reinforcement, modeled as SECTION_BEAM	61
Table 4.6 – CARD 4 for preliminary reinforcement, modeled as SECTION_BEAM	62
Table 4.7 – CARD 1 for preliminary modeling of reinforcement as a Plastic Kinematic Material.....	62
Table 4.8 – CARD 1 for pendulum mass, modeled as an Isotropic Elastic Plastic material.....	70
Table 4.9 – CARD 1 for Honeycomb Material	74
Table 4.10 – CARD 2 for Honeycomb Material	75
Table 4.11 – CARD 3 for Honeycomb Material	75
Table 4.12 – Load Curve Definition CARD	77

List of Figures

Figure 1.1 – TxDOT T203 bridge barrier with concrete parapet	1
Figure 1.2 – Testing Plan to Accomplish Project Objectives	4
Figure 2.1 Schematic of laboratory impact test pendulum.....	9
Figure 3.1 – “Program Manager” screen of LS-DYNA.....	15
Figure 3.2 – Example of three-dimensional input geometry created using the pre-processor (eta/FEMB-PC)	16
Figure 3.3 – Sample model crash animation using the post-processor (PostGL) .	17
Figure 3.4 – Example force-time graph using post-processor (eta Graph)	18
Figure 3.5 – Typical PART menu and card	22
Figure 3.6 – Typical node-creation menu	23
Figure 3.7 – Examples of proper and improper node-selection techniques	24
Figure 3.8 – Example of geometric line framework	25
Figure 3.9 – Order of line selection in mesh creation	26
Figure 3.10 – Example of element property selection	28
Figure 3.11 – Sample menu for material selection.....	30
Figure 3.12 – Sample material input card	30
Figure 3.13 – Sample menu for creating a node set	32
Figure 3.14 – Initial Condition menu	33
Figure 3.15 – Example of how to create an Initial Velocity CARD	34
Figure 3.16 – Sample display of Initial Velocity	34
Figure 3.17 Boundary condition menu.....	35
Figure 3.18 – Example of assigning SPC boundary conditions	36
Figure 3.19 – Menu of types of Contact surface	37
Figure 3.20 – List of three-dimensional Contact types	38
Figure 3.21 – AUTOMATIC_SURFACE_TO_SURFACE CARD	39
Figure 3.22 – “DYNA Miscellaneous” Output Control Menus	41
Figure 3.23 – Output-control menus for Contact Forces (RCFORC)	42
Figure 3.24 – Starting the LS-DYNA Solver	43
Figure 3.25 – Menu with Solver settings	44
Figure 3.26 – Example Solver screen during an analysis	45
Figure 4.1 – TxDOT T203 bridge barrier with intermittent base and concrete parapet	47
Figure 4.2 – Cast-in-place laboratory specimen representing a segment of a TxDOT T203 barrier with continuous base and concrete parapet	47
Figure 4.3 – TxDOT Details of Type T203 Traffic Rail (TxDOT 2004)	49
Figure 4.4 – DYNA model of cast-in-place concrete barrier	51
Figure 4.5 – Placement of reinforcing bars in cast-in-place barrier	54

Figure 4.6 – Schematic of proposed retrofit barrier design.....	55
Figure 4.7 – Selection of elements to be deleted to form ducts for reinforcement or anchors	57
Figure 4.8 – Re-creation of element at top of hollow duct	58
Figure 4.9 – Division of LS-DYNA element for attachment of reinforcing bar...	59
Figure 4.10 – Analytical representation of post-installed reinforcement as a line element inside a hollow duct	60
Figure 4.11 – Spring Elements added at ends of barrier segments to simulate the restraining effects of infinitely long barriers.....	64
Figure 4.12 – Assumptions used in developing stiffnesses of equivalent springs to represent an infinitely long barrier	65
Figure 4.13 – Assumptions used in developing equivalent beam stiffness for finite-length section.....	66
Figure 4.14 –Laboratory pendulum mass.....	67
Figure 4.15 – Creating initial mesh for DYNA model of laboratory pendulum...	68
Figure 4.16 – Simplified DYNA model of laboratory pendulum mass	69
Figure 4.17 – Preliminary design of tubular steel crush package	71
Figure 4.18 – Crush package in position on pendulum during a crash test.....	72
Figure 4.19 – DYNA model of preliminary crush package	73
Figure 4.20 – Stress-strain curve for honeycomb material	77
Figure 5.1 – Acceleration-time history for full-scale vehicular crash test of Geo Metro under TL-3 of NCHRP Report 350	81
Figure 5.2 – Arrangement of steel tubes for static crush test.....	82
Figure 5.3 – Force-deformation curve obtained from static test of first arrangement of steel tubing.....	83
Figure 5.4 – Geometry of preliminary design for crush package for laboratory pendulum and corresponding DYNA model.....	84
Figure 5.5 –Acceleration-time curve for preliminary design of crush package (pendulum testing).....	86
Figure 5.6 – Acceleration-time curve for preliminary design of crush package (LS-DYNA simulation).....	87
Figure 5.7 – Comparison of acceleration-time curves for preliminary design of crush package (LS-DYNA simulation of laboratory pendulum, Geo Metro test, and laboratory pendulum).....	89
Figure 5.8 – Comparison of impulses for real and surrogate tests to NCHRP TL-3 (pendulum tests with preliminary crush package; Geo Metro test; and LS- DYNA simulation of pendulum test with preliminary crush package).....	90
Figure 5.9 – Comparison of peak forces for real and surrogate tests to NCHRP TL-3 (pendulum tests with preliminary crush package, Geo Metro test, and LS-DYNA simulation of pendulum test with preliminary crush package)...	91
Figure 5.10 – Geometry of modified design for crush package, and corresponding LS-DYNA model	93

Figure 5.11 – Acceleration-time curve from laboratory pendulum testing (modified design of crush package)	94
Figure 5.12 – Acceleration-time curve from LS-DYNA simulation of (laboratory test pendulum with modified design of crush package).....	95
Figure 5.13 – Comparison of acceleration-time curves (laboratory pendulum testing with modified design of crush package, LS-DYNA simulation of that testing, and Geo Metro test)	97
Figure 5.14 – Comparison of impulses (laboratory pendulum testing with modified design of crush package, Geo Metro test, and LS-DYNA simulation of pendulum test).....	98
Figure 5.15 Comparison of impulses from different tests and simulations to TL- 3 of NCHRP 350	100

CHAPTER 1

Introduction, Purpose, and Scope

1.1 INTRODUCTION

Bridge railings are an important structural component of concrete bridge systems. In addition to simply providing a physical boundary at the edge of a bridge deck, the rails must be able to withstand the impact of a vehicle, redirect that vehicle back onto the roadway, and deform enough to limit the forces placed on vehicle occupants. To ensure structural integrity and acceptability, they are subjected to both static and dynamic testing, as specified by the Federal Highway Administration (FHWA) requirements, which require that bridge rails conform to the testing standards and performance requirements outlined in the National Highway Cooperative Research Program (NCHRP) *Report 350*. Currently, the Texas Department of Transportation (TxDOT) uses a cast-in-place concrete barrier (Type T203) on some bridges. The T203 bridge rail is a concrete parapet barrier with a continuous upper rail and discrete concrete supports, as shown in Figure 1.1.



Figure 1.1 – TxDOT T203 bridge barrier with concrete parapet

TxDOT is currently seeking a retrofit, pre-cast design for this bridge barrier, which must also conform to the standards of NCHRP 350. A successful retrofit design must perform as least as well as the current cast-in-place design under vehicle impact, must have repeatable, predictable response and behavior, and must be easy to install.

1.2 OBJECTIVES OF PROJECT

The objectives of this project, regarding the retrofit barrier design, are as follows:

- recommend bolting patterns and spacing based upon constructability, structural performance, and behavior;
- present a clearly defined simple method of installation that can be repeated in the field by fabricators; and
- recommend limits for design.

1.3 OBJECTIVES OF THESIS

The objectives of this thesis are to propose a retrofit barrier design; to evaluate that barrier design using finite element analysis software following the guidelines set forth in NCHRP *Report 350*; to verify experimental results from the barrier tests; and to present recommendations for implementation and for future research. Mitchell (2005) presents the design of a laboratory test pendulum, the development of a crush nose for that pendulum, and the initial results obtained using that pendulum with a rigid barrier.

1.4 SCOPE OF PROJECT

A common method of testing bridge rails, and consequently retrofit bridge rails designs, is using vehicle crash tests. These real impact tests, however, are very expensive and difficult to replicate, and for this reason may be used only once on a particular bridge rail design. To remedy this difficulty, various equivalent acceptable alternatives have been developed for impact testing, including pendulum testing and analytical testing. Under the criteria set forth by NCHRP *Report 350*, any test is considered valid if it has the appropriate impact severity, measured in terms of the amount of energy delivered to the bridge barrier system during impact (see Section 2.1.1). As discussed further in Section 2.1.1, NCHRP *Report 350* also states that if a surrogate test vehicle, such as a pendulum, is used in place of an actual vehicle, a test is valid when it can be shown that the surrogate vehicle possesses the necessary properties of the actual vehicle it replaces. For this project, equivalence between the surrogate and actual vehicles was expressed in terms of the impact impulse (area under the force-time curve) for crash tests.

In this project, finite element analyses and pendulum tests are used to evaluate the behavior of the cast-in-place T203 deformable barrier and the retrofit design for that same barrier. An illustration of this project plan, with each type of test, is shown in Figure 1.2. Boxes A through F represent all possible testing scenarios for angles and head-on impacts using analytical and experimental testing. Because full-scale, angled vehicle crash tests (Box A and Box B) cannot be re-created in the laboratory, analytical simulations with LS-DYNA are used as the connection between experimental pendulum testing and actual vehicle impacts. Furthermore, rigid barriers were used to refine the testing procedures before tests on deformable barriers were completed.

Box C represents analytical testing of full-scale vehicles in full-velocity, angled impacts against rigid barriers. Force-time curves from these tests are compared with those of vehicle models in head-on impacts with a frontal velocity equal to the component of velocity perpendicular to the barrier in (Box F). The laboratory pendulum and crush package, which is able to recreate head-on collisions, is the test type shown in Box D. Finite element models developed specifically for the pendulum mass and crush package are then used to generate force-time curves to further validate the connection between the laboratory pendulum and full-scale crash results (Box E).

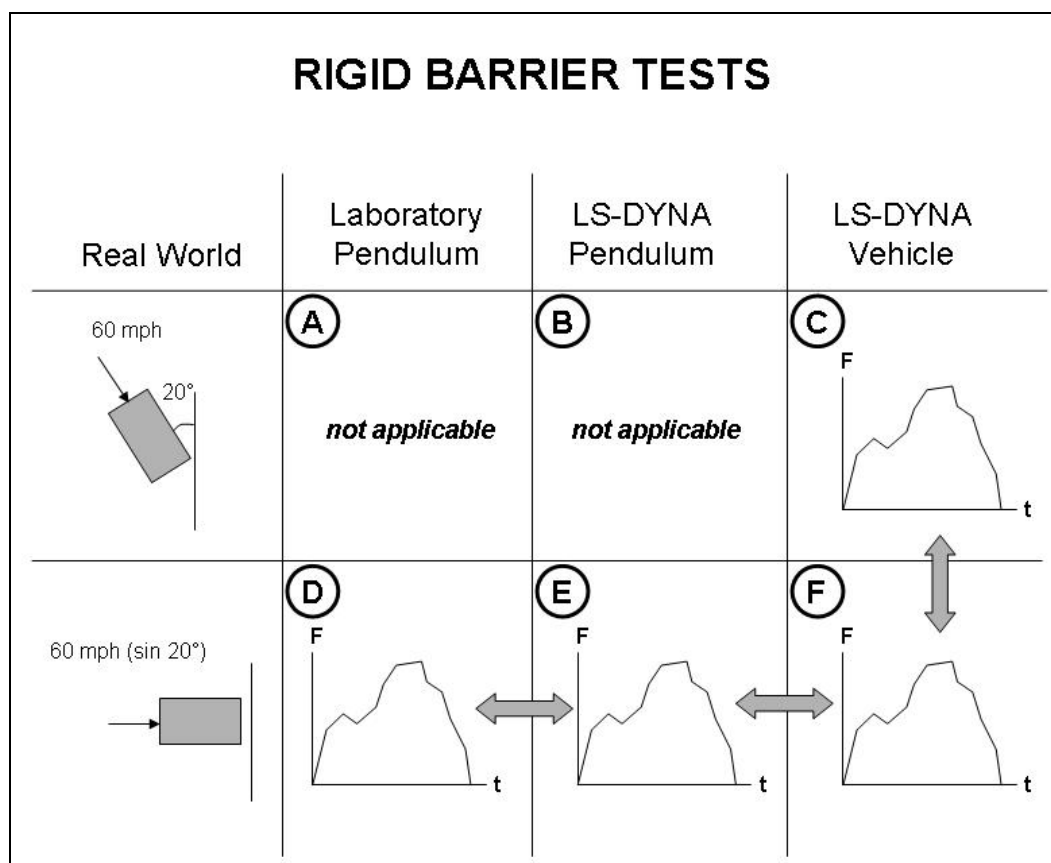


Figure 1.2 – Testing Plan to Accomplish Project Objectives

1.5 SCOPE OF THESIS

Within this thesis, background information related to the development of the retrofit design and to performance testing of bridge barrier systems is presented in Chapter 2. The focus of this thesis is the creation of finite element models and development of the crash simulations, given in Chapters 3 and 4 respectively. The validation process through development of the crushable nose is presented in Chapter 5. Finally, a summary of the research, principal conclusions and recommendations are given in Chapter 6. Background on anchorage to concrete and pendulum testing, the development of the laboratory pendulum and experimental crush package, and recommendations regarding the crush package and experimental barrier tests are given in Mitchell (2005).

CHAPTER 2

Background

2.1 PERFORMANCE TESTING OF BRIDGE RAILS

In the US, performance testing of bridge rails is standardized by the criteria specified in NCHRP *Report 350* (“Recommended Procedures for the Safety Performance Evaluation of Highway Features”), under which a test is considered valid if it has the appropriate impact severity, measured in terms of the amount of energy delivered to the bridge barrier system during impact (Section 2.1.1). As discussed further in that same section, NCHRP *Report 350* also states that

. . . a surrogate test vehicle or device may be used in lieu of a production model test vehicle provided (1) it can be demonstrated that the surrogate possesses essential properties of the production model test vehicle it is intended to replicate and (2) the production model vehicle it is intended to replicate meets the recommendations of [NCHRP 350] Section 2.4.1.1 – production model test vehicles.

NCHRP *Report 350* also states that as of 1993,

. . . there was no widely accepted methodology whereby a surrogate device could be designed and validated to replicate a given vehicle impacting a given safety feature. In absence of such

a methodology, determination of validity and relevance of a surrogate device must be made by the appropriate user agency, that is, the agency responsible for selection and installation of the safety feature being evaluated by the surrogate (1993).

For this project, these criteria were satisfied by developing surrogate vehicles that would have the same mass and impact energy as real vehicles, and equivalence between the surrogate and actual vehicles was verified in terms of the impact impulse (area under the force-time curve) for actual crash tests, laboratory pendulum testing, or LS-DYNA simulations.

2.1.1 NCHRP Report 350 Guidelines

NCHRP *Report 350* requires uniformity in testing procedures for new roadside hardware (such as traffic bridge rails), vehicles, and materials. Because full-scale vehicle crash testing is still the most common way to qualify components and other highway appurtenances, that document specifies the standards and qualifying criteria for such tests (NCHRP 350 1993), and contains criteria for testing, data acquisition, and documentation of roadside tests. For barrier tests and their analytical simulation, criteria include vehicle mass, impact angle, initial velocity, and impact impulse.

To qualify under Test Level 3 (TL-3) of the NCHRP criteria, a longitudinal barrier must be impacted by a vehicle with a mass is $820 \text{ kg} \pm 25 \text{ kg}$, an impact velocity of $100 \text{ km/h} \pm 4 \text{ km/h}$, and an impact angle of $20 \text{ deg} \pm 1.5 \text{ deg}$. The minimum required impact severity is 37.0 kJ, and can be calculated using Eq. 2.1.

$$IS = \frac{1}{2} M (V \sin \theta)^2 \quad (2.1)$$

In Eq. 2.1, IS is the impact severity, M is the test mass, V is the impact velocity, and θ is the impact angle. The suggested tolerance on the impact severity is ± 3 kJ. The above impact parameters are non-mandatory, and are permitted to be modified at the researcher's discretion.

As stated in Section 2.1, NCHRP *Report 350* states that a surrogate test vehicle, such as a pendulum, may be used in place of an actual vehicle if “it can be demonstrated that the surrogate possesses essential properties of the production model test vehicle it is intended to replicate” (1993). For this project, equivalence between the surrogate and an actual vehicle (Geo Metro) was expressed in terms of the impact impulse (area under the force-time curve) for crash tests. Eq. 2.2 shows the impact impulse equation, calculated as the integral of the force-time curve, where P is the force, and dt is the time increment, and I is the impulse. This relationship can be further simplified to multiplying the mass of the vehicle, m , by the integral of the acceleration-time curve (the area under the curve), where a is the acceleration and dt is the change in time.

$$\vec{I} = m \cdot (\vec{v}_o - \vec{v}_f) = \int_{t_o}^{t_f} \vec{P} \cdot dt = m \cdot \int_{t_o}^{t_f} \vec{a} \cdot dt \quad (2.2)$$

2.1.2 Laboratory Pendulum Testing in Study 4823

Surrogate-vehicle testing must meet the required nominal test severity, and must also be compared to real testing in terms of the resulting force-time curve. For this project, it was therefore necessary to develop a testing procedure in which force-time histories could be recorded, integrated to determine the corresponding impulse, and compared with target impulses. A standard laboratory pendulum was selected for impact testing. NCHRP *Report 350* states that the “pendulum

has been used as a surrogate for a small car for low-speed impacts” (NCHRP 350 1993). In this study, a laboratory pendulum was used as a surrogate for high-speed impact tests as well, achieving the required minimum energy in terms of the component of that high-speed velocity normal to the barrier. Figure 2.1 shows a schematic drawing of the impact test pendulum, including the pendulum support frame, pendulum mass, and pendulum mass lifting frame. A crush package (crushable nose) was also developed to attach to the front of the pendulum to simulate the crushing characteristics of a vehicle. Further information on the development of the laboratory pendulum is given in Mitchell (2005).

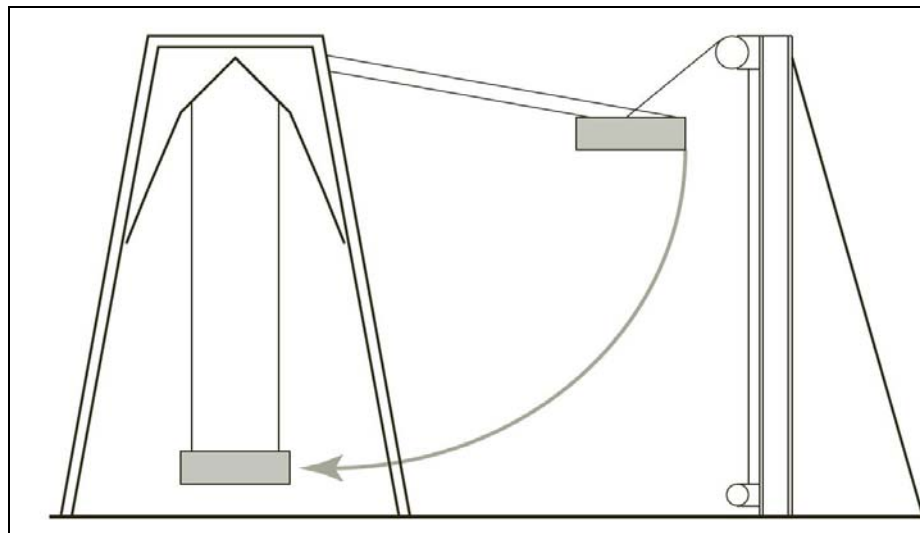


Figure 2.1 Schematic of laboratory impact test pendulum

2.2 ANALYTICAL SIMULATION USING FINITE ELEMENT SOFTWARE

Due to the recent advances in finite element analysis capabilities and the high cost-effectiveness compared with physical testing, analytical simulation using finite element software is becoming a very popular adjunct in crashworthiness studies (Marzougui *et al.* 1996; Sicking 1998). Though prior finite element studies have focused on the crushing characteristics of vehicles (Marzougui *et al.* 1996), finite element analyses are now also used to study the behavior of highway structures during collisions (Sicking 1998). These analyses are addressed in Section 2.2.1 and Section 2.2.2 respectively. Modeling techniques for the crush package are discussed in Section 2.2.3.

2.2.1 Crashworthiness Studies using Finite Element Analysis

The three main applications of nonlinear finite element analysis programs are component design, test extrapolation, and replacement of full-scale crash testing (Sicking 1998).

“Component design” refers to using finite element analysis software to develop accurate models of highway structures, such as barriers or breakaway signposts. Models of other components of crash simulations, such as crushable pendulum noses or specific material designs, can also be developed cost-effectively using finite element analysis. In this research project, finite element analyses were used for component design of the pendulum crush package and for design of the cast-in-place and retrofit barriers.

“Test extrapolation” refers to repeating or modifying full-scale crash tests. Given the high cost of actual vehicle crash tests, it not feasible to conduct multiple tests on a barrier design once that design has been accepted under NCHRP guidelines. Finite element simulation allows for repeated simulations

using a single barrier design under a much wider variety of impact situations (Sicking 1998). In this project, finite element simulation is used for test extrapolation to investigate such scenarios as vehicle snagging and rollover.

“Replacement” refers to the use of finite element simulation as a complete alternative to full-scale or surrogate-vehicle testing. Though analytical simulations for full-scale crashes are becoming more accurate, they cannot yet completely replace full-scale crash testing (Sicking 1998). NCHRP guidelines still require some physical testing, using either a full-scale or a surrogate vehicle.

2.2.2 Using LS-DYNA for Crash Simulations

The LS-DYNA3D (Livermore Software Technology Corporation 2005) program is widely used in the automotive industry to predict the impact behavior of vehicles and highway appurtenances. The National Crash Analysis Center has a collection of LS-DYNA models of test vehicles and roadside hardware available for download specifically for the study of roadside structures during an impact (FHWA 2005).

Two recent crashworthiness studies on barriers using LS-DYNA exemplify this use. One study (Bank *et al.* 1998) involved LS-DYNA simulations and laboratory pendulum impacts on steel W-beam guardrails. Another study (Reid *et al.* 1996) involved analysis of approach terminal sections of highway barriers to develop retrofit designs using LS-DYNA crash simulations and full-scale vehicle crash tests. Though modeling of the contact surfaces between the vehicle and terminal barrier sections posed some difficulties, an appropriate contact was defined, and finite element analysis was beneficial for retrofit design. In both studies, LS-DYNA was chosen for its ability to model large deformations accurately, and it was shown to be a feasible method of testing barriers.

2.2.3 Modeling of Crush Packages with LS-DYNA

Typical research (Eskandarian *et al.* 1996) used the honeycomb material model in LS-DYNA to simulate a crush package as part of a surrogate test vehicle, which was then used in crash simulations against breakaway sign posts. Results indicate that LS-DYNA was a good tool for simulating crash tests and predicting the behavior of highway structures, and that the honeycomb material model in LS-DYNA was very accurate in modeling those researchers' crush package, built using an aluminum honeycomb. In Study 4823, that commercially available honeycomb was not used; instead, a steel-tube crush package with similar load-deformation behavior was developed and used, and was also simulated in LS-DYNA.

CHAPTER 3

Using LS-DYNA for Analysis

3.1 FINITE ELEMENT COMPUTER PROGRAMS

Over the past 30 years, computer programs designed to analyze structures using the finite element method have become a mainstay of structural engineering design. As discussed in Chapter 2, such programs have also found a role in the development of vehicular crash barriers. Examples of commercially available software for finite element structural analysis include *LS-DYNA*, *ANSYS*, and *ABAQUS*. Such programs typically have three main components: a pre-processor; a solver; and a post-processor.

- The pre-processor is typically a graphical interface. With it, a user defines the structure's physical dimensions and geometry; specifies its materials, initial conditions, and boundary conditions; and indicates the desired output information.
- The solver carries out the computation associated with the problem as defined, without additional user interaction.
- The post-processor is used to display and interpret the analytical results, including such items as animated displacements, element stress and strain contours, and velocities. Possibly included may be a graphical processor, which can be used to display more detailed plots of desired information, such as forces and contact interfaces, or accelerations of various model parts.

3.2 SELECTION OF LS-DYNA FOR USE IN THIS STUDY

LS-DYNA is a three-dimensional finite element software package, developed in the late 1970s in nuclear weapons laboratories under US government contract, for the analysis of structures subjected to impact loads. Many subsequent updates have been released, with advances in features such as additional material models, element types, and integration techniques. In the late 1980s, significant advances were made to the software, including development of a commercial version, intended for application to vehicular impact problems (Livermore Software Technology Corporation 2003). LS-DYNA3D has since become an industry standard for crashworthiness studies involving vehicles and roadside appurtenances. Many analytical models of vehicles are available in the public domain for use with LS-DYNA. The Windows® version of LS-DYNA was selected for this project based upon its advanced modeling capabilities and current use in industry. The version of LS-DYNA used for analysis in this research project running on a dual-processor personal computer is PC-DYNA version 970 Rev 5434, June 2004, produced by Livermore Software Technology Corporation in Livermore, California.

3.3 LS-DYNA PROGRAM MANAGER

The main executable file for LS-DYNA is the *Program Manager*, whose screen window is shown in Figure 3.1.

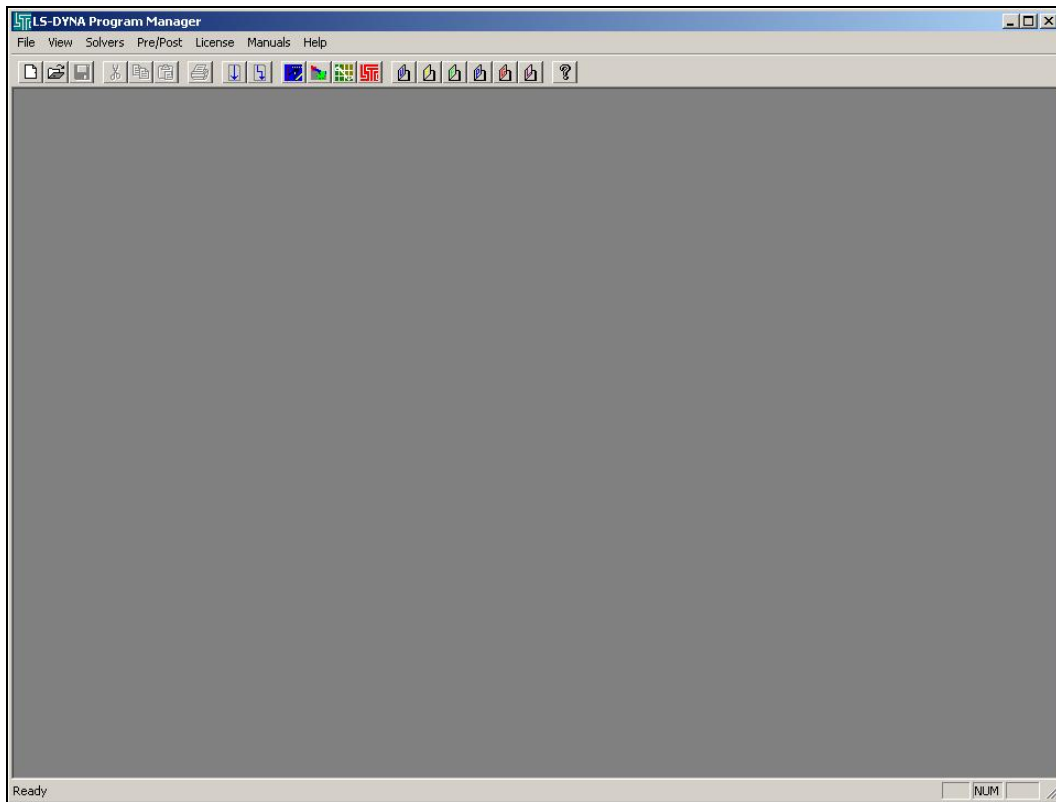


Figure 3.1 – “Program Manager” screen of LS-DYNA

This window is used to run the finite element solver and launch LS-DYNA’s necessary sub-applications, including the pre-processor (*eta/FEMB-PC*), the solver, the post-processor (*PostGL*), and the graph processor (*eta Graph*). LS-DYNA user manuals for pre-processing, post-processing, graph processing and theory are available within the *Program Manager* in Adobe Acrobat (pdf) format.

3.3.1 Pre-processing

Within the pre-processor (*eta/FEMB-PC*), models are created and edited. The pre-processor can be launched either by selecting the appropriate icon from

the *Program Manager* task bar, or by opening it through the *Pre/Post* menu located at the top of the *Program Manager* screen. As shown in Figure 3.2, the pre-processor can graphically display the three-dimensional geometry of the structure being modeled. The pre-processor also includes menu commands for creating an input file for the solver.

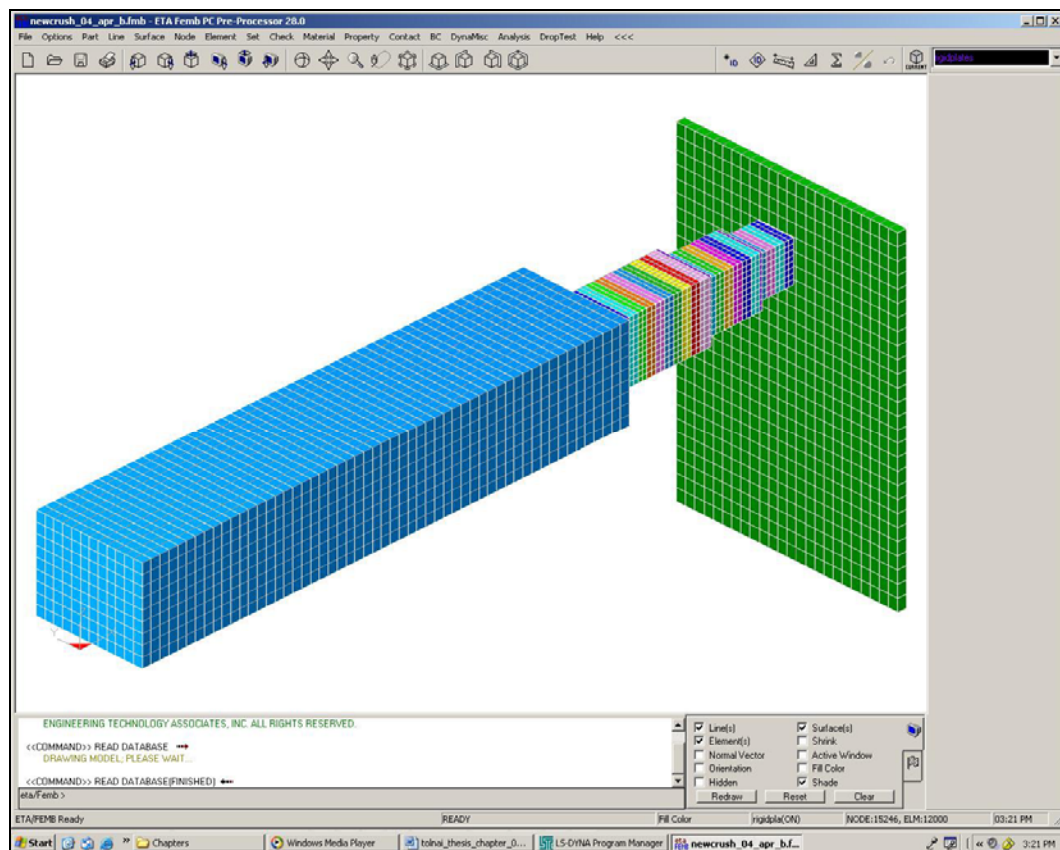


Figure 3.2 – Example of three-dimensional input geometry created using the pre-processor (eta/FEM-PC)

3.3.2 Post-Processing

The post-processor (*PostGL*) allows the user to display many types of output, including the following: three-dimensional animations of model simulations; animated contour plots of stresses and strains within model elements; and the time variation of displacement or velocity of a specified node within the model. Figure 3.3 depicts one frame of a typical crash animation using the post-processor.

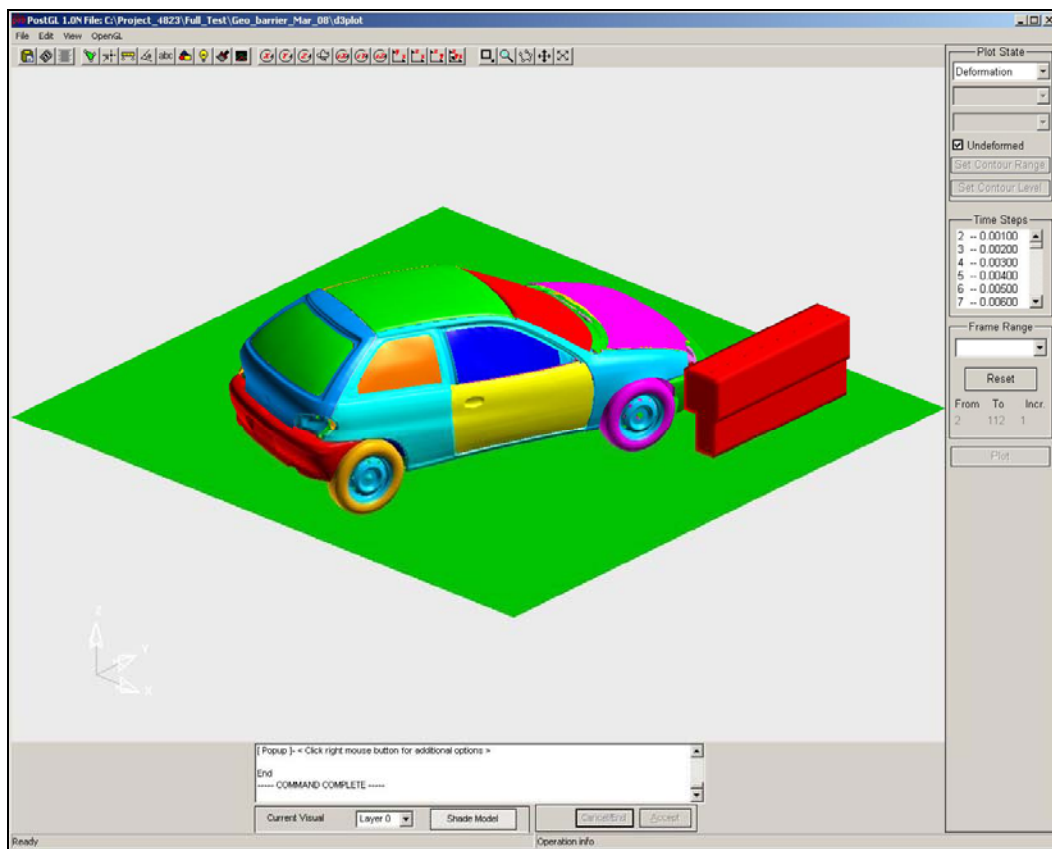


Figure 3.3 – Sample model crash animation using the post-processor (*PostGL*)

3.3.3 Graph Processing

While the post-processor is capable of producing realistic animations of the crash simulations, the graph processor (*eta Graph*) offers additional graphing capabilities. Within a given model, using *eta Graph*, the user can define and then display the desired output information, including the time variations of forces at contact surfaces, displacements, velocities and accelerations of various nodes, and model energies. Figure 3.4 shows one such plot of contact forces with respect to time. In addition, several plots can be overlapped for comparison, and areas under curves can be calculated, which is useful in calculating the impulse of a given crash.

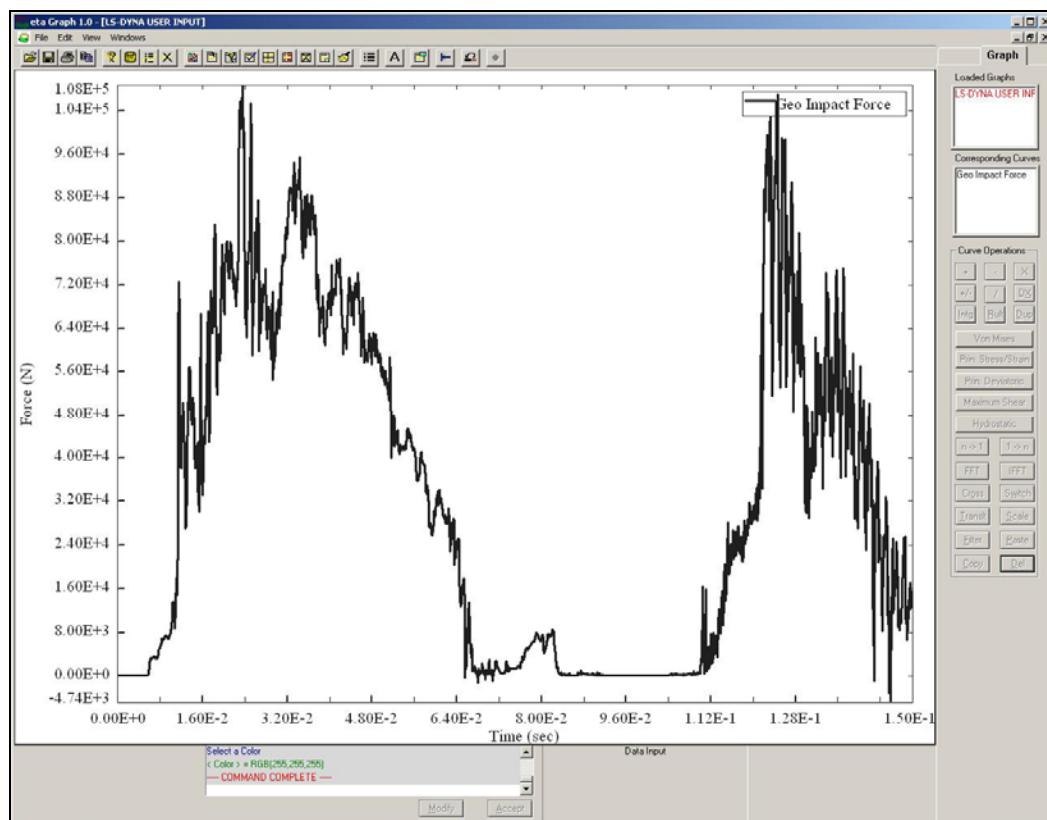


Figure 3.4 – Example force-time graph using post-processor (*eta Graph*)

3.4 BEFORE BEGINNING TO USE LS-DYNA

A variety of existing LS-DYNA-compatible models exist for free download on established websites, such as that of the FHWA/NHTSA Crash Analysis Center (NCAC 2004). Downloaded models of approved crash vehicles and roadside hardware can be combined with user-defined barrier models to simulate complex crashes.

For a vehicle data file to be available for importing, it must be saved onto the hard drive of the same computer that will be used to perform the LS-DYNA analyses. From within the LS-DYNA pre-processor, the import command is given under the *File* menu. The user is then prompted to select the file to be imported. For FHWA vehicle models, appropriate files for importation are those with the file extension *.key*. The process by which a vehicle model is downloaded and used is explained in Chapter 4 of this thesis.

LS-DYNA has no fixed system of units, requiring only a consistent set of units. Establishing a consistent set of units before beginning is important for continuity of the model, and for interpreting the corresponding results. When importing models built by other users, one has the option to select the desired set of units, to ensure that imported models and user-generated models are compatible.

3.5 OVERVIEW OF MAJOR STEPS INVOLVED IN USING LS-DYNA

A user can choose among many ways to generate finite element simulations for crashworthiness studies. The general steps used to simulate a crash simulation using LS-DYNA are the following:

- create a file and folder for the model;
- define each *PART* comprising the model;

- create nodes and lines for each part;
- create elements and a mesh for each part;
- define element properties for each *PART*;
- select and modify material models for each *PART*;
- set up initial conditions and boundary conditions;
- create contact surfaces;
- choose information for output; and
- run the defined model.

Each step is addressed further in the following sections. Generation of models specific to Project 4823 is discussed in Chapter 4.

3.6 CREATE A FILE AND FOLDER FOR THE MODEL

It is important to set up a file folder for each model. The program runs more quickly if the folders and files are stored on a local hard drive rather than a network fileserver. Each folder should contain the model file used in the pre-processor, the file used in the LS-DYNA solver, and all output files. LS-DYNA does not permit the user to run two model files from within the same folder, because output files for different models have the same names and cannot be overwritten. Because LS-DYNA does not have an “undo” button, it is vital to save each version of a model. It is best to create a completely new folder and re-save when making changes to existing models. In this way, if a particular change does not produce the desired result, or if a model should become corrupted, the previous version of the model still exists.

The files used by the LS-DYNA solver have the suffix *.dyn*. Each such file is a text file composed of a series of “*CARDS*” which are essentially blocks of

input information relating to a single aspect of a model, such as nodal locations, selected materials, or boundary conditions. The required format of each *CARD* is given in the LS-DYNA *User's Manual*, and a user could potentially create the text file and cards manually. It is easier, however, to use the pre-processor (*eta/FEMB-PC*), which automatically produces the *.dyn* file in the correct format when a built model is exported. Each *CARD* can also be defined in detail through the menu options within the pre-processor. Slight modifications to the *.dyn* file can then be made manually. A sample *.dyn* file is given in Appendix A.

3.7 DEFINE EACH *PART* COMPRISING THE MODEL

The first step in creating a three-dimensional finite element model in LS-DYNA is to define the model geometry, including the size and shape of the objects to be analyzed, and the components comprising them. Within the LS-DYNA pre-processor, each component of the entire model must be designated as a separate “part.” For instance, a bridge railing model may consist of two parts: the concrete portion and the post-installed reinforcing bars. A laboratory pendulum may be composed of the steel body and a crush package mounted on the front of that body. Each *PART* can be assigned different properties and material definitions, but a *PART* may have at most one material and property. Though the *PART* menu, one may create, name, and edit various *PART* cards. The *PART* menu, along with an example card, is shown Figure 3.5.

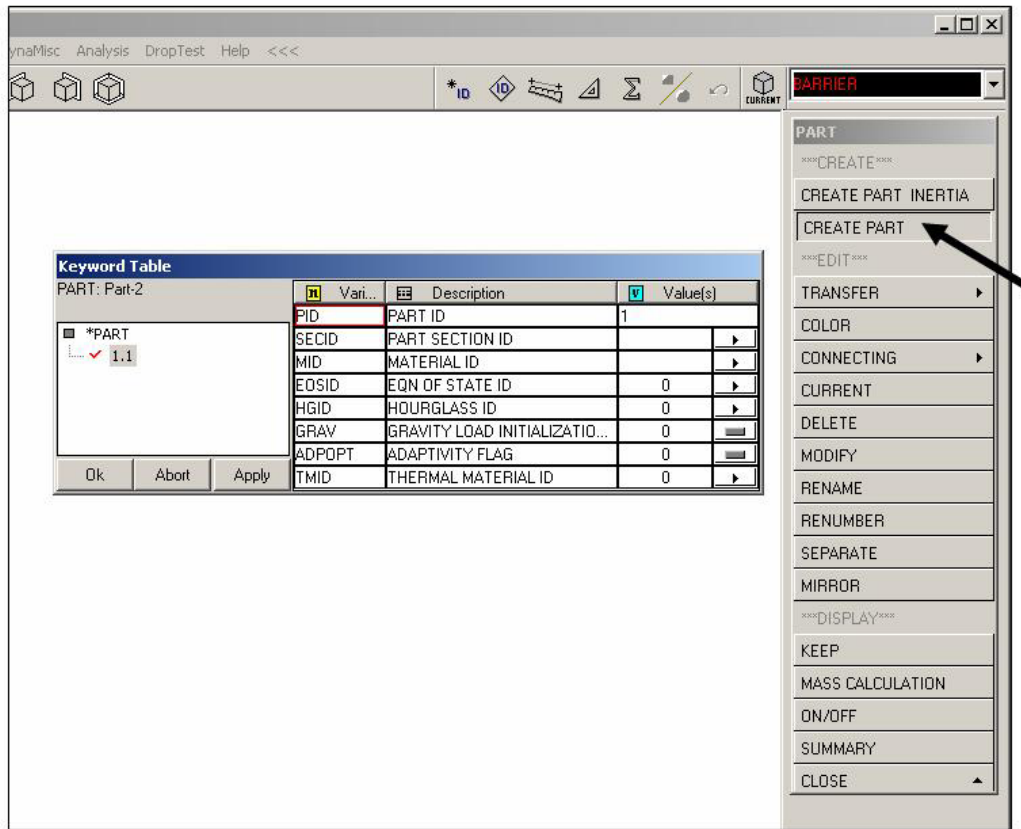


Figure 3.5 – Typical PART menu and card

3.8 CREATE NODES AND LINES FOR EACH PART

Once each *PART* has been created, the physical boundaries of each part must be established. In the case of geometrically regular, block-like objects, such as a barrier or a laboratory pendulum, the easiest way to establish boundaries is to create nodes in three-dimensional space that define the perimeter of the *PART*. Although a *PART* can theoretically be oriented in any direction, it is helpful to orient it in a meaningful manner. For instance, it may be beneficial to orient it so that the initial conditions (for example, initial velocity) occur predominantly in a single global direction, or so that the desired output forces occur in a global

direction. Commands for defining nodes by global coordinates are given under the *NODE* menu. Once a *PART* has been created using a convenient initial orientation, that orientation can be changed using the *TRANSFORM* command in the *NODES* menu.

3.8.1 Create Nodes for Each *PART*

To begin creating nodes, one must make sure that the desired *PART* is listed in the current window. After selecting *CREATE* under the *NODE* menu, the nodes can be defined by global coordinates using the *Key-In* command. Figure 3.6 depicts a typical node creation command window.

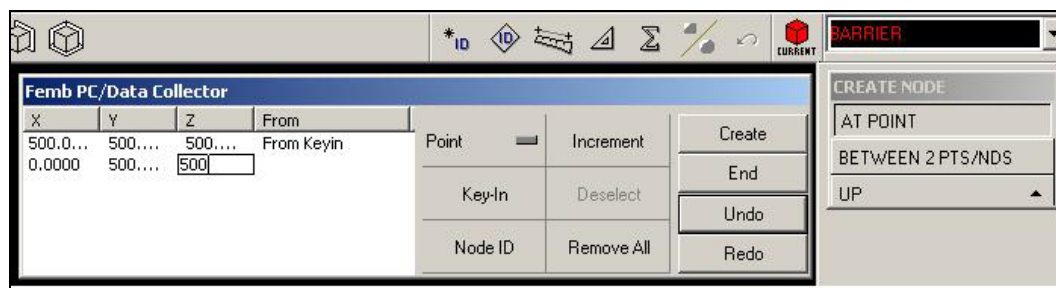


Figure 3.6 – Typical node-creation menu

3.8.2 Create Lines for Each *PART*

Once all nodes are defined, they must be connected by lines to create a skeleton outline of the geometry of the *PART*. Using the *CREATE* command within the *LINE* menu, one creates lines by selecting two nodes with the cursor, and then selecting *CREATE*. To create lines between nodes, *NODE* (rather than *POINT*) must be active in the selection window. Each line between two nodes must be created separately; otherwise, it is possible that two line segments having

two different axial orientations will be viewed by the solver as a single line. Examples of proper and improper node selection are shown in Figure 3.7.

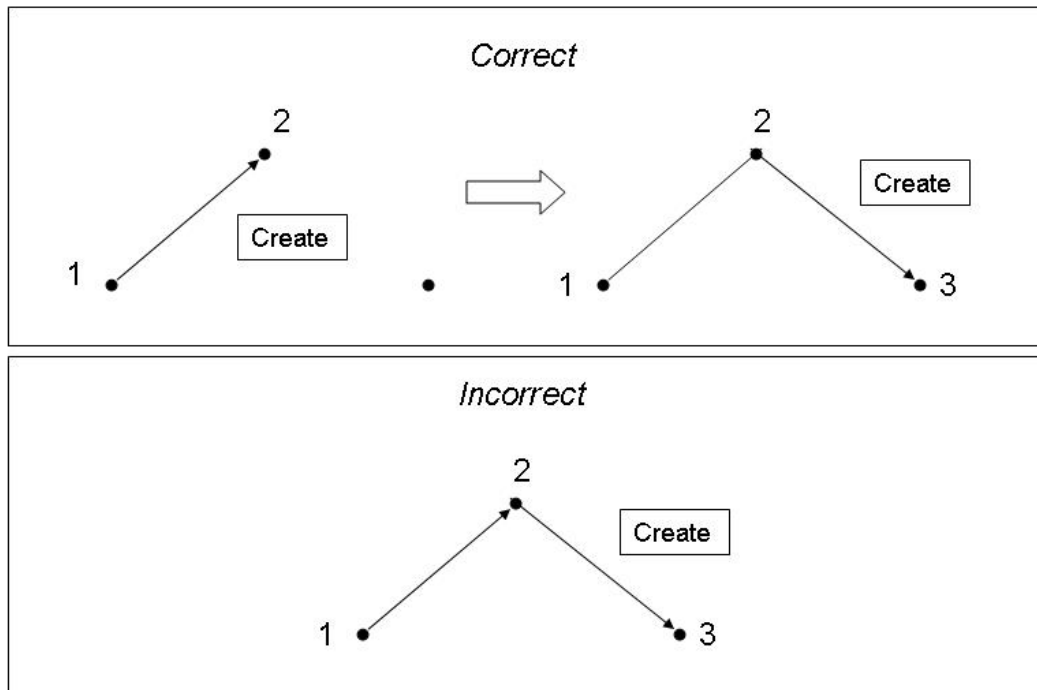


Figure 3.7 – Examples of proper and improper node-selection techniques

Upon completion of line creation, each geometrically regular shape (such as a rectangular solid) consists of twelve lines, as shown in Figure 3.8. This framework of lines is then used to create the three-dimensional solid mesh of finite elements. If an object (like a T203 bridge rail), can be broken down into two simple component shapes, each shape should be created separately within the same *PART*. Thus, a single *PART* may consist of twenty-four lines instead of twelve.

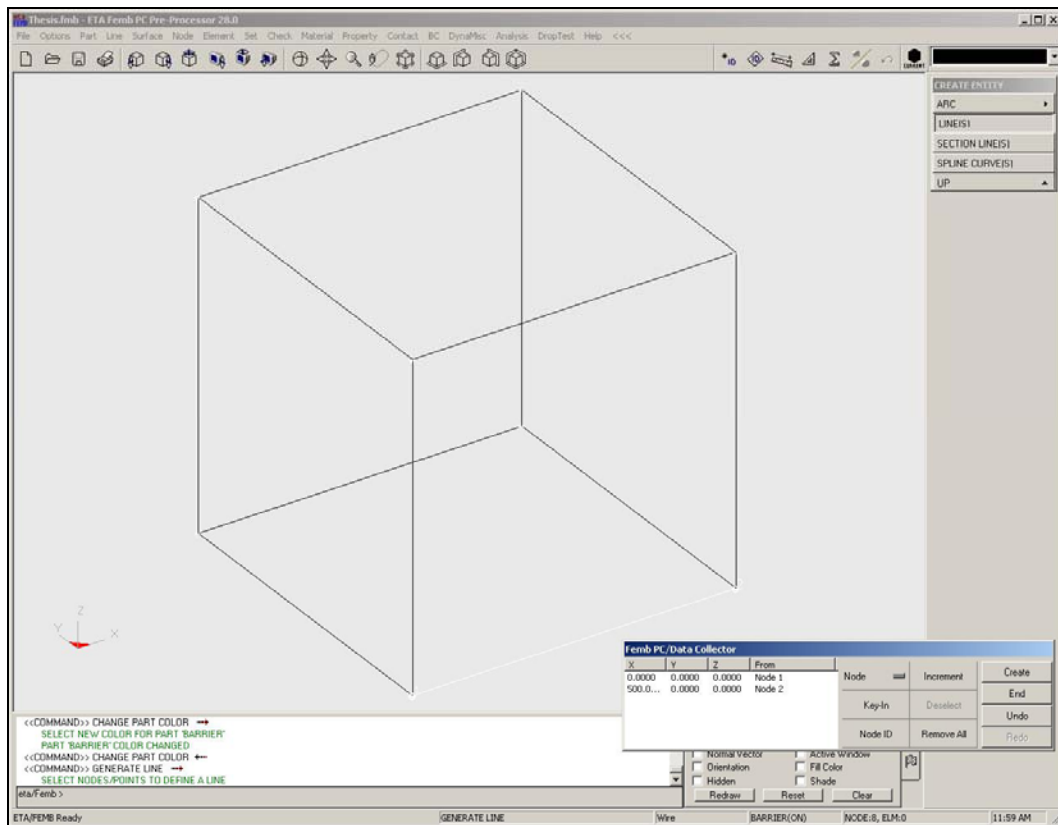


Figure 3.8 – Example of geometric line framework

Commands for creating and editing lines are given under the *LINE* menu. All newly created nodes and lines are associated with whichever part is listed in the *CURRENT* field. Thus, when all nodes and lines for a particular *PART* are defined, the user must select a new *PART* in the *CURRENT PART* field before creating nodes and lines for a new part.

3.9 CREATE ELEMENTS AND A MESH FOR EACH PART

The next step in creating a usable finite element model is to “mesh” the defined parts, including defining the density and arrangement of finite elements.

There are many ways to create a solid mesh with LS-DYNA. A relatively easy way to create solid brick elements from the previously created lines is to use a 12-line plate/solid meshing tool. This tool requires the user to click on the twelve lines which define the part, and then allows the user to define the fineness of element size in each local direction. Options related to this task are given in the pre-processor under the *ELEMENT* menu.

One begins by selecting the four coplanar lines defining one face of the part to be meshed. Though the direction is irrelevant, the user must select these lines in a clockwise or counter-clockwise direction. Accordingly, once a line is selected, the next line chosen must be in contact with that first line, and so on. Lines must be selected in a consistent order – either clockwise or counterclockwise. The final four lines are then selected in order, with the first line connecting the corners formed by Lines 1 and 4, the second line connecting the corners formed by Lines 1 and 2, and so on (Figure 3.9).

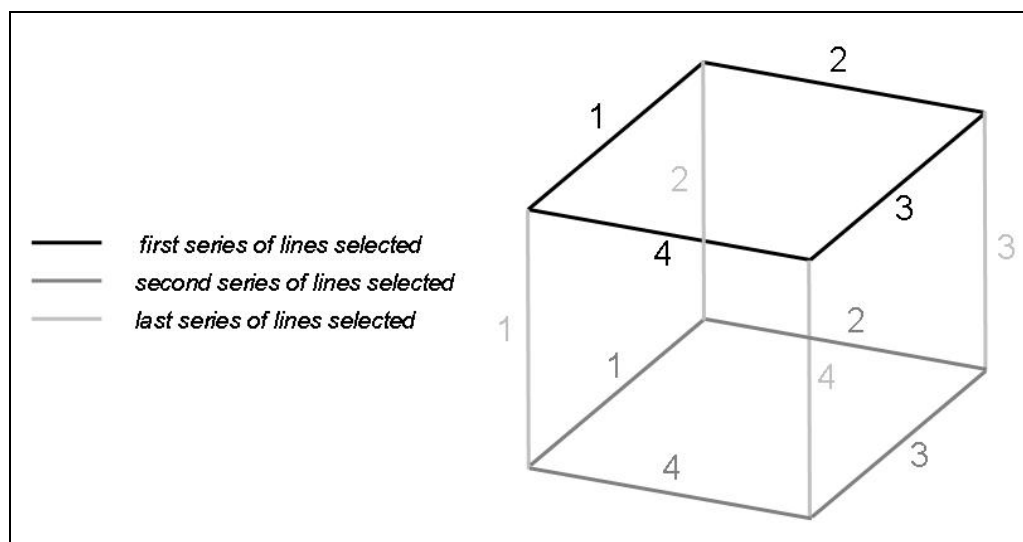


Figure 3.9 – Order of line selection in mesh creation

Once all lines are selected, the user is prompted to enter the number of elements desired along each of the three local axes. The final result of meshing is a three-dimensional solid object consisting of smaller solid elements of the specified size. Once an object is meshed, a user has the option of modifying the size of individual elements using commands in the *ELEMENT* menu. Elements of arbitrary size and shape can also be created manually by selecting a series of eight nodes that outline the desired element shape.

The ratio of the longest dimension to the shortest dimension of an element is called its aspect ratio. Because of how finite element programs calculate displacements at the element boundaries, elements with smaller aspect ratios (that is, elements that are approximately cubical) are generally more accurate (Logan 1993). The National Crash Analysis Center (NCAC) at George Washington University recommends keeping aspect ratios between 1.0 and 5.0 (NCAC 2005). Another consideration in creating a mesh is the size of the elements relative to the size of the object that they comprise. In general, the smaller the elements (the denser the mesh), the more accurate the analysis, and also the greater the required computational effort.

3.10 DEFINE ELEMENT PROPERTIES FOR EACH *PART*

A *PART* can be assigned one of several types of element properties, including shells, solids, beams, and springs. Downloaded vehicle models typically consist of shell elements, which are three- and four-noded elements used to model three-dimensional plate-like surfaces and membranes (Livermore Software Technology Corporation 2003). To model solid, three-dimensional objects, the *SOLID* property is a logical choice. Beams are defined as two-noded elements used to represent members such as three-dimensional beams or truss

members (Livermore Software Technology Corporation 2003). Beams can be used to create axially-loaded members such as concrete reinforcing bars. Other element properties also exist, such as spring/damper elements. *PART* properties are defined through the *PROPERTY* menu within LS-DYNA, as shown in Figure 3.10. Once a property is defined, it must be assigned to the desired *PART* using the *ASSIGN* command.

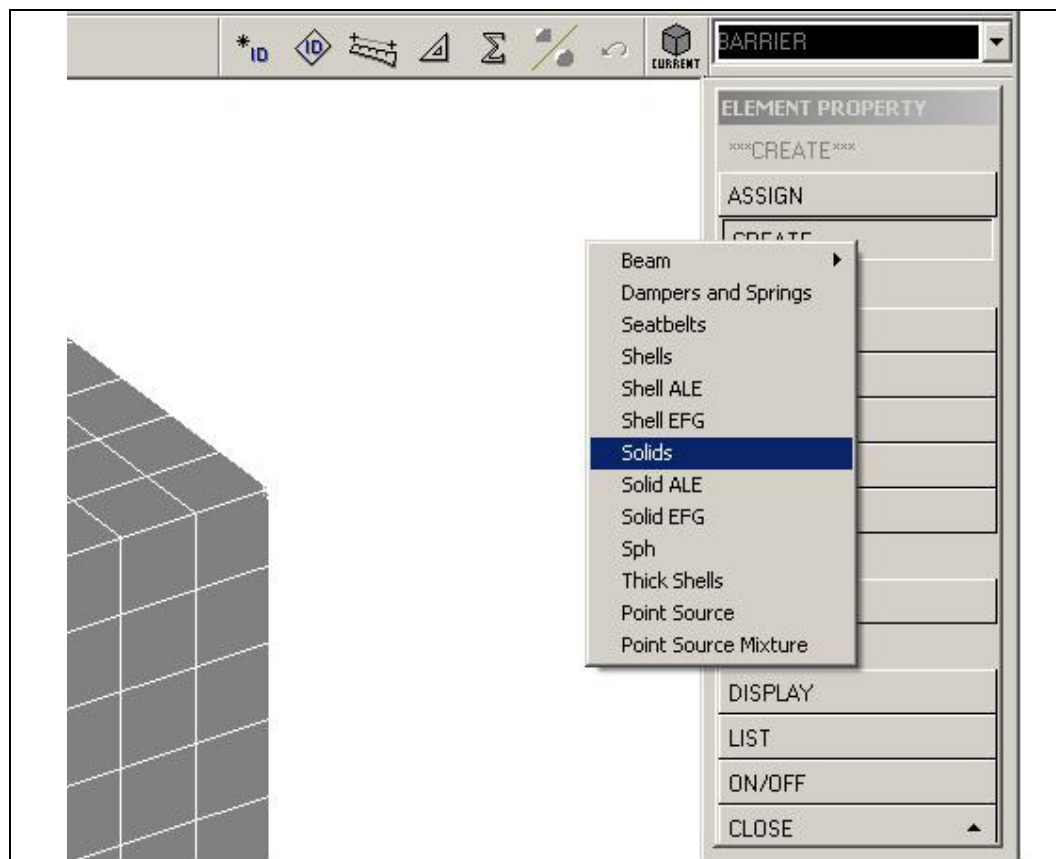


Figure 3.10 – Example of element property selection

3.11 SELECT AND MODIFY MATERIALS FOR EACH PART

Within the *MATERIAL* menu, the user can define, edit, and assign material properties to the created *PARTS*. Selecting an appropriate material model is perhaps the most significant part of creating a model. LS-DYNA has over two hundred predefined material models, some of which can be used only for specific element types, or to represent specific material properties. The elastic material model, for instance, can be used for all solid and shell elements and most beam elements, but does not address failure or strain-rate effects. A honeycomb material model, in contrast, can be used only for solid brick elements, but can address both failure and strain-rate effects (Livermore Software Technology Corporation 2003).

Each material model consists of one or more cards of input information, which are automatically produced when that material model is selected, and which contain the appropriate user prompts for that material. Material properties common to most predefined models are mass density, modulus of elasticity, and Poisson's ratio. Other properties, such as yield stress, failure strain, or tangent modulus, may be required for particular material models. Simpler material models, such as elastic or plastic with kinematic hardening, require a limited number of input values. Some more complex models also require the user to enter load-displacement or stress-strain curves, using the *LOAD CURVE* command in the *DYNA MISCELLANEOUS* menu.

To create a specific material in the pre-processor, the user selects the *CREATE* option in the *MATERIAL* menu, and is prompted to select either a structural or a spring/damper type material, as shown in Figure 3.11. Depending on which is chosen, a list of applicable material types appears. Once a specific material type is selected, LS-DYNA automatically displays the appropriate cards and prompts the user for the necessary information. A sample input card is shown

in Figure 3.12. After a material is created, it can be assigned to one or more *PARTS* within the model.

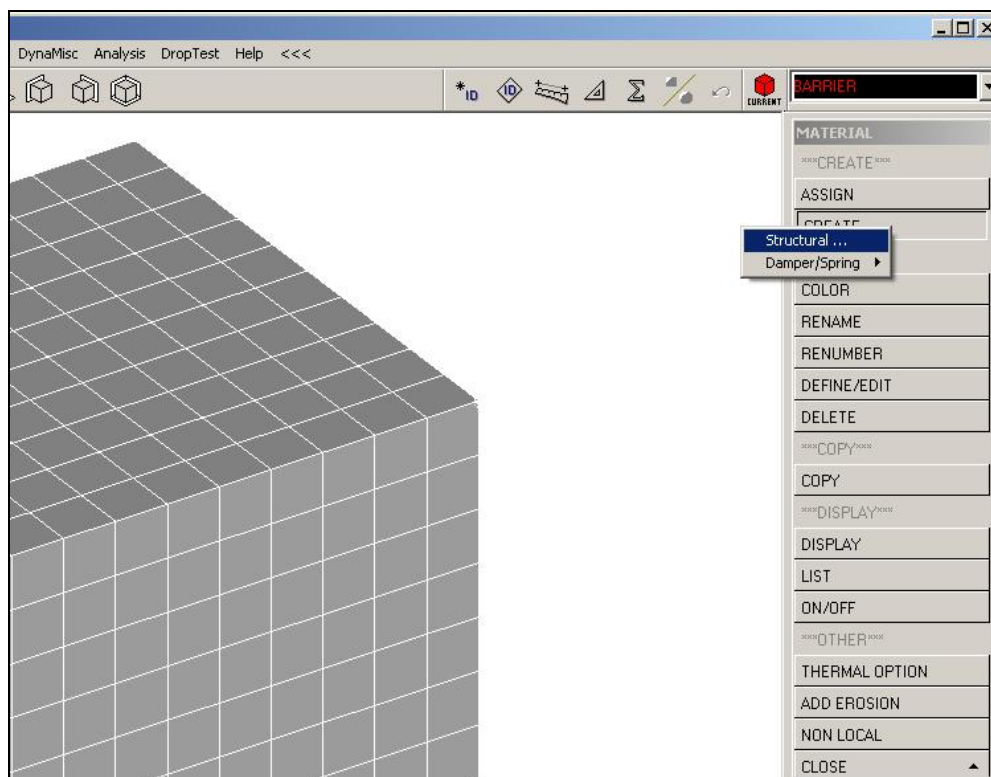


Figure 3.11 – Sample menu for material selection

Keyword Table			
M-1	Vari...	Description	Value(s)
*MAT_ELASTIC	MID	MATERIAL ID	1
1.1	RD	MASS DENSITY	
	E	YOUNG'S MODULUS	
	PR	POISSON'S RATIO	
	DA	AXIAL DAMPING FACTOR	0.0000e+000
	DB	BENDING DAMPING FACTOR	0.0000e+000

Ok Abort Apply

Figure 3.12 – Sample material input card

3.12 SET UP INITIAL CONDITIONS AND BOUNDARY CONDITIONS

The next step in creating a finite element model with LS-DYNA is to apply initial conditions and boundary conditions. Commands related to such conditions are given in the *B.C.* menu. Initial conditions and boundary conditions can be assigned to an object or group of nodes either by individually selecting the nodes comprising the object, or by creating a *NODE SET* to which the conditions can be applied. The latter is discussed in the next subsection.

3.12.1 Create a Node Set for Initial Conditions or Boundary Conditions

Instead of selecting nodes individually, or even by a given region, a user can create a *NODE SET* to which boundary conditions can be applied. This process simplifies the application of boundary conditions, and also ensures that all desired nodes are included, as when an initial velocity is applied to all nodes in a specified *PART*. In addition, one *NODE SET* can be used to apply more than one type of boundary condition, making model creation more user-friendly. Various *NODE SETs* can be defined using the *SET* menu, selecting *NODE*, and then selecting the desired nodes by part, by region, or individually. The menu for creating a *NODE SET* is shown in Figure 3.13. To the same end, a user can create sets of parts or elements for applying various conditions in the model.

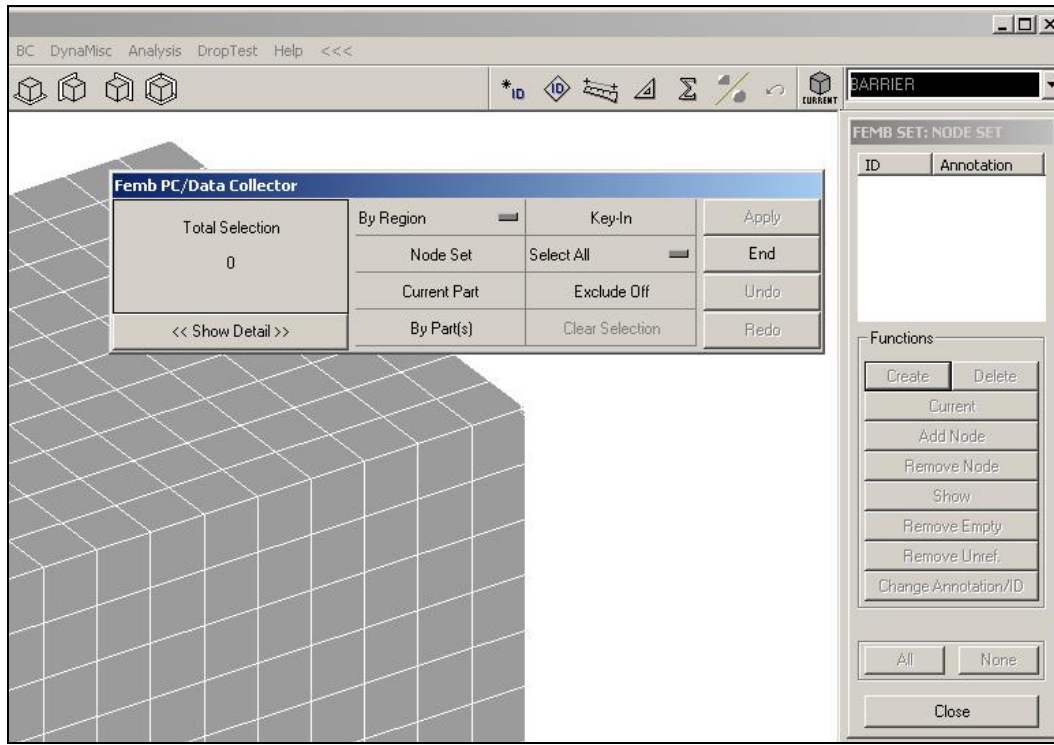


Figure 3.13 – Sample menu for creating a node set

3.12.2 Apply Initial Conditions

Useful initial conditions for crash simulations include characteristics (such as velocities or accelerations) imposed on *PARTS* and *NODES*. For vehicle impact simulation, initial velocity is most useful. The *INITIAL CONDITION* menu (within *B.C.*) allows the user to select initial *VELOCITY*, as shown in Figure 3.14.

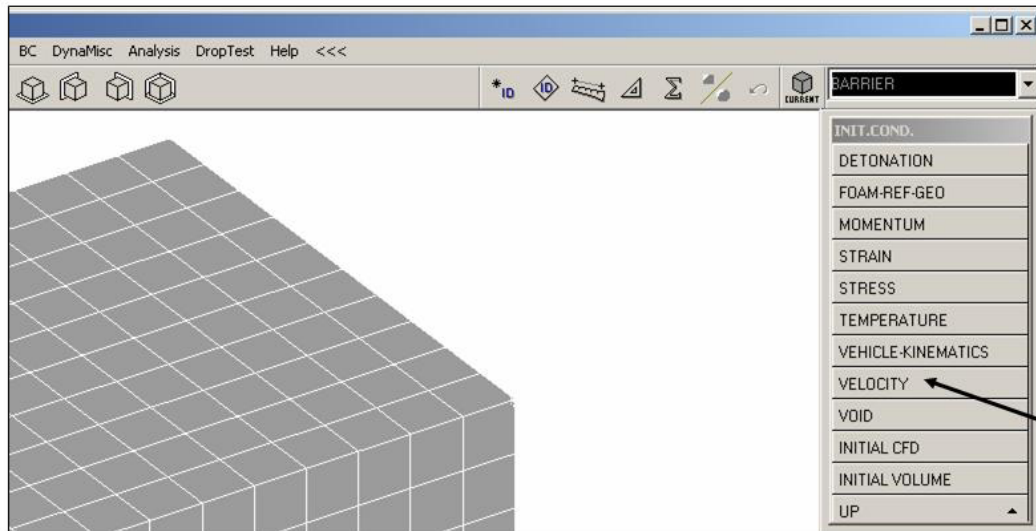


Figure 3.14 – Initial Condition menu

When the user selects *VELOCITY*, an initial velocity card is created, using either individual nodes or a *NODE SET*. Initial translational or rotational velocities can be defined in global coordinates, using the input menu shown in Figure 3.15. Once initial velocities are defined, the resultant velocity vector at each node is displayed as in Figure 3.16.

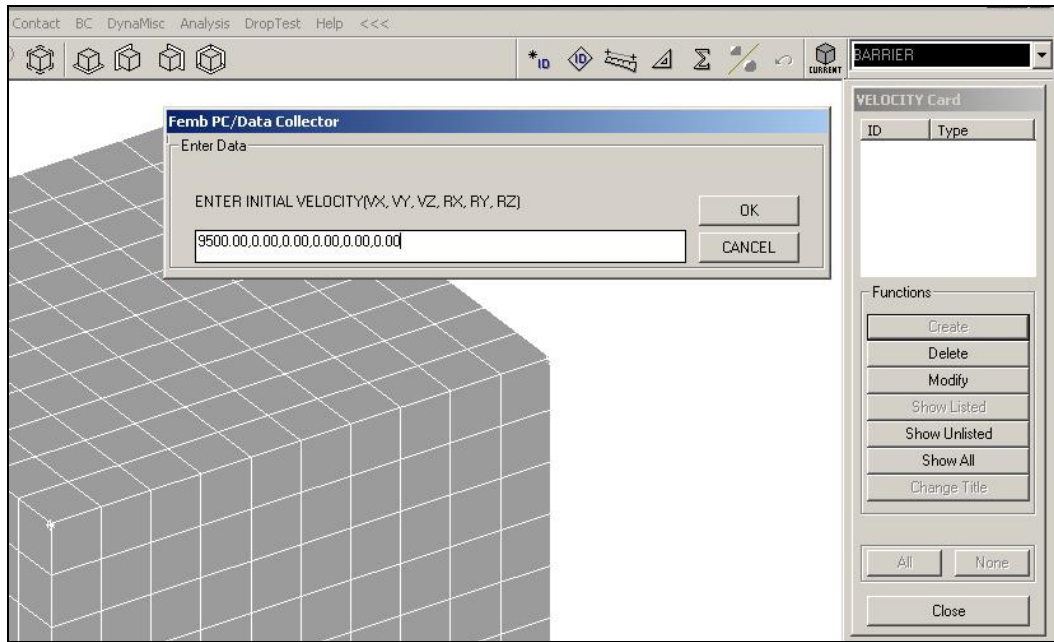


Figure 3.15 – Example of how to create an Initial Velocity CARD

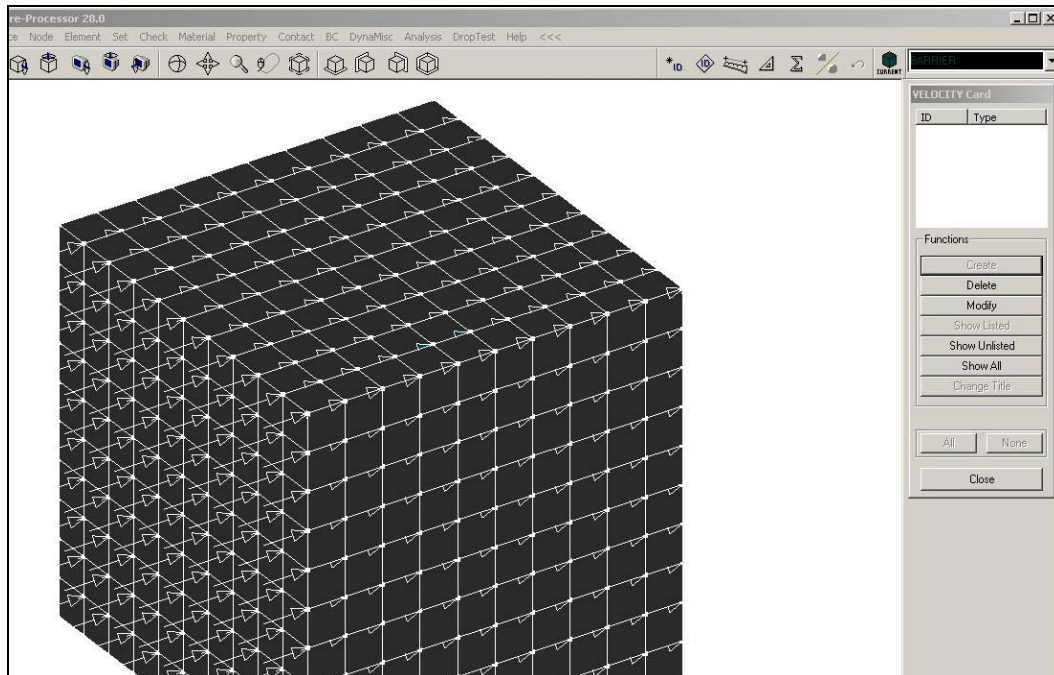


Figure 3.16 – Sample display of Initial Velocity

3.12.3 Apply Boundary Conditions

Boundary conditions are applied by selecting, within the *B.C.* menu, the *BOUNDARY* option. As shown in Figure 3.17, many types of boundary conditions can be applied in many ways. The *SPC* (Single Point Constraint) option is often the most useful of these, and allows a user to apply any combination of translational or rotational restraint in global coordinates.

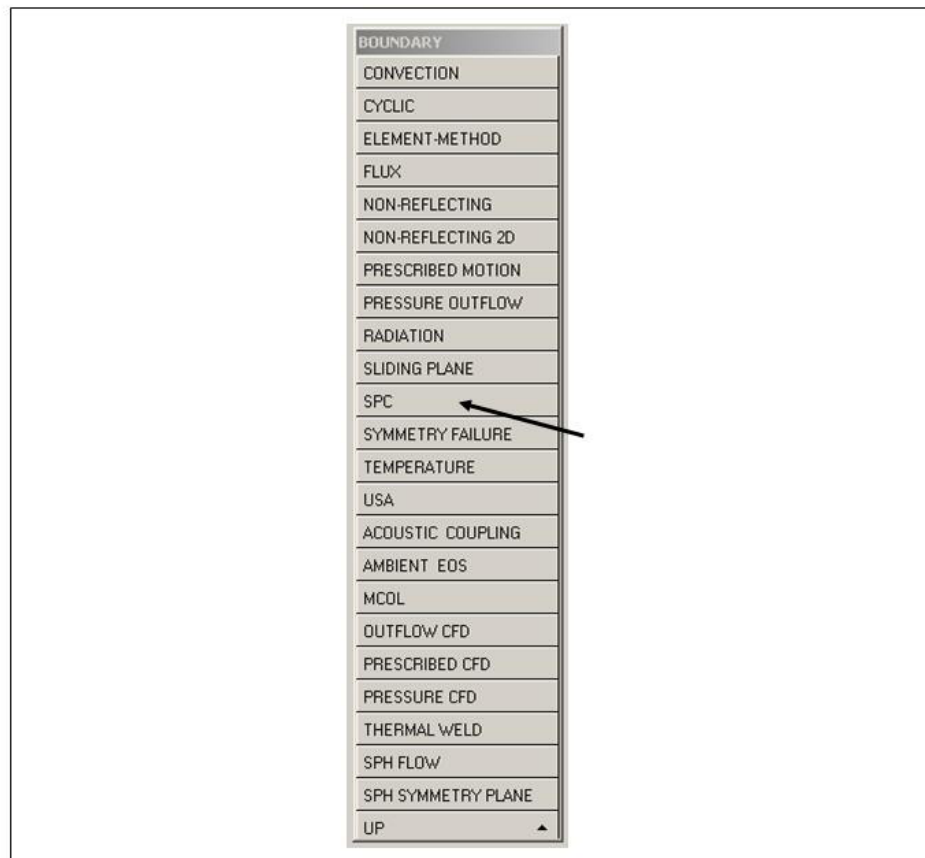


Figure 3.17 Boundary condition menu

Once a user opts to create an *SPC CARD*, a menu appears in which the restraints can be selected, after which they are displayed by number at the

appropriate nodes. In the example shown in Figure 3.18, restraints 1 (x -translation), 2 (y -translation), and 6 (z -rotation) are applied to every node in a cube.

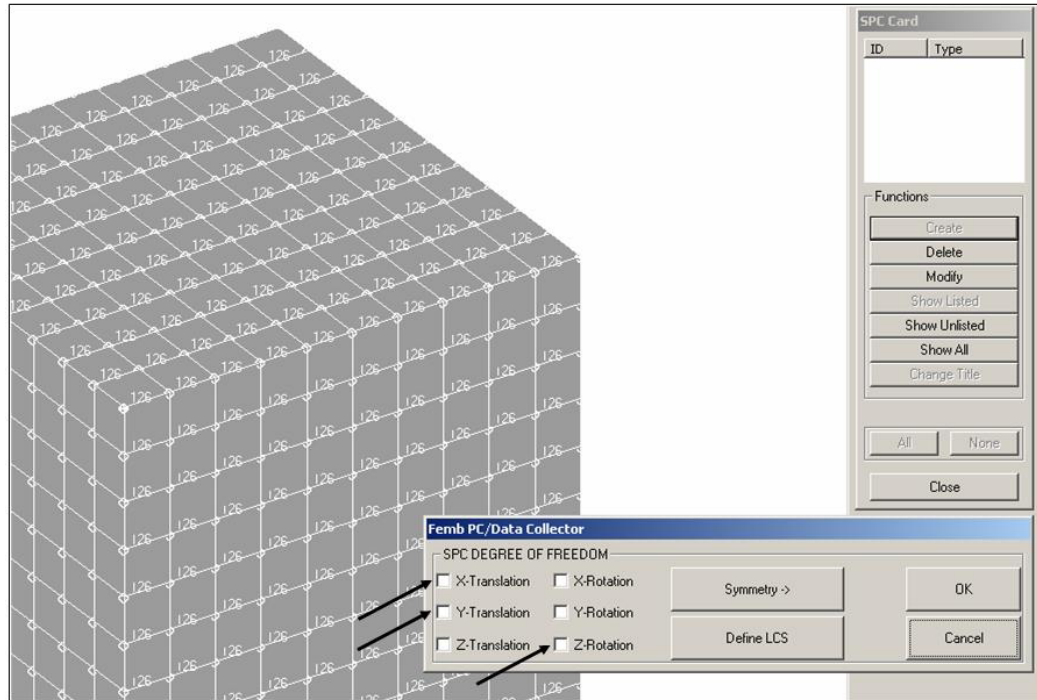


Figure 3.18 – Example of assigning SPC boundary conditions

3.13 CREATE CONTACT SURFACES

After boundary conditions and initial velocities are applied to their respective *PARTs*, the fact that two *PARTs* may be in contact for the analysis must be explicitly declared in the model by creating a *CONTACT* card. To create a contact surface, the user must first select *CREATE*, and then *CONTACT*. Several types of contact surface options are then displayed (Figure 3.19). A three-dimensional contact option is appropriate for crash simulations, as most *PARTS* in

these models are three-dimensional and their surfaces, rather than only their nodes, are anticipated to be in contact with each other.

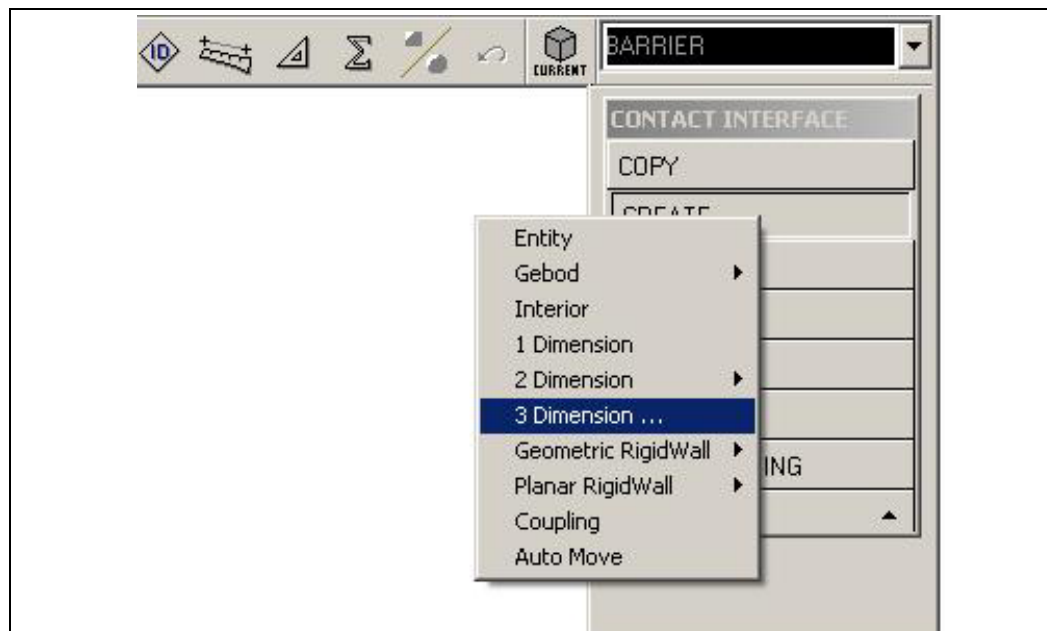


Figure 3.19 – Menu of types of Contact surface

Once the three-dimensional contact has been selected, a list of contact surface types appears (Figure 3.20). Of these, the most versatile and useful for impact analyses is the *AUTOMATIC_SURFACE_TO_SURFACE* contact, which can be used for almost all impact situations and requires little input information from the user. Contacts should be defined for all surfaces in the model where contact is anticipated. No default contact is defined in LS-DYNA. If a contact *CARD* is not created, objects that touch simply pass through each other, occupying the same space at the same time.

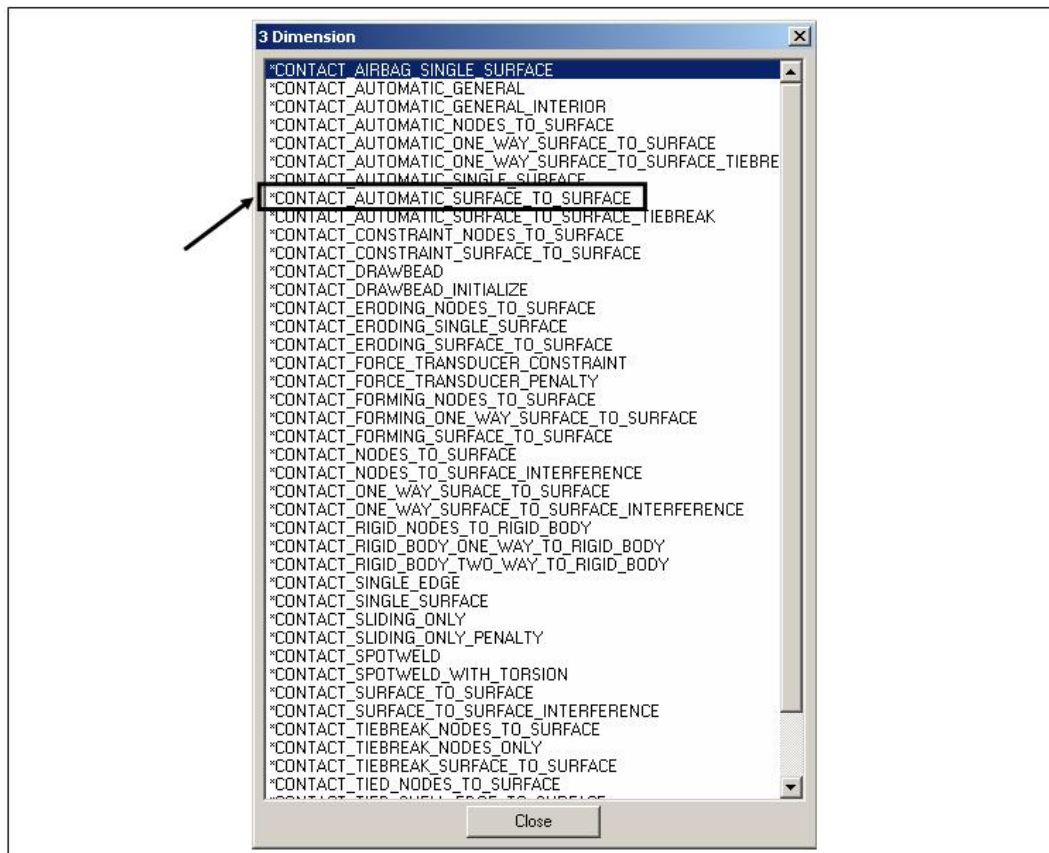


Figure 3.20 – List of three-dimensional Contact types

Once the *AUTOMATIC_SURFACE_TO_SURFACE* contact type is selected, the *AUTOMATIC_SURFACE_TO_SURFACE CARD* appears (Figure 3.21). Fields requiring user input are slave and master designations and slave and master IDs. When two objects are to be considered in potential contact, one must be selected as the master surface, and the other as the slave surface. Under most circumstances, the nodes of the slave surfaces cannot penetrate the geometry of the master surface. To minimize anomalies in applying this concept, the master surface should be the stiffer of the two materials in question or the larger surface with the coarser mesh (AC Engineering, Inc. 1996). The other surface

should therefore be selected as the slave surface. LS-DYNA allows a user to define the master and slave surfaces in a variety of ways, the easiest of which is to select the surfaces by *PART*. Other options in the contact *CARD* include static and dynamic coefficients of friction for contact surfaces, and toggling checks for small penetrations between surfaces.

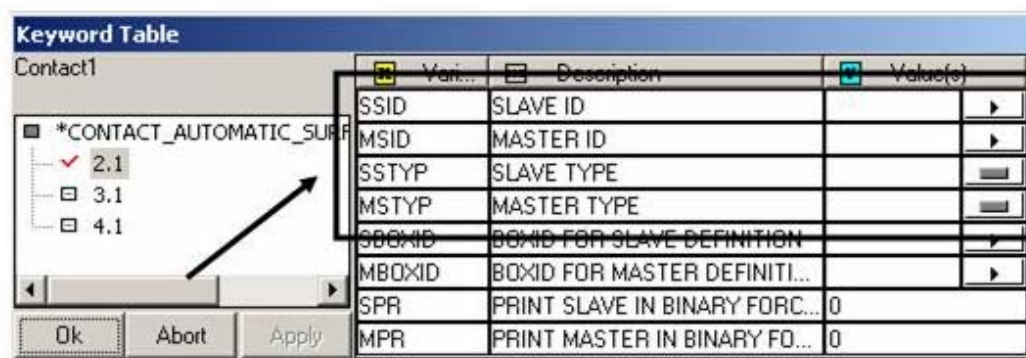


Figure 3.21 – AUTOMATIC_SURFACE_TO_SURFACE CARD

3.14 SELECT INFORMATION FOR OUTPUT

When the geometric definition of the model is finished, output parameters must be selected through the *DYNA MISCELLANEOUS* menu, shown in *Column A* of Figure 3.22. From within that menu, *CONTROL* and *DATABASE*, shown respectively in *Columns B* and *C* of Figure 3.22, are the two most useful output categories. Within *CONTROL*, a user is permitted to define the termination time (time at which the analysis should end). To capture the period from 0.0 to 0.15 seconds in real time of a crash simulation, for instance, the termination time should be defined as 0.15 sec. This menu also permits the user to modify the time interval at which the solver integrates the solution, the way in which contact

surfaces are calculated, and the energy equations on which the solutions are based.

The *DATABASE* menu contains two important sub-categories for specifying the desired output information: *ASCII* and *BINARY*. As shown in Column C of Figure 3.22, within those subcategories, *ELOUT*, *NODOUT* and *RCFORC* are useful for crash simulations. *ELOUT* and *NODOUT* refer to “element output” and “node output” respectively. By defining a time interval for these two output types, the user can obtain response histories for forces within beam elements, and displacement and acceleration histories for specified nodes. The beam elements and nodes for which output is desired must be selected within the *HISTORY* card, which is also given in the *DATABASE* menu. *RCFORC*, which stands for “resultant contact force,” is additional useful information from a crash simulation. By defining a time interval for output, the user can create force-time histories for any of the model’s contact surfaces, such as the surface between the barrier and vehicle. The menus for setting up *RCFORC* for output are given in Figure 3.23.

Finally, to create stress-contour plots or displacement animations, the *D3PLOT* command must be defined with a time interval for output, as shown in Column D of Figure 3.22.

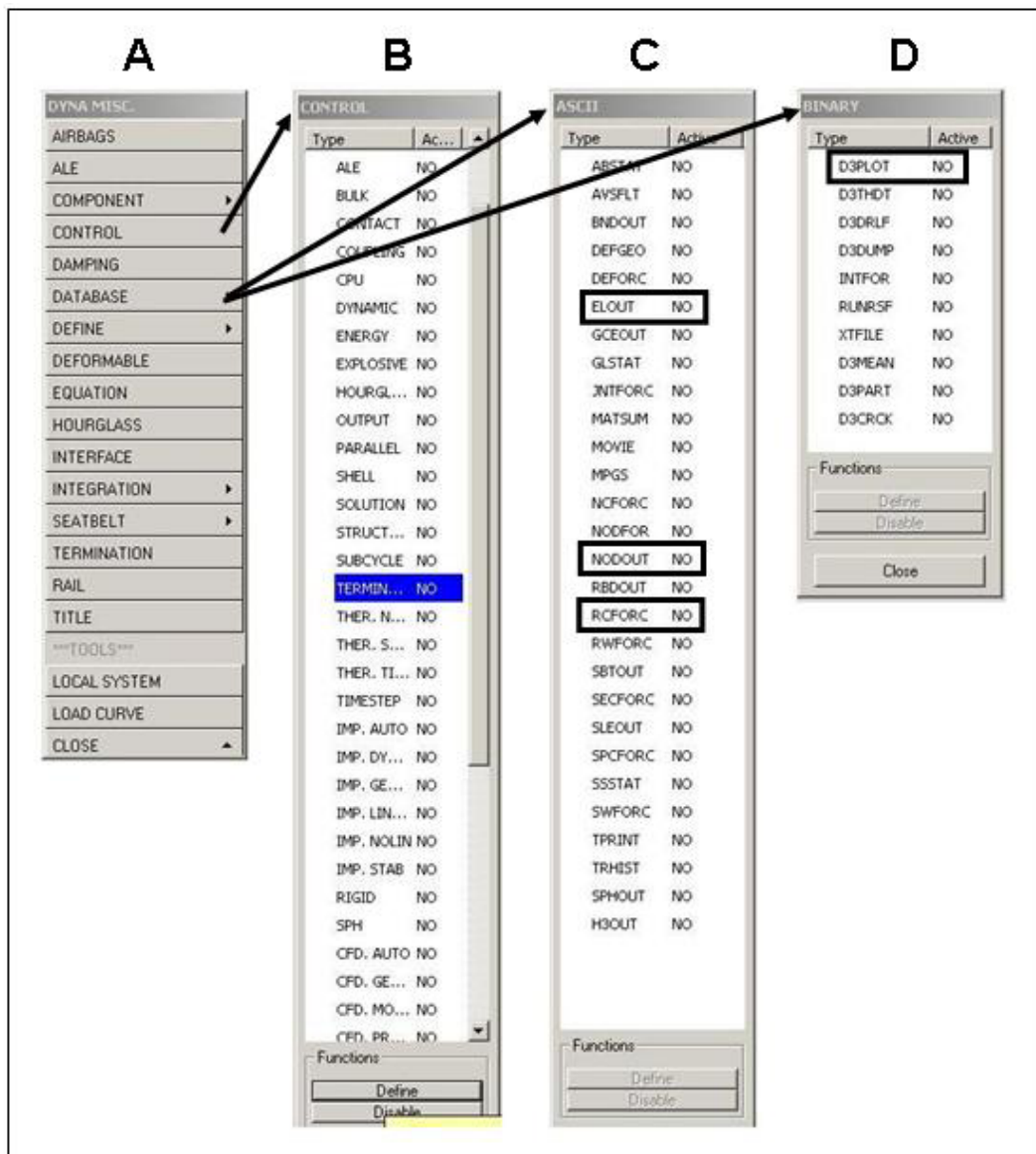


Figure 3.22 – “DYNA Miscellaneous” Output Control Menus

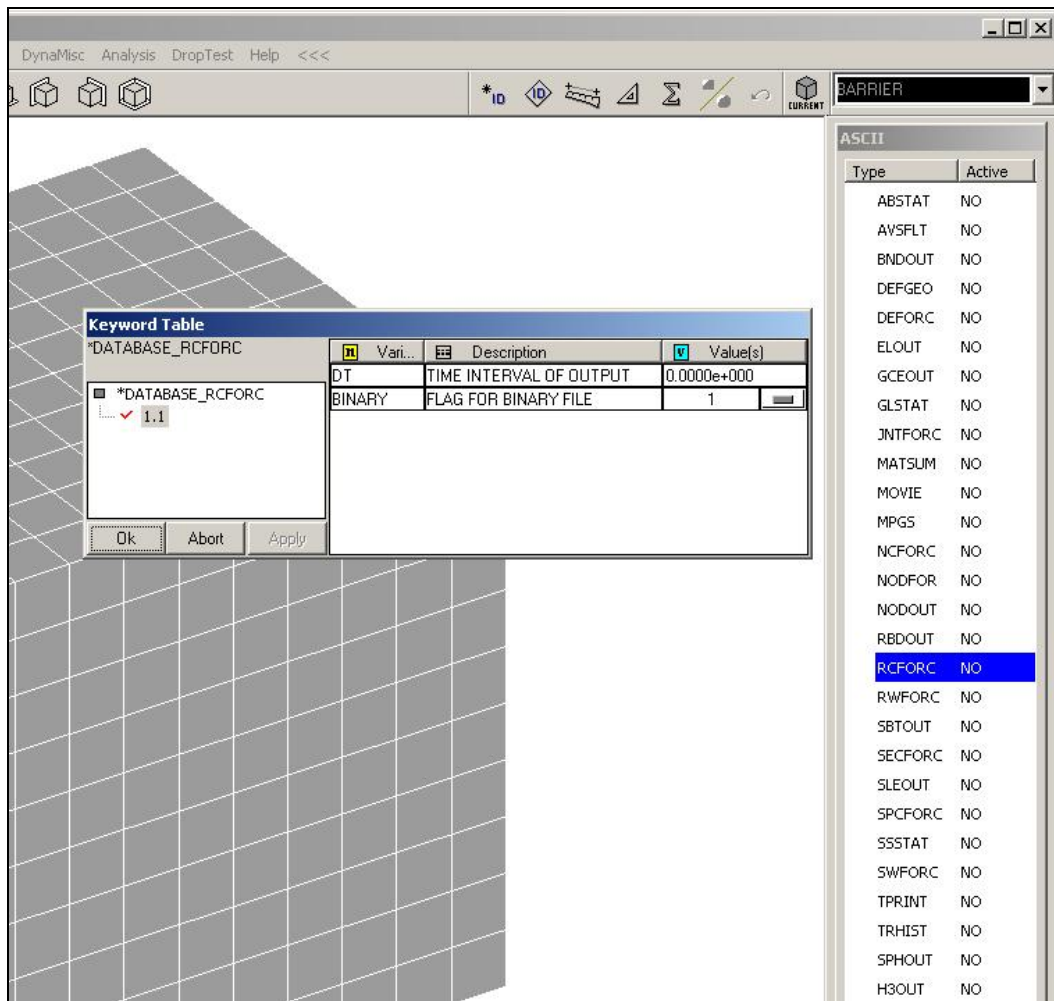


Figure 3.23 – Output-control menus for Contact Forces (RCFORC)

3.15 RUN THE DEFINED LS-DYNA MODEL

Once all necessary *CARDS* are defined as described in the preceding sections, the model is ready to be analyzed. Previously created files have the file extension *.fmb*. The LS-DYNA solver, however, requires the file extension *.dyn*. To create this file, the model must be exported (menu heading *FILE, EXPORT*

command), and assigned an appropriate file name. The preprocessor program is not needed for the model solution. As shown in Figure 3.24, the user must use the *SOLVERS* command in the *LS-DYNA Program Manager* to run an analysis.

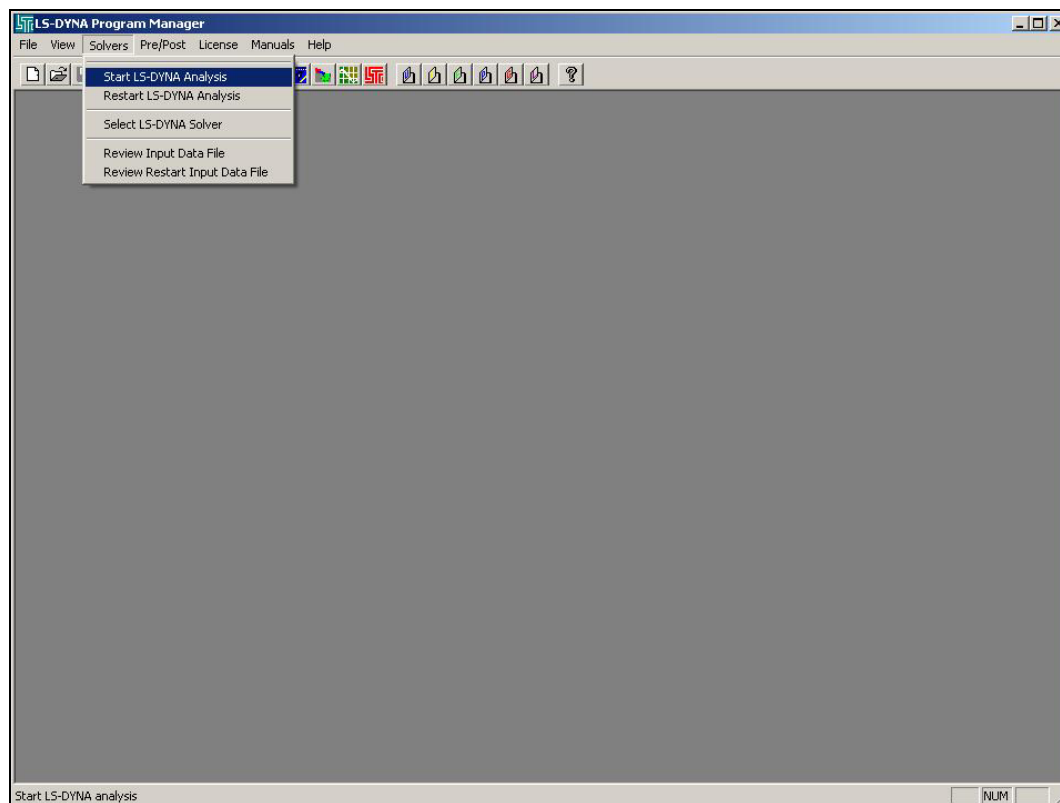


Figure 3.24 – Starting the LS-DYNA Solver

Upon selecting “Start LS-DYNA Analysis,” the menu commands for setting up the analysis run are displayed (Figure 3.25). The desired analysis file can be selected using the *BROWSE* command within the *INPUT FILE* field. The *OUTPUT FILE* field should be filled in automatically by the program, because the output file destinations have already been specified indirectly within the preprocessor by selecting output information categories. If the analysis is run on a

dual-processor micro-computer, the *NCPU* field, under the heading “Set Command Line Parameters,” should be changed to “2,” indicating two processors. If the input file is extremely large, the user may have to manually increase the number in the *MEMORY* field, under the heading “Set Command Line Parameters,” also shown in Figure 3.25. Once the input and output parameters are specified, clicking “OK” starts the analysis. While the analysis is running, a progress window automatically displays total input energies, and also updates the analysis time steps and eroded elements if erosion (i.e., failure and removal from the model) criteria have been specified. A typical progress window is shown in Figure 3.26.

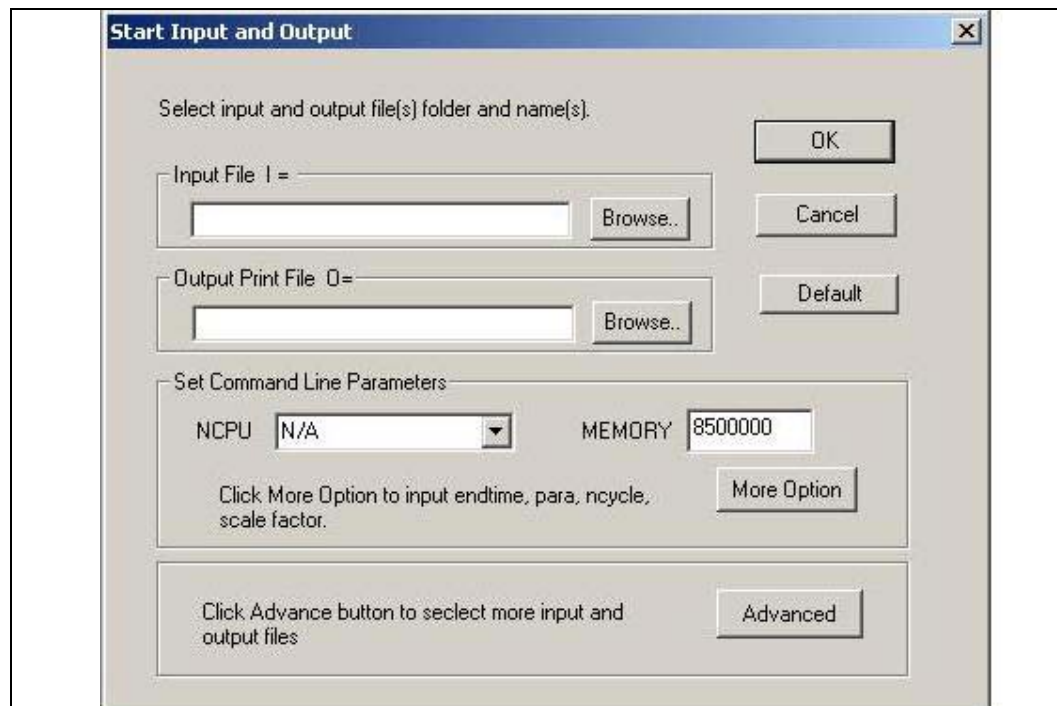


Figure 3.25 – Menu with Solver settings

```

C:\I-C\PROJEC~1\HONEYC~1\HOAEB4~1\HONEYC~1.DYN O=C:\PROJEC~1\HONEYC~1\HOAEB4~1\d3hsp NCPU=2
-----
Unauthorized use infringes LSTC copyrights
-----
Input file: C:\PROJEC~1\HONEYC~1\HOAEB4~1\HONEYC~1.DYN

The native file format      : 32-bit small endian
Memory size from default   : 8500000

on UNIX computers note the following change:

ctrl-c interrupts ls-dyna and prompts for a sense switch.
type the desired sense switch: sw1., sw2., etc. to continue
the execution.  ls-dyna will respond as explained in the users manual

-----
type           response
-----
sw1.          a restart file is written and ls-dyna terminates.
sw2.          ls-dyna responds with time and cycle numbers.
sw3.          a restart file is written and ls-dyna continues calculations.
sw4.          a plot state is written and ls-dyna continues calculations.

***** notice ***** notice ***** notice *****
*
* This is the LS-DYNA Explicit Finite Element code.
* Neither LSTC nor the authors assume any responsibility for
* the validity, accuracy, or applicability of any results
* obtained from this system. The user must verify his own
* results.
*
* LSTC endeavors to make the LS-DYNA code as complete,
* accurate and easy to use as possible.
* Suggestions and comments are welcomed. Please report any
* errors encountered in either the documentation or results
* immediately to LSTC through your site focus.
*
* Copyright (C) 1990-2003
* by Livermore Software Technology Corp. (LSTC)
* All rights reserved
*
***** notice ***** notice ***** notice *****

input of data is completed

initial kinetic energy = 0.39704668E+08

The LS-DYNA time step size should not exceed 0.172E-05
to avoid contact instabilities. If the step size is
bigger then scale the penalty of the offending surface.

initialization completed

dt of cycle      1 is controlled by solid      element 84137

time..... 0.00000E+00
time step..... 1.41640E-06
kinetic energy..... 3.97027E+07
internal energy..... 1.00000E-20
spring and damper energy..... 1.00000E-20
system damping energy..... 0.00000E+00
sliding interface energy..... 0.00000E+00
external work..... 0.00000E+00
eroded kinetic energy..... 0.00000E+00
eroded internal energy..... 0.00000E+00
total energy..... 3.97027E+07
total energy / initial energy.. 1.00000E+00
energy ratio w/o eroded energy.. 1.00000E+00
global x velocity..... 1.99332E+03
global y velocity..... 0.00000E+00
global z velocity..... 0.00000E+00
cpu time per zone cycle..... 0 nanoseconds
average cpu time per zone cycle... 0 nanoseconds
average clock time per zone cycle.. 4159 nanoseconds

estimated total cpu time = 0 sec ( 0 hrs 0 mins)
estimated cpu time to complete = 0 sec ( 0 hrs 0 mins)
estimated total clock time = 3282 sec ( 0 hrs 54 mins)

```

Figure 3.26 – Example Solver screen during an analysis

CHAPTER 4

Developing LS-DYNA Models for Study 4823

4.1 OVERVIEW OF PROJECT 4823 MODELS

To create LS-DYNA models for barrier crashworthiness studies, four components must be modeled: the cast-in-place barrier to be studied; the retrofit barrier intended to replace that cast-in-place barrier; the pendulum intended for laboratory use in evaluating that barrier's performance; and the specific crush package attached to the nose of that pendulum. Each component must be modeled analytically, using appropriate dimensions and materials. In this chapter, the development of LS-DYNA analytical models for each component is presented. In addition, because those LS-DYNA models can be used with pre-existing finite element models of various test vehicles, the process of incorporating pre-existing models is also presented.

4.2 DEVELOPMENT OF LS-DYNA MODEL FOR CAST-IN-PLACE BARRIER

Development of an LS-DYNA model for the cast-in-place bridge barrier is essential for studying the behavior of such barriers, and for determining a suitable retrofit design with similar behavior. A typical field installation of a TxDOT T203 cast-in-place barrier is shown in Figure 4.1. In Figure 4.2 are shown photos of a laboratory specimen representing a segment of that same type of barrier (TxDOT 2004). An appropriate LS-DYNA analytical model was created for the same barrier, considering its geometry, element size, materials, and treatment of the steel reinforcement.



Figure 4.1 – TxDOT T203 bridge barrier with intermittent base and concrete parapet

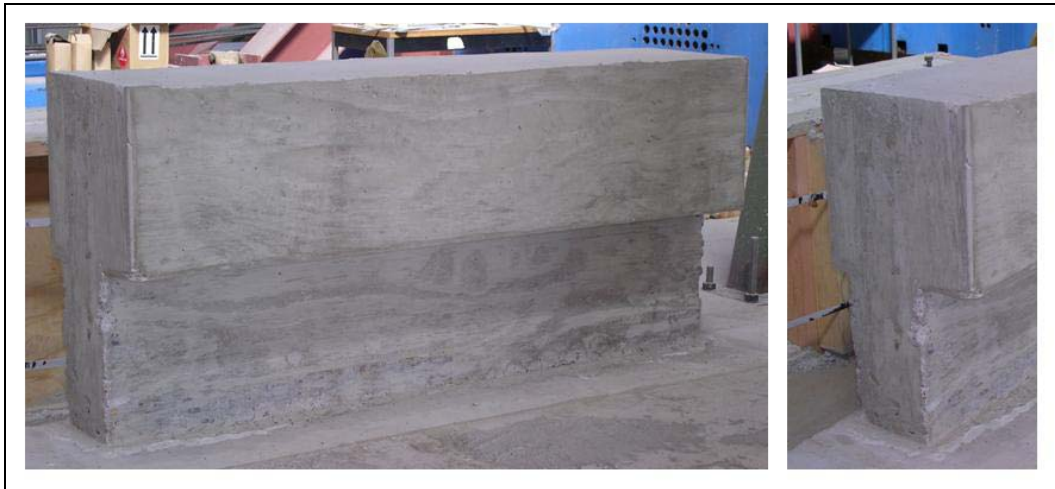


Figure 4.2 – Cast-in-place laboratory specimen representing a segment of a TxDOT T203 barrier with continuous base and concrete parapet

4.2.1 Geometry of Cast-in-Place Barrier

The geometry of the Type T203 bridge barrier, based on TxDOT standards, is shown in Figure 4.3. Though some characteristics must be modified slightly for ease of modeling, the geometry of the analytical model must still be consistent with those standards. The outer dimensions of that geometry were used to create the finite element model. Modeling of the steel reinforcement in the cast-in-place barrier is discussed in Section 4.2.5, and modeling of the deck slab is discussed in Section 4.4.3.

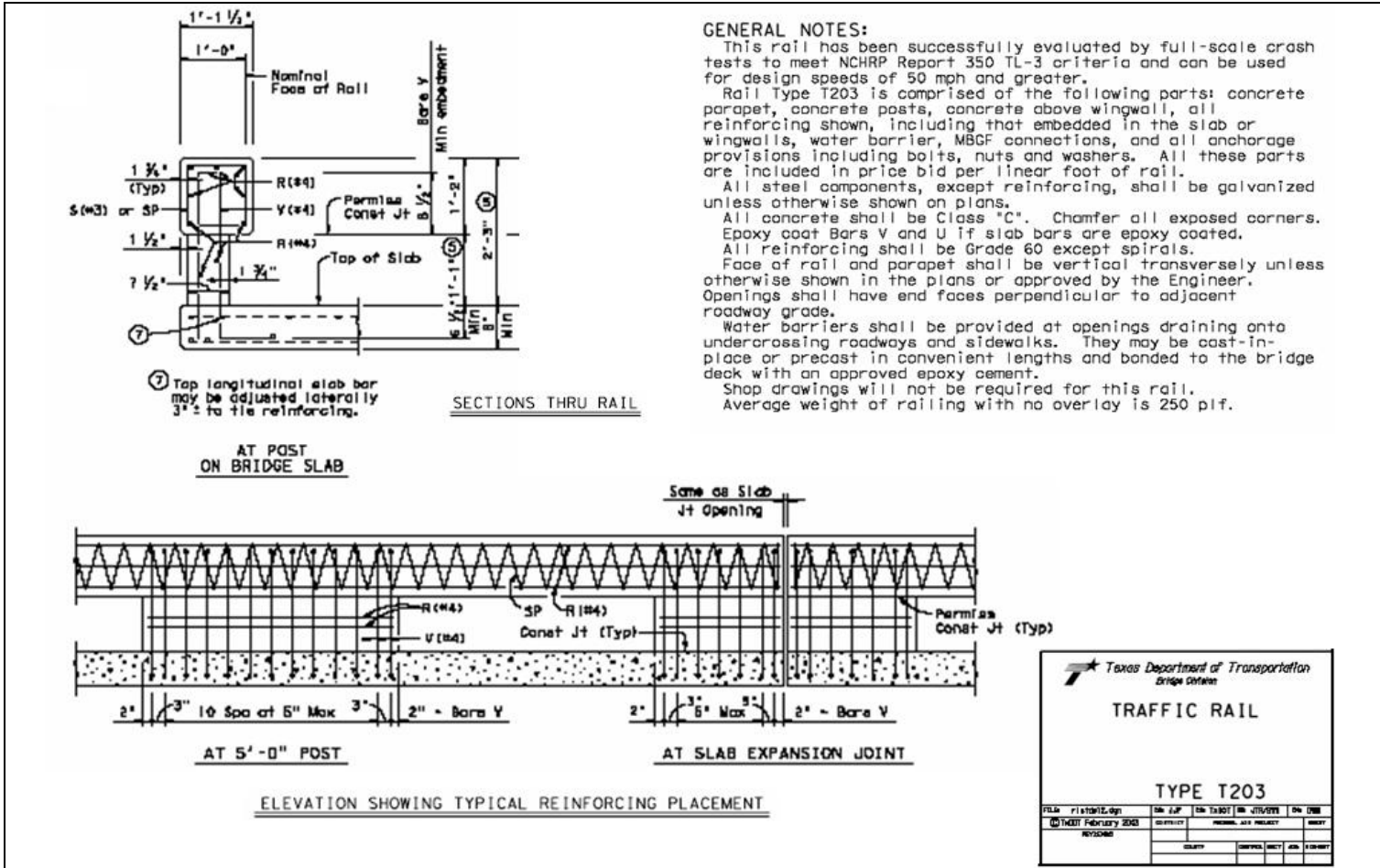


Figure 4.3 – TxDOT Details of Type T203 Traffic Rail (TxDOT 2004)

4.2.2 Develop Each PART

The easiest way to create the correct geometry for a five-foot section of barrier is to create two rectangular prisms and then join them together. The process of meshing and joining the prisms is discussed in Section 4.2.3. The dimensions of each barrier portion are specified in Table 4.1. The upper portion of the barrier must be positioned globally so that its base is at the same elevation as the top of the lower portion. In addition, the top portion must extend 114 mm (4.5 in.) over the front and 38 mm (1.5 in.) over the back of the lower portion. The correct positioning of each piece is shown in Figure 4.4.

Table 4.1 – Dimensions (mm) of Cast-in-place T203 barrier

<i>Barrier Portion</i>	<i>Length</i>	<i>Width</i>	<i>Height</i>
Lower	1524	190.5	330.2
Upper	1524	342.9	355.6

4.2.3 Create the Mesh

Once both barrier sections have been created, they must be meshed individually. Mesh sizes should be selected so that elements are the same size in each barrier section. In addition, element width should be no larger than 38.1 mm (1.5 in.) so that elements line up in the upper and lower barrier portions. The mesh selected for most of the barrier models consisted of cubic elements measuring 38.1 mm (1.5 in.) in each dimension (Figure 4.4). After meshing each barrier section, they are joined to form a single entity, using the *CHECK COINCIDENT* command under the *NODES* menu. The user is prompted to select

a tolerance value, or distance between nodes, for checking for nodal coincidences. The default value of 0.01 mm (3.94×10^{-4} in.) is acceptable for this purpose, though other values can be selected to suit individual modeling needs. Once a tolerance value is selected, a region must be chosen where coincident nodes will be checked. The user should select the entire region over which the upper and lower barrier portions are in contact. LS-DYNA will give the user the option of merging the nodes located at the same positions. The *MERGE* option should be selected to create a unified barrier.

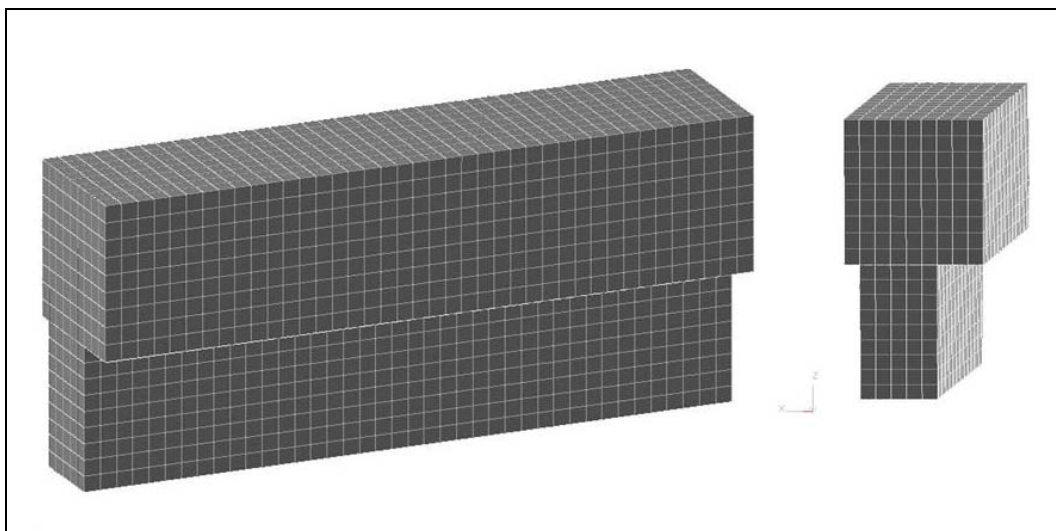


Figure 4.4 – DYNA model of cast-in-place concrete barrier

4.2.4 Select the Concrete Material Model

Concrete is a relatively difficult material to model using finite element analyses due to its brittle behavior, the effects of confinement and reinforcement, and its descending-branch response characteristics. One way of dealing with the

material characteristics of concrete is to use a simple material model, such as an elastic material, and include criteria for erosion of elements. To model the cast-in-place barrier, the *ISOTROPIC_ELASTIC_FAILURE* material was selected. The failure criteria were set so that elements would erode if the strain in an element reached 0.06. The *CARD* for this material, specifying each property that defines it, is shown in Table 4.2. Criteria for element failure and erosion, defined on the second *CARD*, are shown in Table 4.3.

Table 4.2 – CARD 1 for concrete, modeled as Isotropic Elastic Failure Material

<i>Variable</i>	<i>Description</i>	<i>Value</i>	<i>Units</i>
MID	Material ID	-	-
RO	Mass Density	2.4028e-009	ton/mm ³
G	Shear Modulus	1.0807e+004	MPa
SIGY	Yield Stress	2.7579e+001	MPa
ETAN	Plastic Hardening Modulus	0	MPa
BULK	Bulk Modulus	1.1836e+004	MPa

Table 4.3 – CARD 2 for concrete, modeled as Isotropic Elastic Failure Material

<i>Variable</i>	<i>Description</i>	<i>Value</i>	<i>Units</i>
EPF	Plastic Failure Strain	6.0000e-002	-
PRF	Failure Pressure	0	-
REM	Element Erosion Option	0	-
TREM	Time step for Element Erosion	0	-

4.2.5 Treatment of Steel Reinforcement

For the cast-in-place barrier, due to the distribution of reinforcing bars, it is efficient to assume that the concrete and steel act compatibly. The assumption is valid if the bond between concrete and reinforcement is adequate. The end conditions, however, and specifically the connection between the barrier section and the deck slab, need to be modeled appropriately. It was assumed that these elements are primarily axial in behavior. Individual spring elements were created for each reinforcing bar, and they extend between the base of the barrier and deck slab. In total, 26 spring elements were created, each with the appropriate equivalent stiffness, calculated as EA/L for axial elements, where L is the length of the flexural reinforcement. The length, L , for the cast-in-place barrier is approximately the height of the barrier, 686 mm (27 in.) (Figure 4.5). Other material properties are Young's modulus for steel, and the cross-sectional area of a #4 bar. The appropriate material for this type of element is *ELASTIC SPRING*. The *CARD* for this material is shown in Table 4.4.

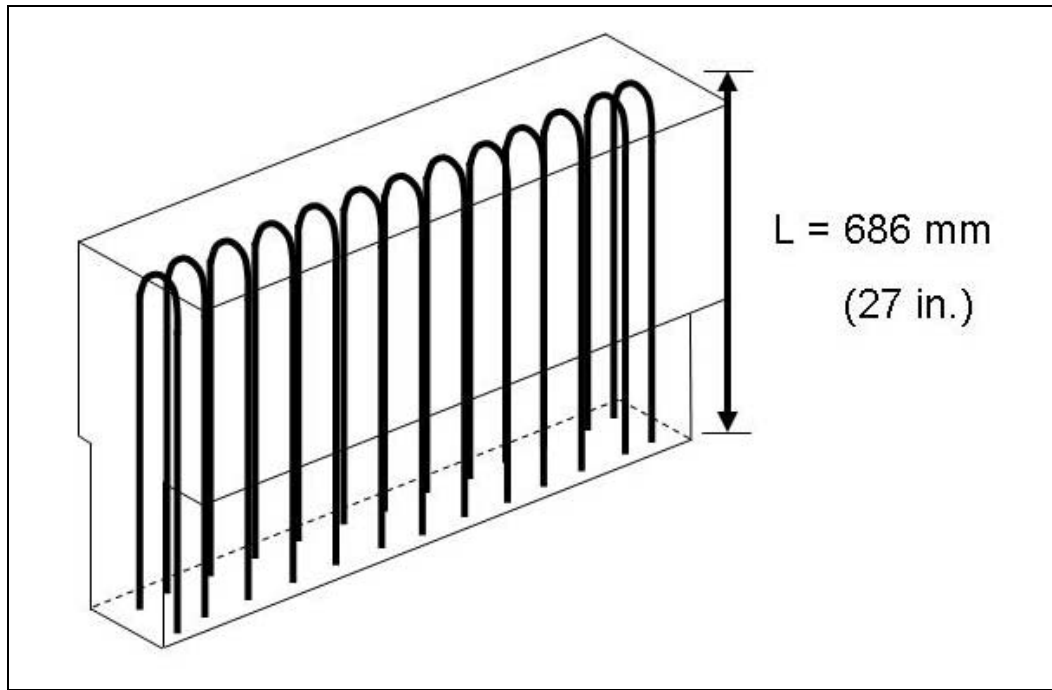


Figure 4.5 – Placement of reinforcing bars in cast-in-place barrier

Table 4.4 – CARD 1 for Reinforcing Bars, modeled as Elastic Spring Material

<i>Variable</i>	<i>Description</i>	<i>Value</i>	<i>Units</i>
MID	Material ID	-	-
K	Spring Stiffness	3.7620e+004	N/mm

4.3 ANALYTICAL MODELING OF RETROFIT BARRIER

An analytical model of the proposed retrofit barrier design was needed for comparison with the cast-in-place model. The model for the retrofit barrier used the same dimensions, materials and mesh as the cast-in-place barrier model.

The retrofit barrier design, which is the subject of the experimental and analytical testing, is described in the following section. Based upon the current state of knowledge on anchorage to concrete using post-installed mechanical anchors (Mitchell 2005), the retrofit barrier design shown in Figure 4.6 was proposed. It will likely require further modification based on the results of future research in this study.

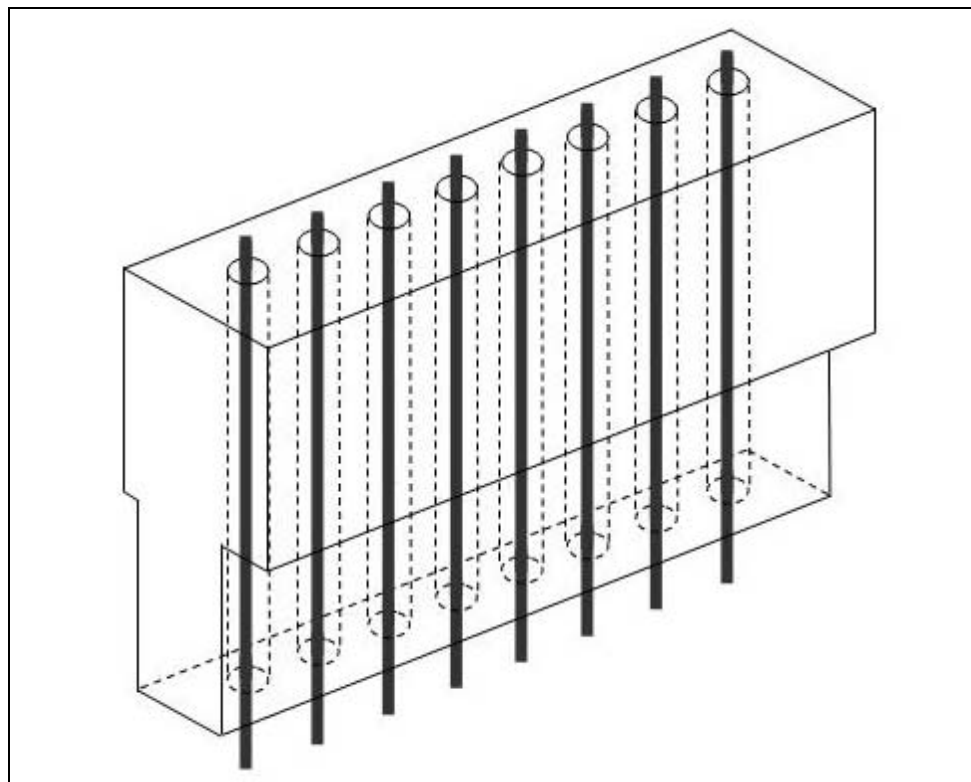


Figure 4.6 – Schematic of proposed retrofit barrier design

This design has the advantage of utilizing a precast concrete section, allowing easy installation in replacement of a damaged cast-in-place barrier. The

retrofit barrier does not have the same steel reinforcement as the cast-in-place design. Its flexural reinforcement will be post-installed, and the amount of steel will be varied depending on the desired barrier response under impact loads. For this purpose, the pre-cast barrier section contains hollow ducts, spaced at approximately 165 mm (6.75 in.) on center, with a diameter that can be varied depending on the amount of steel to be installed. The current proposal for the post-installed steel is threaded rods held underneath the deck with external nuts.

4.3.1 Modify the Cast-in-Place Barrier

The LS-DYNA analytical model for the retrofit barrier begins with the completed cast-in-place model, excluding the reinforcing-bar elements. The models differ principally in the inclusion, in the retrofit design, of hollow ducts into which post-installed reinforcement or anchors can be placed. One must first determine, based on the dimensions of the finite elements, how many elements must be deleted to create the correct cross-sectional area of the void space representing the hollow ducts. For this preliminary retrofit design, a series of eight equally spaced ducts had to be created. Based upon the element cross-sectional area of 1451 mm² (2.25 in.²), a void one element wide in each radial direction was needed. Once the void was created, elements at the top of each hollow void were re-created so that the reinforcing bar could be anchored to them. The process for accomplishing this task is described in the following sections.

4.3.2 Create Hollow Ducts for Retrofit Reinforcement or Anchors

To delete the necessary elements in an efficient manner, the user should use a two-dimensional view of the top of the barrier model. Using the *DELETE* command under the *ELEMENT* menu, elements can be deleted from the given

region by clicking and dragging the mouse over them in that view. Vertically aligned elements in the dragged window are deleted, creating a vertically oriented, elongated void in the barrier. In other words, to create the vertically oriented three-dimensional void, the user must select elements defining the cross-sectional area of each duct in a horizontal plane. This procedure is shown in Figure 4.7.

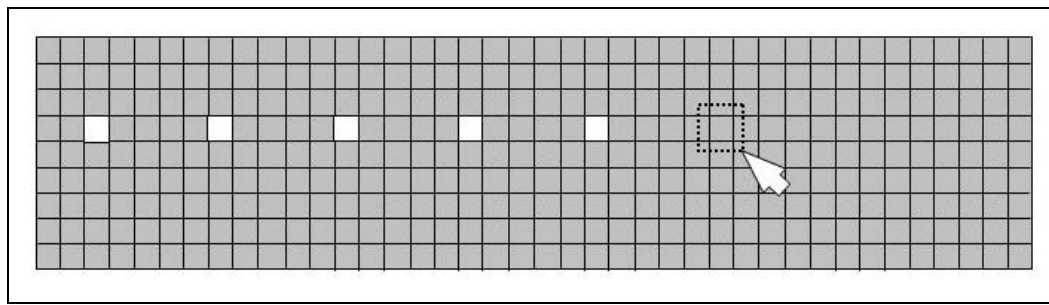


Figure 4.7 – Selection of elements to be deleted to form ducts for reinforcement or anchors

4.3.3 Create Elements for Anchorage of Reinforcement

Even though the reinforcing steel in the actual retrofit design is anchored outside of the dimensions of the concrete, the reinforcing steel in the analytical model is anchored at the upper boundary of the barrier. This modeling approach should not affect the overall behavior significantly. The user must first create the anchorage points by re-creating a single element at the top of each hollow duct, preferably when the barrier is in the three-dimensional view and the *fill-color* view option is selected. Under the *ELEMENT* menu, the user selects *CREATE* followed by *SOLID*, and is then prompted to select eight nodes to define a single

element. It is easiest to select the eight nodes of the surrounding elements to define a single cube at the top of each duct (Figure 4.8). Once the element has been created, it must be subdivided to allow the axial reinforcing steel elements to be attached in the center of the hollow duct. Subdividing the element is accomplished using the *SPLIT* command under the *ELEMENT* menu. The correct option under the *SPLIT* menu is the *SOLID TO 8 SOLIDS* option. When the desired element is selected, LS-DYNA automatically subdivides the cubic element into eight identical smaller cubic elements (Figure 4.9).

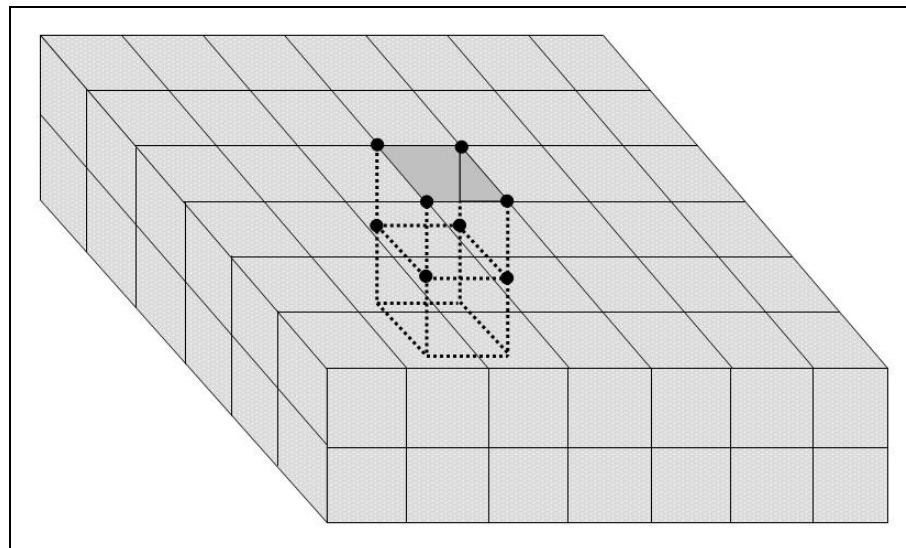


Figure 4.8 – Re-creation of element at top of hollow duct

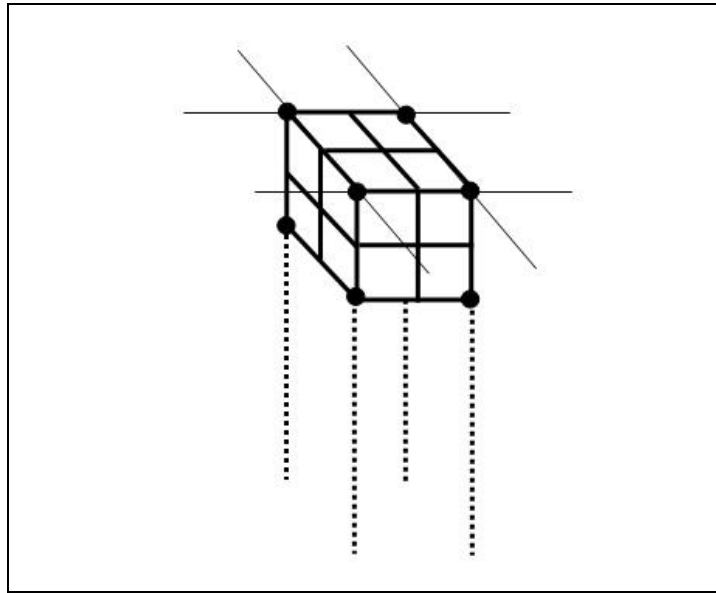


Figure 4.9 – Division of LS-DYNA element for attachment of reinforcing bar

4.3.4 Treatment of Post-Installed Reinforcing Bars

Post-installed reinforcing bars were created using line elements, assuming primarily axial behavior and a standard threaded rod with an effective diameter of approximately 31.75 mm (1.25 in.). This assumption may be modified by future research.

First, lines defining each reinforcing bar must be created within a separate *PART*, connecting the node at the center of the elements at the top of the hollow duct with a corresponding node located directly below the first node in the rigid deck. The finished element should appear as shown in Figure 4.10.

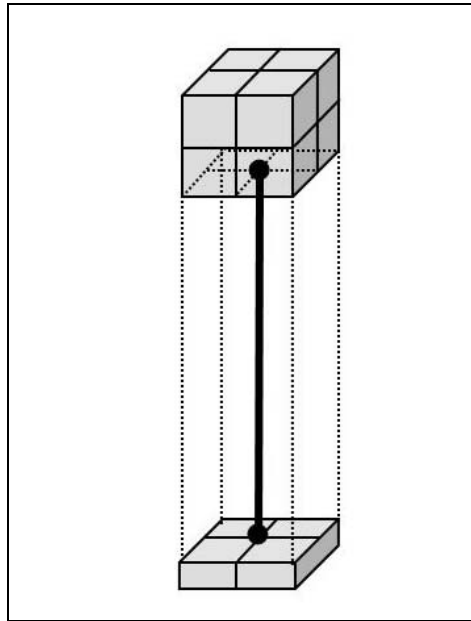


Figure 4.10 – Analytical representation of post-installed reinforcement as a line element inside a hollow duct

Next, each line is subdivided into the desired number of elements (for this research project, ten elements). Under the *ELEMENT* menu, the user selects the *LINE MESH* command, followed by the *BEAM ELEMENT* option, and is then prompted to select the lines to be meshed and the number of elements into which each line should be subdivided.

Because LS-DYNA lists truss elements under the heading of “beam,” beam elements were used, with a cross-sectional area equal to the effective cross-sectional area of the threaded rod, and a moment of inertia equal to zero. Under the *SECTION* menu, the *BEAM* option was selected. When the input *CARDS* are displayed, the user must select an *element formulation* option in addition to inputting other information, all shown in Table 4.5 below. Most values were kept as the default values, with the exception of the cross-section type which was

changed to Option 1, tubular. According to the *LS-DYNA Theory Manual*, an appropriate choice of element properties for a circular cross-section beam element is the Belytschko-Schwer beam element (Livermore Software Technology Corporation 1998). This type of element is given as Option 5 within the *ELFORM* field, also shown in Table 4.5. LS-DYNA then automatically displays the appropriate *CARDs* for the beam section depending on which option is selected. Once selected, LS-DYNA also displays *CARD 4* for user input, which includes information on beam dimensions. Values used for the preliminary design of the reinforcing steel are shown in Table 4.6. In Table 4.6, TS1 and TS2 refer to the outer diameter of the element at nodes 1 and 2, respectively. TT1 and TT2 refer to the inner diameter at the same nodes.

Table 4.5 – CARD 1 for reinforcement, modeled as SECTION_BEAM

<i>Variable</i>	<i>Description</i>	<i>Value</i>	<i>Units</i>
SECID	Section ID	-	-
ELFORM	Element Formulation	5	-
SHRF	Shear Factor	1.0000e+000	-
QR/IRID	Quadrature Rule	2	-
CST	Cross Section Type	1	-
SCOOR	Location of Triad	0	-
NSM	Nonstructural Mass Per...	0.0000e+000	-

**Table 4.6 – CARD 4 for preliminary reinforcement, modeled as
SECTION_BEAM**

<i>Variable</i>	<i>Description</i>	<i>Value</i>	<i>Units</i>
TS1	Beam Thickness in s-dir	3.2258e+001	mm
TS2	Beam Thickness in s-dir	3.2258e+001	mm
TT1	Beam Thickness in t-dir	0.0000e+000	mm
TT2	Beam Thickness in t-dir	0.0000e+000	mm

Although many different material models can be used to model steel within LS-DYNA, the selection of beam elements for the reinforcing bar limits the material models that can subsequently be selected. A model in which the steel could yield and deform was desirable for assessing overall barrier behavior in the inelastic range. After reviewing several possibilities, the plastic-kinematic material model was selected, with the input variable values shown in Table 4.7.

**Table 4.7 – CARD 1 for preliminary modeling of reinforcement as a Plastic
Kinematic Material**

<i>Variable</i>	<i>Description</i>	<i>Value</i>	<i>Units</i>
MID	Material ID	-	-
RO	Mass Density	7.9291e-009	ton/mm ³
E	Young's Modulus	1.9995e+005	MPa
PR	Poisson's Ratio	3.0000e-001	-
SIGY	Yield Stress	3.4474e+002	MPa
ETAN	Plastic Hardening Modulus	2.7579e+003	MPa
BETA	Hardening Parameter	0	-

In contrast with the cast-in-place barrier model for which the reinforcing bar and concrete were considered as a single solid entity, the retrofit barrier model used distinct concrete barrier and steel elements with an associated contact surface. The standard *AUTOMATIC_NODES_TO_SURFACE* contact for contact with two-dimensional elements was selected, using the concrete as the master surface and the reinforcing bar as the slave surface.

4.4 OVERALL CONSIDERATIONS IN MODELING BARRIERS

Once all components of the barrier models are developed, several other aspects must still be considered to finish the creation of a useful, comprehensive model. The two most important of these issues are the treatment of finite versus infinitely long barriers, and the modeling of the bridge slab.

4.4.1 Modeling of Finite-Length versus Infinitely Long Barriers

The critical structural case for bridge rails is a barrier with a finite length of 1.5 m (5.0 ft), representing a reasonable lower limit for out-of-plane stiffness and strength. Therefore, the default analytical model of the barrier used that length. This section addresses the modifications required to address the opposite limiting case of an infinitely long barrier.

4.4.2 Modeling of Infinitely Long Barriers

An infinitely long barrier can be handled analytically as a 1.5-m (5.0 ft) barrier with out-of-plane springs at each end, with stiffness values calculated to match the case of an infinitely long barrier. Spring elements were created in the horizontal direction for each node at the face of the upper parapet sections at each

end of the barrier, as shown in Figure 4.11, and represent only the out-of-plane translational stiffness due to adjacent barrier segments.

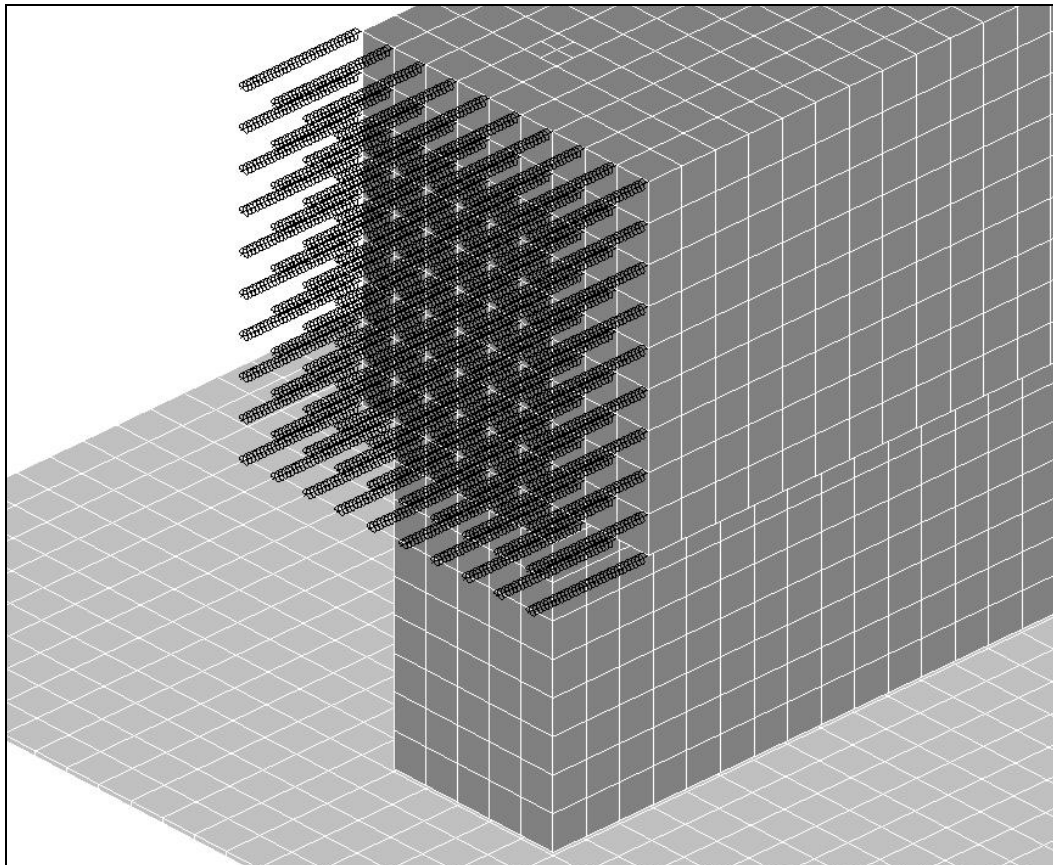


Figure 4.11 – Spring Elements added at ends of barrier segments to simulate the restraining effects of infinitely long barriers

At this point in the research project, it is not known what stiffness assumptions are the most accurate, and the spring stiffnesses proposed here may be modified in the future. An upper bound on the stiffness was established by considering the sum of two translational stiffness components.

The first contribution to the translational stiffness is based on the assumption that two segments, adjacent to the barrier segment being modeled, are allowed to deflect while their far ends are fixed. The total out-of-plane stiffness that they provide, k_t , is equal to $\frac{24 EI}{\ell^3}$. The stiffness contribution of one adjacent barrier segment is depicted in Figure 4.12.

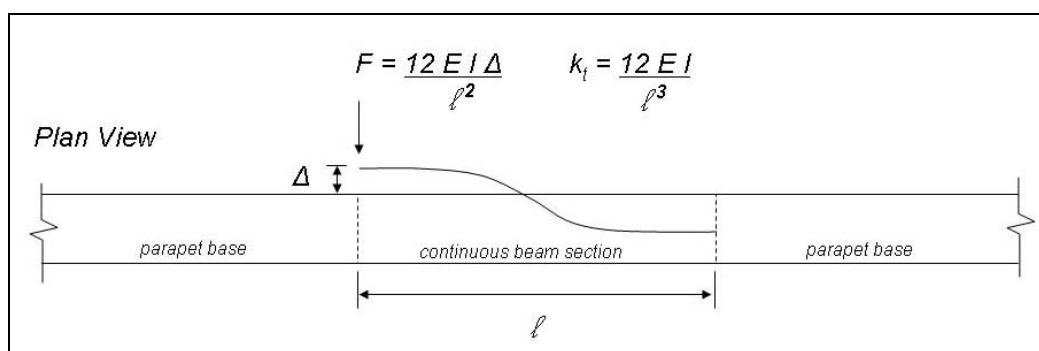


Figure 4.12 – Assumptions used in developing stiffnesses of equivalent springs to represent an infinitely long barrier

The other translational stiffness considered was that of the segment alone, based on a preliminary crash simulation with the finite-length barrier section and a Geo Metro vehicle model. That stiffness, $k_{segment}$, is equal to the out-of-plane force at the interface divided by the out-of-plane barrier deflection (Figure 4.13). This stiffness value was much smaller than the beam stiffness value. The upper-bound stiffness for an infinitely long barrier was assumed as the sum of the two translational stiffness contributions, k_t and $k_{segment}$. Once laboratory pendulum tests are completed, the data should permit refinement of the necessary boundary stiffnesses.

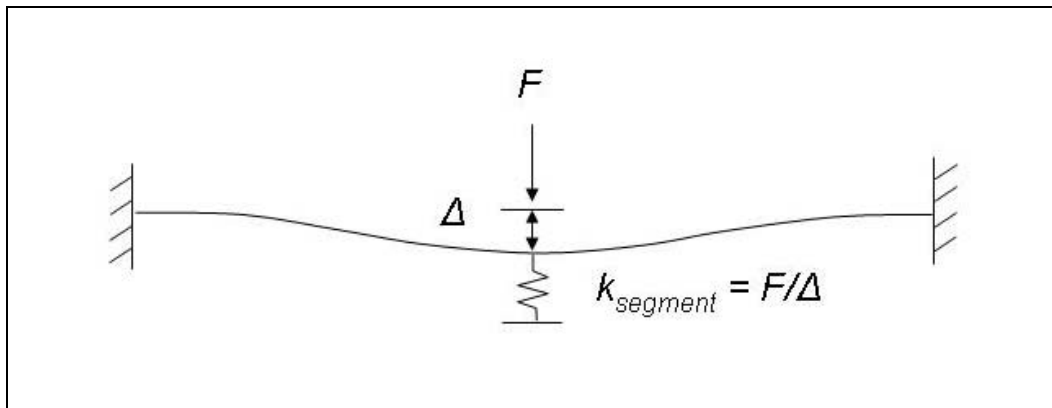


Figure 4.13 – Assumptions used in developing equivalent beam stiffness for finite-length section

4.4.3 Analytical Model of Reinforced Concrete Bridge Deck

To develop the crush package and analyze the cast-in-place barriers and preliminary retrofit designs, the concrete deck was modeled as a rigid base. Fixed boundary conditions were applied to all degrees of freedom attached to it, and it was used as an anchorage point for cast-in-place and post-installed reinforcing bars. Though the behavior of the barrier is the focus of this study, that behavior is influenced by the behavior of the deck. Therefore, future analytical models will include a deformable bridge deck.

4.5 DEVELOPMENT OF ANALYTICAL MODEL FOR IMPACT PENDULUM

The mass of the laboratory impact pendulum, shown in Figure 4.14, consists of a long center spine plate, two end plates, a top plate, and several smaller side plates added to achieve the desired weight. A finite element model of the pendulum mass was created using those components and steel material properties, as described in the following sections.



Figure 4.14 –Laboratory pendulum mass

4.5.1 Geometry of Pendulum Mass

The steel plates of the laboratory pendulum mass are 25.4-mm (1-in.) thick. It measures 1447-mm (57-in.) long, 457-mm (18-in.) wide, and 304.8-mm (12-in.) high. The plates and dimensions were modeled as accurately as possible, though the plates used for additional weight were modeled as a single part.

4.5.2 Creation of Finite Element Mesh for Laboratory Pendulum Mass

Due to the orientation, dimensions, and connectivity of the steel plates in the laboratory pendulum, a detailed mesh needed to be created. The mesh became more complex with smaller elements where the steel plates needed to be joined with geometric accuracy. For instance, as shown in **A** of Figure 4.15, the long, center vertical plate could only be joined at the center of the front plate. **B** of Figure 4.15 shows a similar connection between the center vertical plate and the

horizontal top plate. While a mesh of elements of approximately 16387 mm^3 (1 in.^3) would have been sufficient to capture pendulum behavior, a mesh of elements approximately 2048 mm^3 (0.125 in.^3) was necessary to allow for the joining of plates as described previously. An example of the resulting meshed pendulum is shown in **C** of Figure 4.15. Due to the large number of relatively small elements, however, computer run times using this pendulum model were unreasonably long. A simpler pendulum model was therefore developed to give shorter run times.

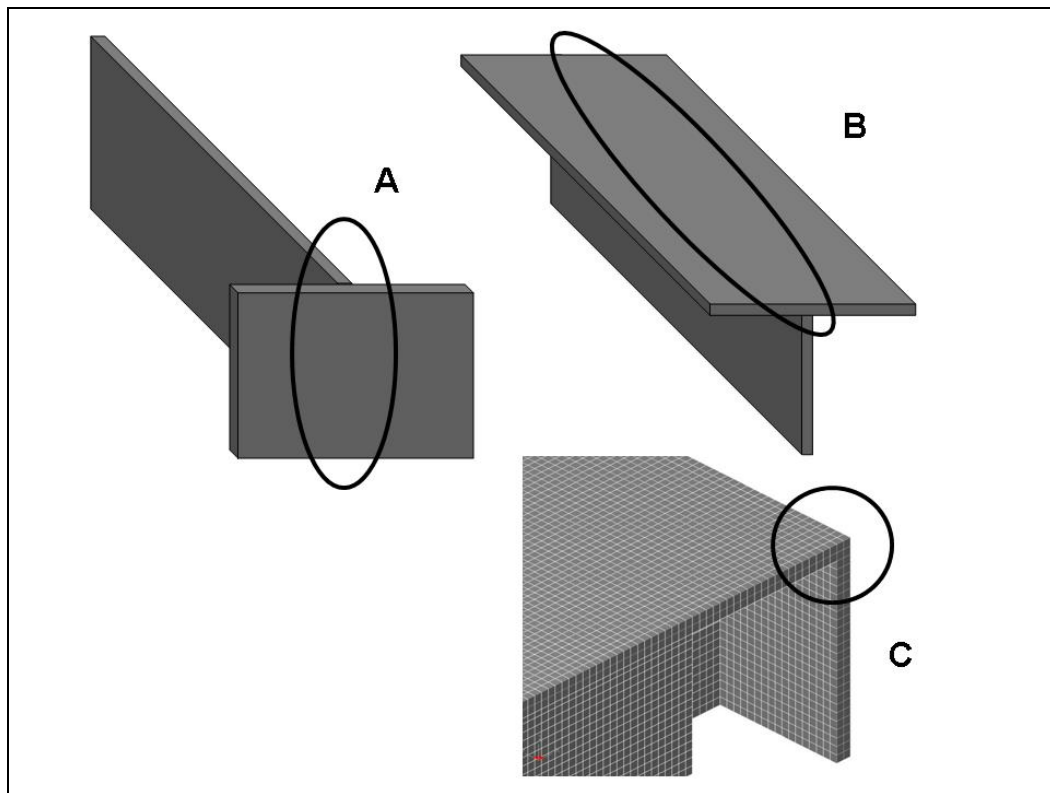


Figure 4.15 – Creating initial mesh for DYNA model of laboratory pendulum

4.5.3 Mesh for Simplified DYNA Model of Pendulum Mass

Several factors were considered when creating the mesh for a simplified DYNA model of the pendulum mass. Most important, the mass of the pendulum had to be preserved in order to preserve the impact impulse. Also, the overall length of the pendulum mass was essentially maintained to preserve the time that an axial stress wave would take to travel the length of the pendulum during a crash simulation. The resulting simplified pendulum mass was 1397-mm (55-in.) long, 305-mm (12-in.) wide, and 229-mm (9-in.) high. Its frontal cross-sectional area was still sufficient to allow placement of the crush package. The simplified pendulum model is shown in Figure 4.16.

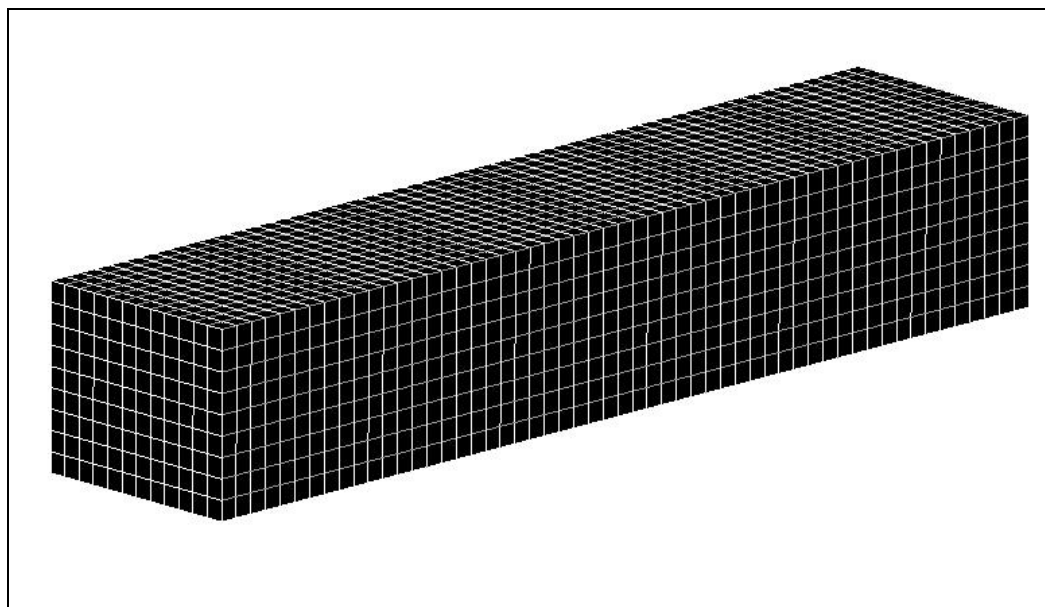


Figure 4.16 – Simplified DYNA model of laboratory pendulum mass

4.5.4 Material Model for Laboratory Pendulum Mass

The material model for the laboratory pendulum mass was selected to address elastic and plastic behavior. The simplest material model including these features is the *ISOTROPIC_ELASTIC_PLASTIC* material model, which requires only basic material properties for its definition. The values for steel, shown in Table 4.8, were used as input to LS-DYNA.

Table 4.8 – CARD 1 for pendulum mass, modeled as an Isotropic Elastic Plastic material

<i>Variable</i>	<i>Description</i>	<i>Value</i>	<i>Units</i>
MID	Material ID	-	-
RO	Mass Density	7.9278e-009	ton/mm ³
G	Shear Modulus	7.9903e+004	MPa
SIGY	Yield Stress	4.1369e+002	MPa
ETAN	Plastic Hardening Modulus	2.7579e+003	MPa
BULK	Bulk Modulus	1.6662e+005	MPa

4.6 DESIGN OF CRUSH PACKAGE

Development and calibration of the crush package design is discussed in detail in Chapter 5. The process by which a crush package is created and appropriately modeled is covered in this section, however.

4.6.1 Overview of Preliminary Design of Crush Package

The crush package is a structure attached to the front of the pendulum mass, intended to absorb impact energy and thereby replicate the crushing characteristics of a vehicle during an impact. The preliminary crush package was created using 25-mm (1-in.) hollow tubular steel arranged in layers with the cross-section perpendicular to the direction of impact, as shown in Figure 4.17. In that figure, the left end of the package impacts the barrier, and the right end is attached to the pendulum mass. The crush package is shown in its proper orientation with the pendulum during a crash test in Figure 4.18.



Figure 4.17 – Preliminary design of tubular steel crush package



Figure 4.18 – Crush package in position on pendulum during a crash test

4.6.2 Creation and Connection of Layers for Model of Preliminary Crush Package

Using the processes described in Chapter 4, each layer of the crush package must be created as a separate *PART*. Each layer of steel crushes individually, and creating separate *PART*s for each layer allows the analytical model to behave in the same way.

Once each layer of steel tubes is created and meshed individually, the *FIND COINCIDENT* command under the *NODES* menu heading is used to merge the nodes at the interface of each layer and also at the interface between the pendulum and the crush package. In the preliminary design of the crush package, each layer had a cross section of 152 mm (6 in.) by 152 mm (6 in.) and a depth of

25 mm (1 in.). A total of 18 layers were joined to form the complete crush package (Figure 4.19).

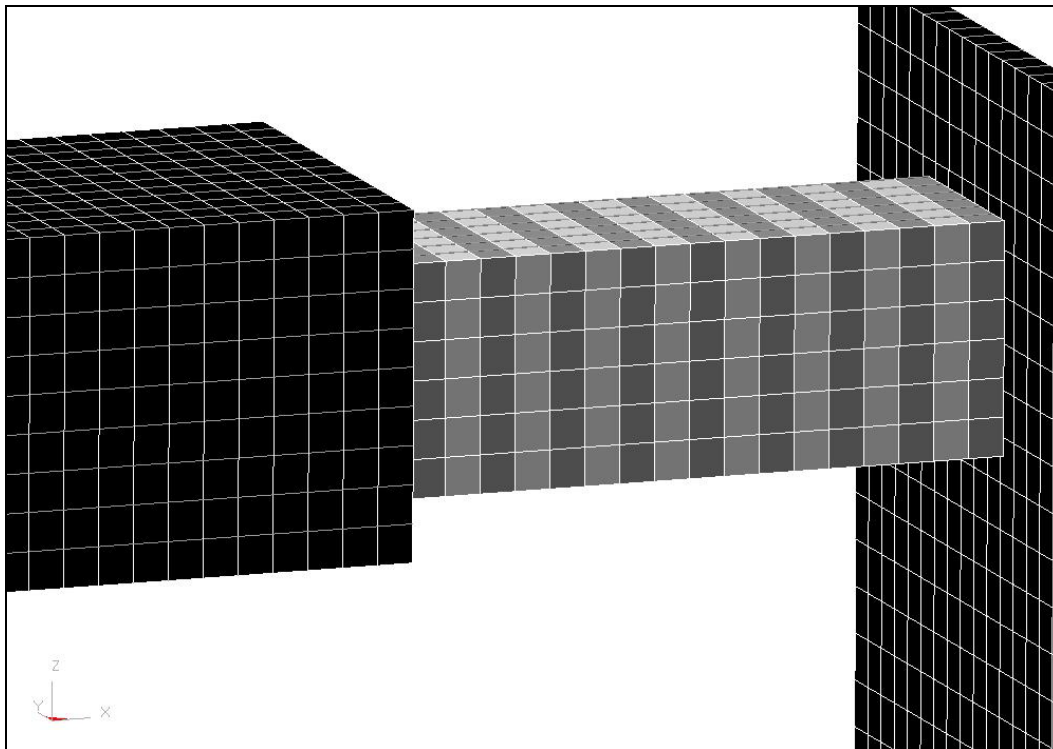


Figure 4.19 – DYNA model of preliminary crush package

4.6.3 Material Model for Preliminary Crush Package

The crush package consists of distinct steel layers that crush individually. The LS-DYNA material model most suited for this type of behavior is the *HONEYCOMB* material model, intended for metal materials that crush with a defined load curve. The first *CARD* and the values for input for that model are

shown in Table 4.9. Each value given is standard for steel, with the exception of the mass density, which represents the overall density of the crush package, including voids as well as steel.

Table 4.9 – CARD 1 for Honeycomb Material

<i>Variable</i>	<i>Description</i>	<i>Value</i>	<i>Units</i>
MID	Material ID	-	-
RO	Mass Density	1.1654e-009	ton/mm
E	Young's Modulus	1.9995e+005	MPa
PR	Poisson's Ratio	3.0000e-001	-
SIGY	Yield Stress	4.1369e+002	MPa
VF	Fully Compacted Rel. Vel.	3.8000e-001	-
MU	Material Viscosity Coefficient	5.0000e-002	-
BULK	Bulk Viscosity Flag	0	-

The second *CARD* of input information used to define the honeycomb material (Table 4.10), supplies force-deformation information for the honeycomb material. A single load curve can be used for each of the LCA, LCB, LCC, and LCS variables. LCA, LCB, LCC, and LCS represent the load curve ID for the normal stress-volumetric strain curve for each of the primary coordinate axes. LCAB, LCBC, LCCA, and LCSR are the load curve IDs for the shear stress-volumetric strain for each of the primary axes. If the fields for the variables LCAB, LCBC, LCCA, and LCSR are left blank, those variables are assumed to have the same values as those of the direct stress-volumetric strain curves. The

input of the load curve is described in Section 4.6.4. The final *CARD* used to define the honeycomb material is shown in Table 4.11. Values for elastic and shear moduli are listed for each axis.

Table 4.10 – CARD 2 for Honeycomb Material

<i>Variable</i>	<i>Description</i>	<i>Value</i>	<i>Units</i>
LCA	LCID: Sigma-AA vs. Vol.	#	-
LCB	LCID: Sigma-BB vs. Vol.	#	-
LCC	LCID: Sigma-CC vs. Vol.	#	-
LCS	LCID: Shear Stress vs. Vol.	#	-
LCAB	LCID: Sigma-AB vs. Vol.	-	-
LCBC	LCID: Sigma-BC vs. Vol.	-	-
LCCA	LCID: Sigma-CA vs. Vol.	-	-
LCSR	LCID: Strain Rate Effects	-	-

Table 4.11 – CARD 3 for Honeycomb Material

<i>Variable</i>	<i>Description</i>	<i>Value</i>	<i>Units</i>
EAAU	Elastic Modulus, EAAU	6.2580e+001	MPa
EBBU	Elastic Modulus, EBBU	6.2580e+001	MPa
ECCU	Elastic Modulus, ECCU	6.2580e+001	MPa
GABU	Shear Modulus, EABU	2.2100e+001	MPa
GBCU	Shear Modulus, EBCU	4.6423e+001	MPa
GCAU	Shear Modulus, ECAU	2.2100e+001	MPa
AOPT	Material Axes Option	-	-

4.6.4 Input of Load Curve

The load curve specified in the *CARDs* for the honeycomb material model must be manually added by the user, and can be created using the *LOAD CURVE* command under the *DYNA MISC.* menu. Using this command, the user is prompted to enter information into a *CARD* similar to the material model *CARDs*. The values used to define the load curve are given in Table 4.12 and were obtained from a static crush test on the layers of hollow steel tube, converted to a curve of stress versus volumetric strain, and entered into LS-DYNA. A further description of this static testing procedure is given in Section 5.1.1. The load-displacement data were converted to stress-volumetric strain data by dividing each load value by the cross-sectional area being loaded, and dividing each displacement value by the overall length of the specimen. In Table 4.12, the ordinate scale factor (*SFO*) has a value of 1.2, reflecting the probable higher strength of the material under dynamic loading conditions. Once the *DEFINE CURVE CARD* is completed, the user can enter the stress and strain values that define the load curve itself (Figure 4.20).

Table 4.12 – Load Curve Definition CARD

<i>Variable</i>	<i>Description</i>	<i>Value</i>	<i>Units</i>
LCID	Load Curve ID	#	-
SIDR	Stress Initialization Opt.	0	-
SFA	Scale Factor: Abscissa Value	1.0000e+000	-
SFO	Scale Factor: Ordinate Value	1.2000e+000	-
OFFA	Offset Value: Abscissa	0.0000e+000	-
OFFO	Offset Value: Ordinate	0.0000e+000	-
DATTYP	Data Type	0	-

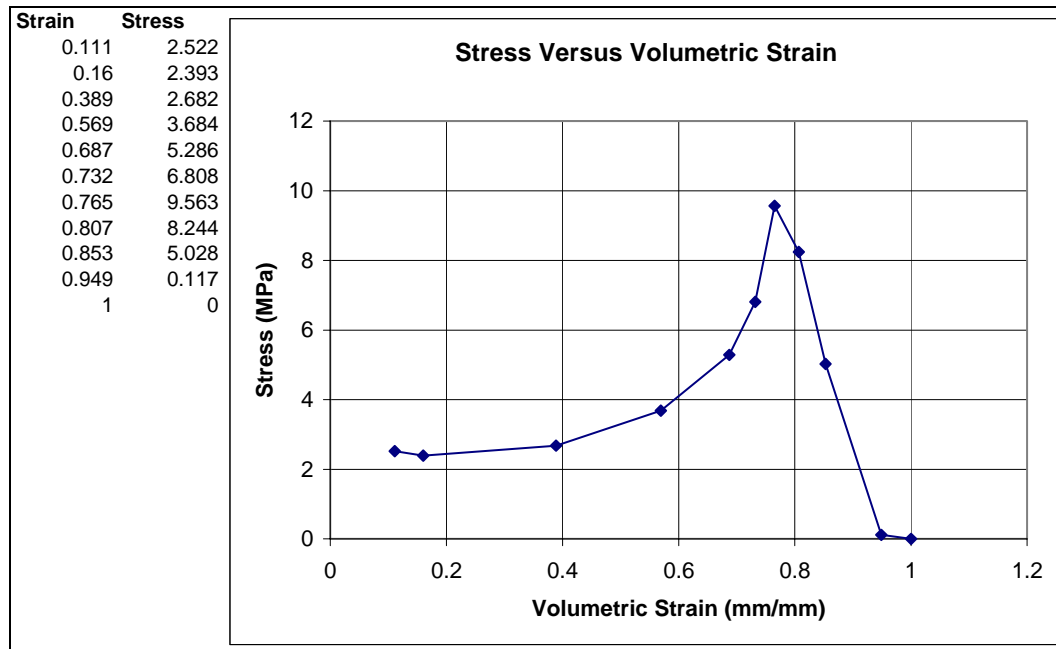


Figure 4.20 – Stress-strain curve for honeycomb material

4.7 INCORPORATION OF FHWA VEHICLE MODELS INTO LS-DYNA MODELS

To use LS-DYNA to simulate real vehicular impacts, it is necessary to incorporate previously developed FHWA vehicle models, distinguished as previously discussed by a *.key* suffix. Once downloaded, the *.key* file of the vehicle model can be introduced into a pre-existing barrier model using the *IMPORT* command under the *FILE* menu. Manipulation of these models for use in various crash simulations is described in the following sections. To achieve TL- 3 under NCHRP *Report 350* guidelines, a vehicle within 820 ± 25 kg must be used (1993). The coarse Geo Metro model mass is within that tolerance and should be used.

4.7.1 Spatial Location and Orientation of Imported Vehicle Model

Each previously developed vehicle model has a pre-defined spatial location and orientation, which may or may not be correct for the desired crash simulation. The vehicle model can be translated and rotated as desired using the *TRANSLATE* and *ROTATE* commands under the *TRANSFORM* and *NODE* menus. Alternatively, the barrier itself can be translated and rotated. Whether the vehicle or the barrier is moved depends on the user's preference for the axis along which force output information is desired.

4.7.2 Initial Conditions for Pre-defined Vehicle Models

Just as the vehicle models have pre-defined locations and orientations, they also have initial translational and rotational velocities, which the user can adjust using the *MODIFY* command after selecting a particular condition under the *B.C.* menu heading.

4.7.3 Contact Surfaces for Pre-defined Vehicle Models

To complete the importation of a pre-defined vehicle model, a contact surface must be defined between the barrier and the vehicle. Most vehicle models have a defined *PART SET* that includes all *PARTs* of the vehicle. Using an *AUTOMATIC_SURFACE_TO_SURFACE* contact definition, the user can select the barrier as the slave *PART* and the vehicle as the master *PART SET*. Though the barrier is actually the least stiff of the barrier and vehicle, it was chosen as the *SLAVE* because its deformation was to be studied.

4.8 OUTPUT CONSIDERATIONS FOR LS-DYNA IMPACT SIMULATIONS

To compare analytical results from LS-DYNA simulations with data from experimental pendulum tests, *RCFORC* and *NODOUT* should be selected for output. The *RCFORC* command gives output for forces at the contact interface between the front of the crush package and the rigid barrier. The *NODOUT* command gives acceleration histories. As described in Section 3.14, this information is requested at specific *NODEs*. For the pendulum model, the selected *NODE* was located at the point where the accelerometer was mounted on the laboratory pendulum.

CHAPTER 5

Design of Crush Package, Validation of Test Methods, and Significance of Results

5.1 PRELIMINARY DESIGN OF CRUSH PACKAGE FOR IMPACT PENDULUM

The crush package attached to the nose of an impact pendulum serves several purposes: it absorbs energy during the impact; it limits the maximum impact force to the prescribed level; and it controls the duration of the impact. It can also simulate the force-time or acceleration-time history of a vehicular impact on the barrier. The acceleration-time history for a typical full-scale vehicular impact test is shown in Figure 5.1 (Mitchell 2005). Key characteristics of this history are a maximum acceleration of about 28 g, corresponding to a force of 246 kN (55.4 kips), and an impact duration of about 0.1 sec. The selected correspondence between vehicle crash tests and the simulated crashes for this research is the impact impulse (area under the force-time curve). The impulse of the simulated tests should match that of a Geo Metro during a crash test, which satisfies TL-3 of NCHRP *Report 350*. The impulse for a Geo Metro vehicular crash test is about 6900 N-sec, and the crush package should be designed to match that impulse.

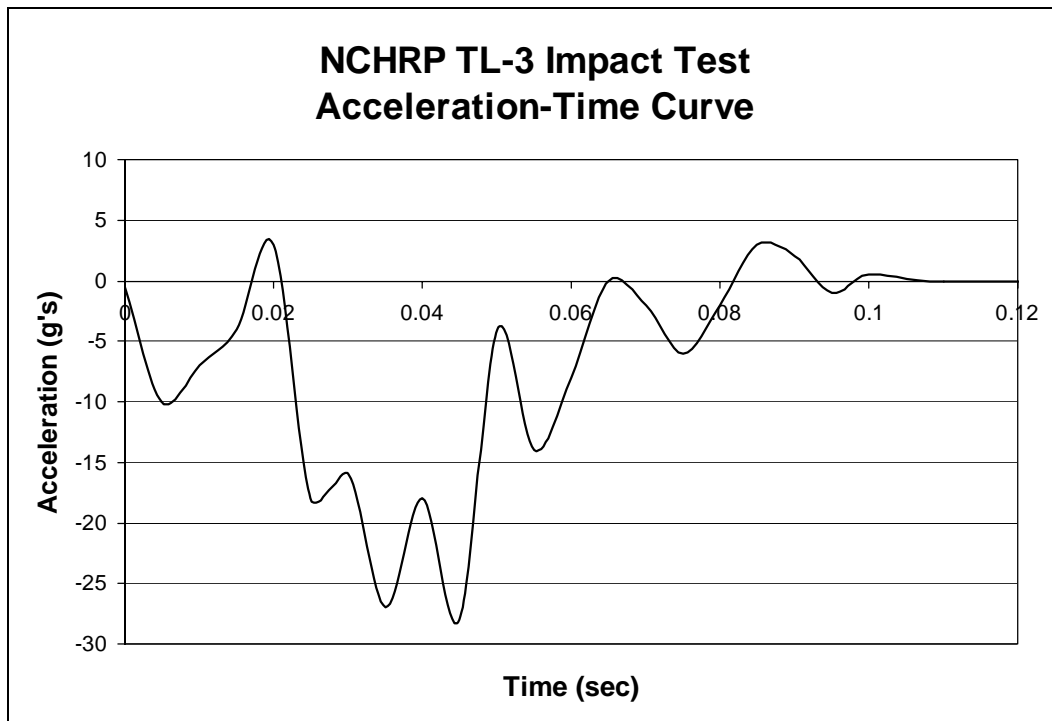


Figure 5.1 – Acceleration-time history for full-scale vehicular crash test of Geo Metro under TL-3 of NCHRP Report 350

5.1.1 Select Material for Crush Package

Two principal options were considered in selecting the material for the crush package: autoclaved aerated concrete (AAC) and tubular steel.

Preliminary tests of an AAC crush package were completed using a block of unreinforced AAC measuring 610-mm (24-in.) long and 200-mm (8-in.) square in cross-section, attached to the front of the pendulum and impacting a rigid barrier. Results showed that the AAC did not have enough strength and stiffness to slow down the pendulum sufficiently during impact or absorb enough energy. After preliminary static testing indicated its general suitability, tubular steel was selected for trial as a potential material for the crush package. It proved to be

appropriately strong, stiff and repeatable in behavior. The static test procedure used to verify these response characteristics is described below.

An initial arrangement of steel tubes was created using 152.4-mm (6-in.) sections of 25.4-mm (1-in.) tubes, placed in six layers (Figure 5.2), alternating the orientation of adjacent layers by 90 degrees. This orthotropic arrangement was selected to reduce the chance of extreme sidesway caused by simultaneous buckling of multiple adjacent layers in the same direction.

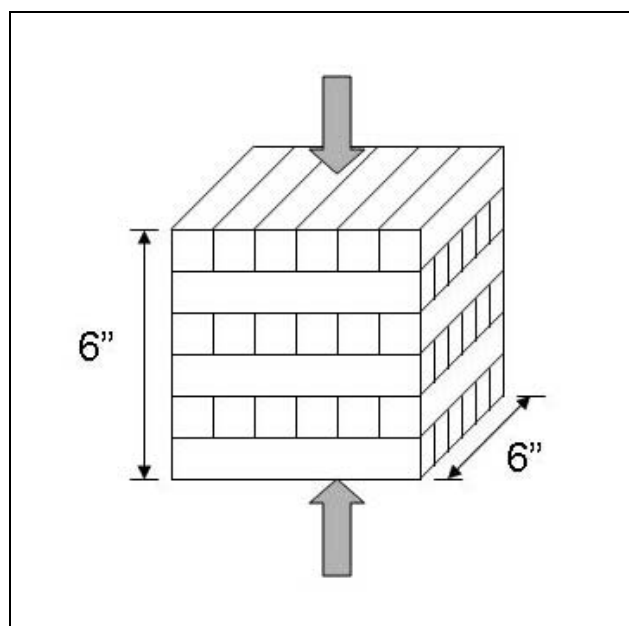


Figure 5.2 – Arrangement of steel tubes for static crush test

The steel tube walls had a thickness of 1.25 mm (0.049 in.). The resulting cubical arrangement of steel tubes was tested statically to determine its load-deformation characteristics (Figure 5.3). As each layer of tubes crushes, it creates a peak in the curve of between 165 and 222 kN (37 and 50 kips), and crushes to about 40

percent of its initial length. The resulting curve was used to design an appropriate crush package as explained in Section 5.1.2.

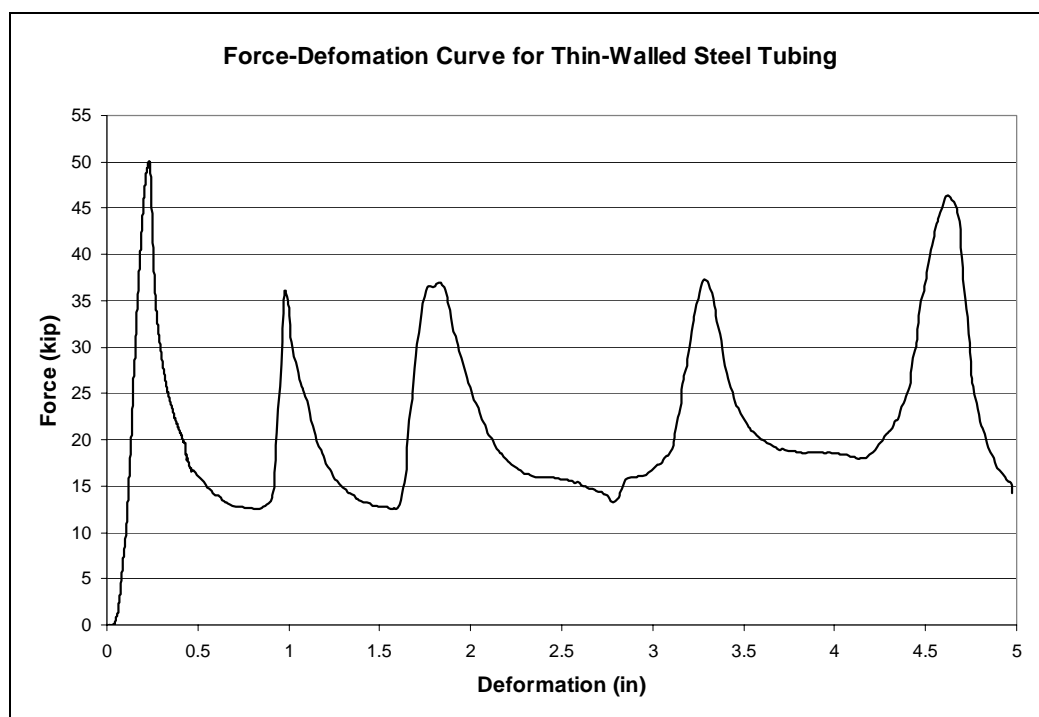


Figure 5.3 – Force-deformation curve obtained from static test of first arrangement of steel tubing

5.1.2 Establish Geometry of Crush Package

The peak load produced during static testing of a crush package with a 152.4-mm (6-in.) square cross-sectional area (222 kN, or 50 kips) was quite similar to the required peak force in an NCHRP 350 crash test to TL-3, indicating that this cross-sectional area of steel tubes would be a good starting point for

design of the crush package. Based upon the area under the force-deformation curve from the static test, and its relationship to the desired amount of energy to be absorbed, an overall length of 457.2 mm (18 in.), representing 18 layers of tubes, was selected for the preliminary design of the crush package for the laboratory impact pendulum. Shown in Figure 5.4 is the resulting geometry for that crush package, and the corresponding LS-DYNA model.

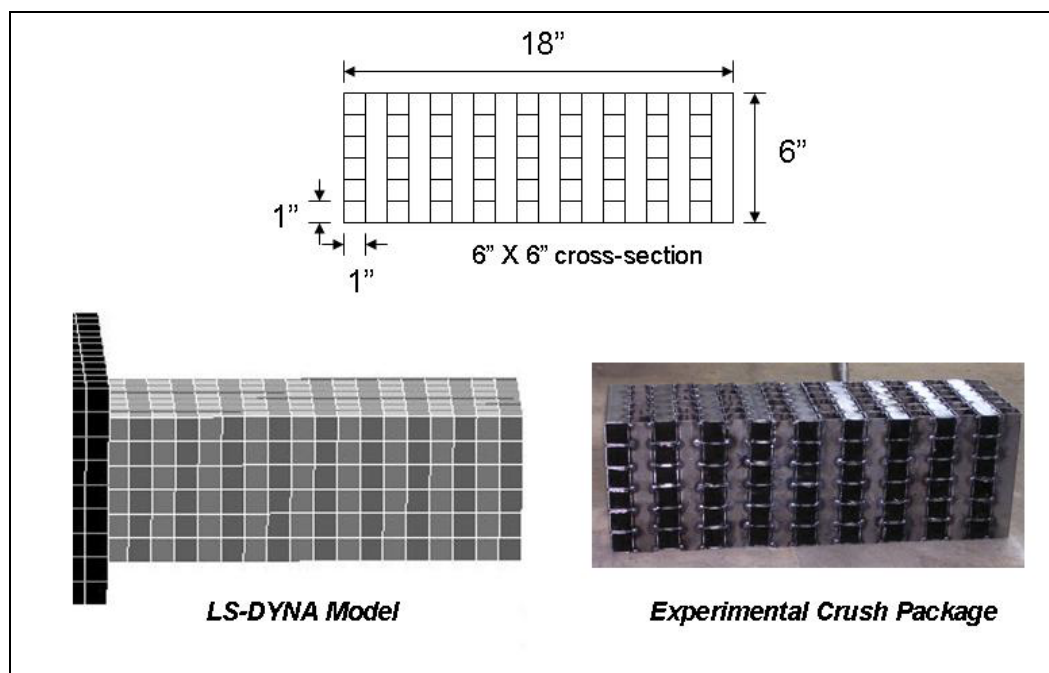


Figure 5.4 – Geometry of preliminary design for crush package for laboratory pendulum and corresponding DYNA model

5.2 TESTING AND SIMULATION OF PRELIMINARY DESIGN OF CRUSH PACKAGE

The preliminary design of the crush package was tested experimentally by pendulum tests against a rigid barrier, and was also simulated analytically using

LS-DYNA. The rigid barrier was used to ensure that the resulting acceleration-time curves would be due to the deformations of the crush package only, independent of the barrier. Results of the experimental tests are given in Section 5.2.1, and results of the analytical simulations, in Section 5.2.2. As described in Section 5.2.3, the crush package design was subsequently modified based on both types of verification.

5.2.1 Results of Experimental Verification using Pendulum Testing

The acceleration-time curve for the preliminary design of the crush package, tested using the laboratory pendulum, is shown in Figure 5.5. The peak acceleration was about 25 g, which, multiplied by the mass of the laboratory pendulum (855 kg), gave a peak force of 210 kN (47 kips). The duration of the impact was about 0.09 sec, and the resulting impulse was about 6600 N-sec. These initial test conditions (vehicle mass and velocity) are within the ranges of variables permitted by NCHRP *Report 350*, and the impulse is also close to that of the Geo Metro, indicating that TL-3 was achieved by that pendulum test.

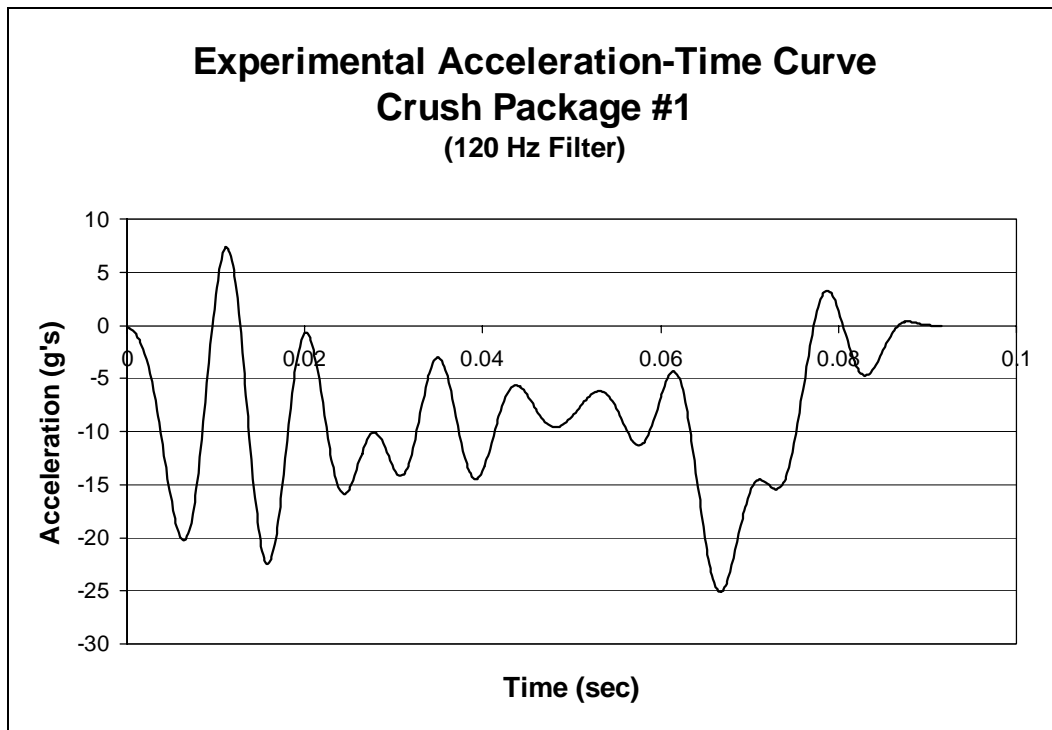


Figure 5.5 –Acceleration-time curve for preliminary design of crush package (pendulum testing)

5.2.2 Results from LS-DYNA Simulation using Preliminary Design of Crush Package

The acceleration-time curve for the preliminary design of the crush package in a LS-DYNA impact simulation is shown in Figure 5.6. The finite-element simulations are used to qualify the pendulum tests to a particular level by NCHRP *Report 350*, and also to verify the results of the experimental tests. Using the preliminary design for the crush package, the LS-DYNA simulation gives a peak force of 291 kN (65.5 kips) with a pendulum mass of 849 kg (836 kg simplified pendulum model and crush package) and an impact duration of about 0.05 sec. Although the duration is less than that of the experimental test, the

impulse is quite similar, about 7700 N-sec. This comparison is consistent with assertions made by the author and others (Chapter 2) that LS-DYNA can be used to corroborate the validity of results from experimental pendulum testing. In addition, the results of the simulations also show that they qualify by themselves at TL-3 of NCHRP *Report 350*.

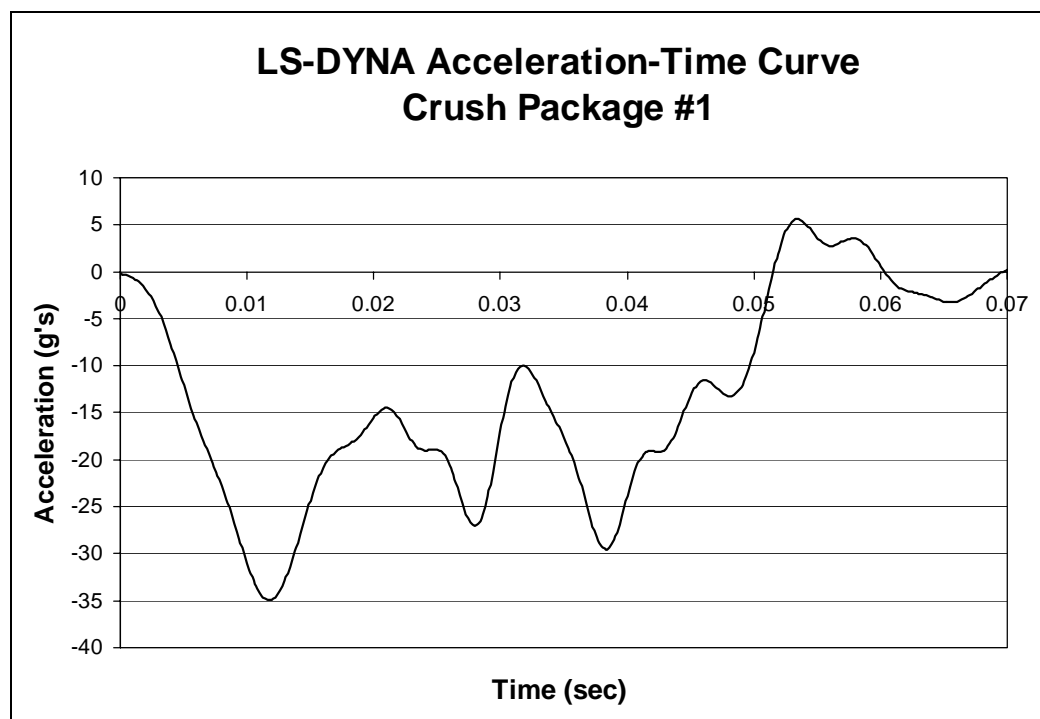


Figure 5.6 – Acceleration-time curve for preliminary design of crush package (LS-DYNA simulation)

5.2.3 Modifications to Preliminary Design of Crush Package

In Figure 5.7, the acceleration-time curves obtained from pendulum testing with the preliminary design of the crush package, and the corresponding curve for the LS-DYNA simulation, are compared with the acceleration-time curve obtained in a real crash test involving angled impact on a real barrier by a Geo Metro. In Figure 5.8 are compared the impulses from each test to TL-3 of NCHRP 350, for the laboratory pendulum with the preliminary design for the crush package, for a Geo Metro impacting a barrier at an angle, and for the LS-DYNA simulation of the laboratory pendulum with the preliminary design for the crush package. Figure 5.9 shows the corresponding peak forces. The impulses from the surrogate vehicles were respectively 3% and 13% different than that of the Geo Metro, and the maximum forces were different by 15% and 18% respectively. These agreements were considered acceptable. Both the pendulum and its LS-DYNA simulation, however, reached their maximum acceleration quite quickly, in contrast to the gradual ramp of the Geo Metro test. The preliminary design of the crush package was therefore modified to achieve a more gradual increase of acceleration to the peak value.

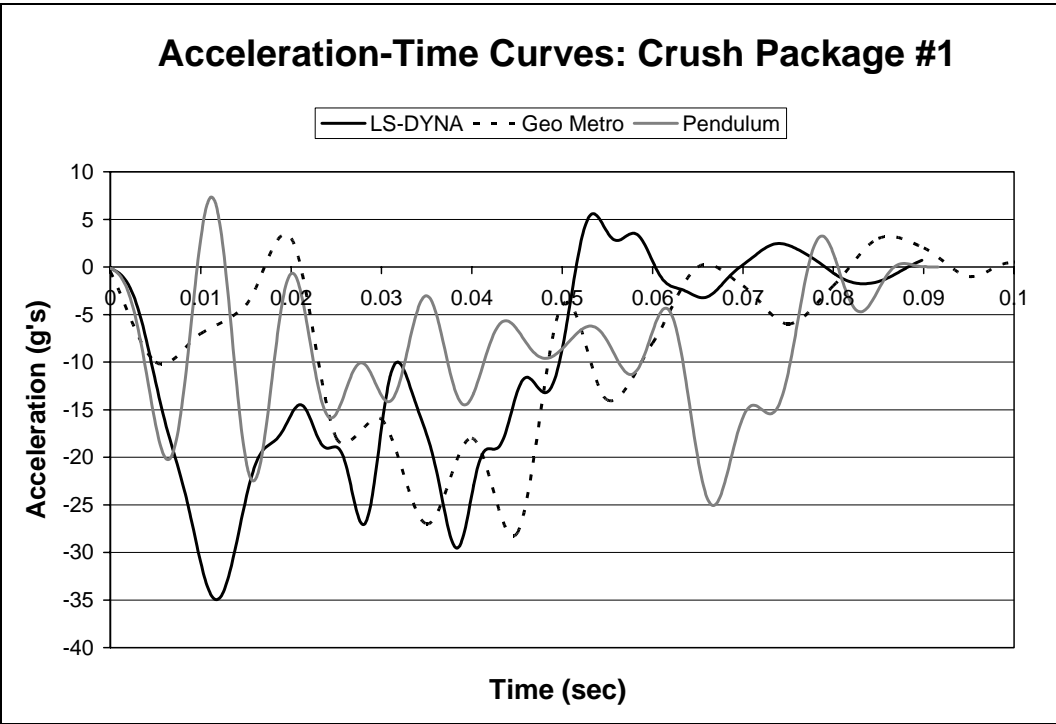


Figure 5.7 – Comparison of acceleration-time curves for preliminary design of crush package (LS-DYNA simulation of laboratory pendulum; Geo Metro test; and laboratory pendulum)

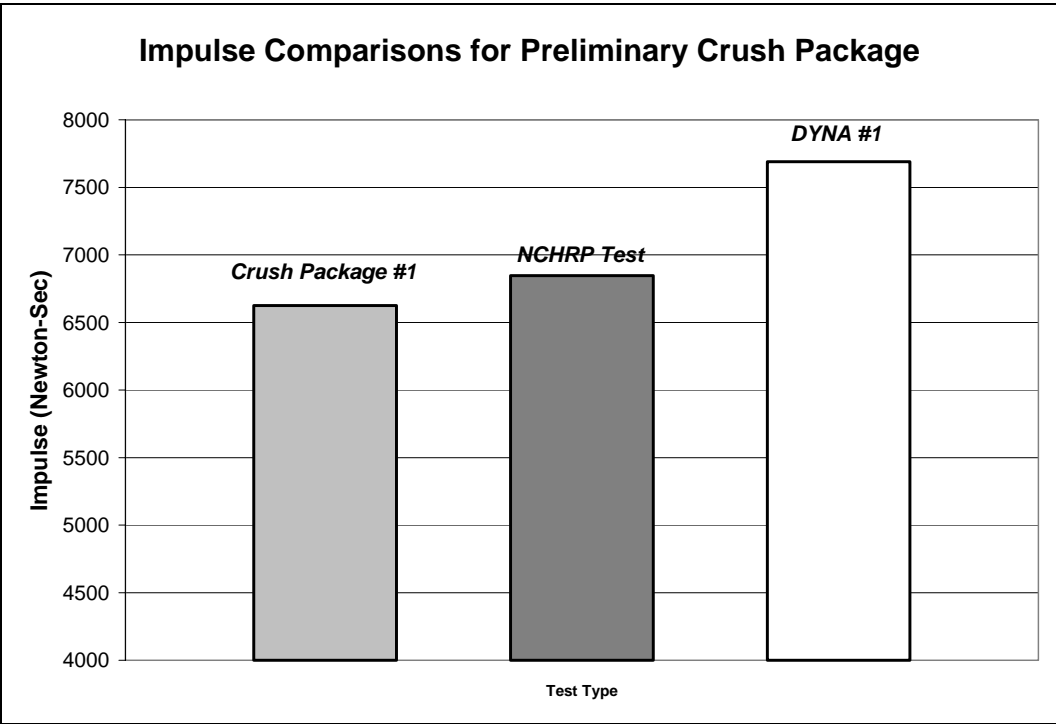


Figure 5.8 – Comparison of impulses for real and surrogate tests to NCHRP TL-3 (pendulum tests with preliminary crush package; Geo Metro test; and LS-DYNA simulation of pendulum test with preliminary crush package)

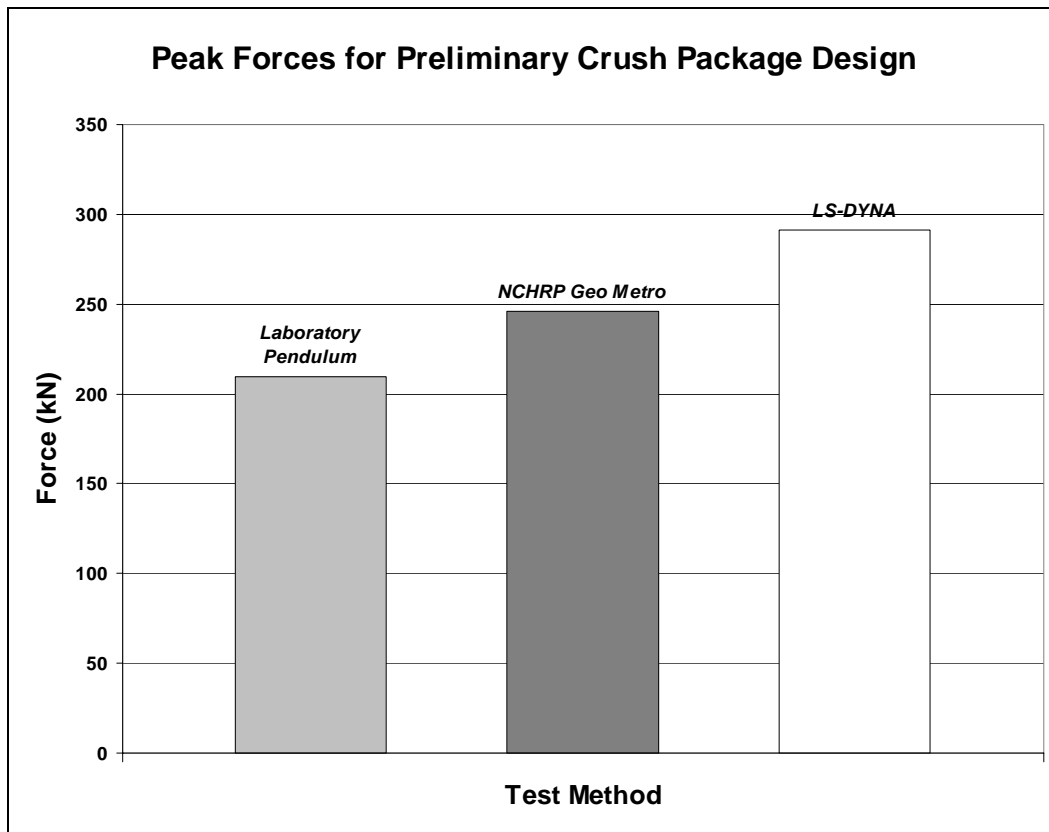


Figure 5.9 – Comparison of peak forces for real and surrogate tests to NCHRP TL-3 (pendulum tests with preliminary crush package; Geo Metro test; and LS-DYNA simulation of pendulum test with preliminary crush package)

5.3 MODIFIED DESIGN OF CRUSH PACKAGE FOR LABORATORY PENDULUM

Because the peak force at which the crush package begins to crush is directly proportional to the package’s cross-sectional area, the design of the crush package was modified so that its cross-sectional area would increase in steps from the front of the package to the point of attachment to the pendulum mass. Each successive layer of increasing cross-sectional area was intended to crush at a

higher force than the preceding layer, resulting in a force-time curve with an more gradual rise to the maximum force.

5.3.1 Geometry of Modified Crush Package

As shown in Figure 5.10, the overall length of the modified crush package was increased to 558.8 mm (22 in.). Because the smaller cross-sectional areas crush at lower forces and absorb less energy, it was anticipated that the increased length would maintain the proper duration of the impact time. The majority of the crush package length (twelve layers) was kept at the 152.4-mm (6-in.) square cross-section used previously for the preliminary design. Added were six layers that were 127 mm (5 in.) square in cross-section, and four layers that were 102 mm (4 in.) square in cross-section. To separate the different cross-sections and ensure that the impact surface would stay flat against the rigid barrier during the crushing process, 6.35-mm (0.25-in.) thick steel plates were inserted between layers of different cross-sections. These steel spacing plates were modeled in LS-DYNA using the same steel material and *PART* properties as the pendulum model.

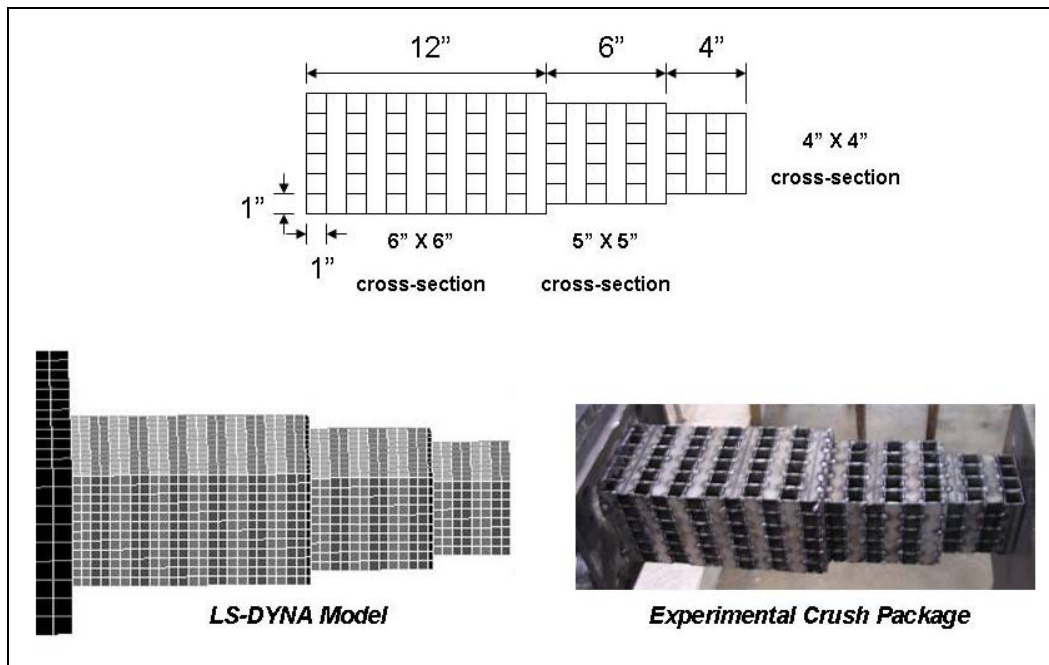


Figure 5.10 – Geometry of modified design for crush package, and corresponding LS-DYNA model

5.3.2 Experimental Results from Pendulum Testing with Modified Design of Crush Package

Figure 5.11 shows the acceleration-time curve for a laboratory pendulum test against a rigid barrier, using the modified design for the crush package. The peak acceleration was approximately 25 g, corresponding to a peak force of about 210 kN (47 kips), the same as with the preliminary design of the crush package. The duration of the impact was again about 0.09 sec. The increase in acceleration to peak did take longer with the modified design than the preliminary design. The resulting impulse, however, was now about 5600 N-sec, lower than before but still similar to that of the real Geo Metro test. The vehicle mass and initial

velocity were also within the tolerances specified by NCHRP *Report 350*. The initial conditions and similar impulse indicate that TL-3 was again achieved.

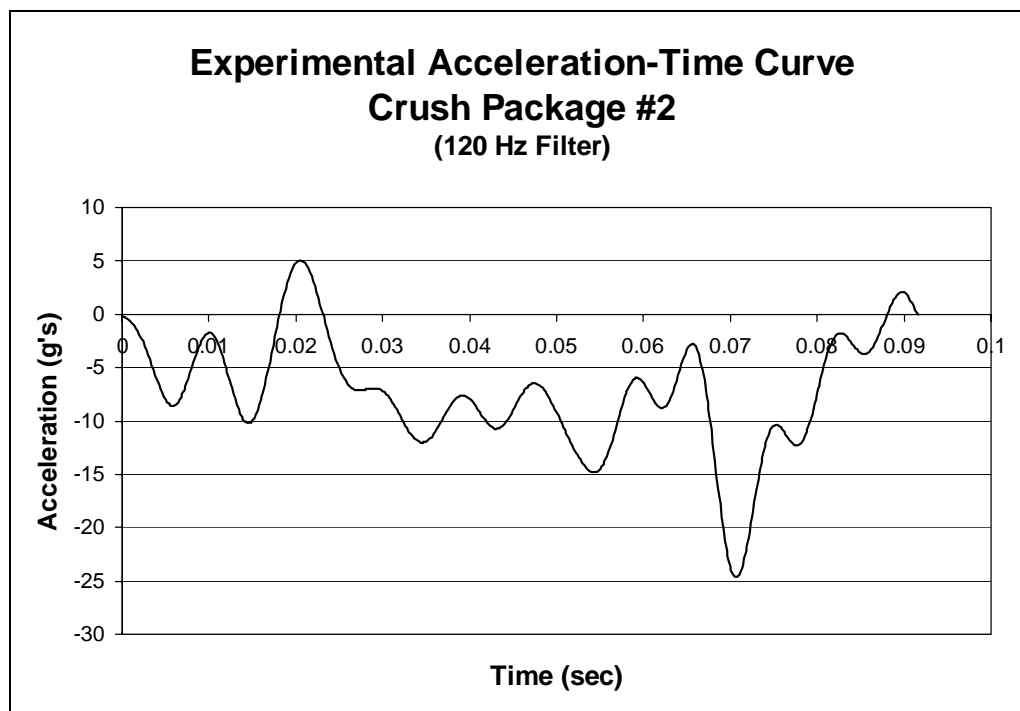


Figure 5.11 – Acceleration-time curve from laboratory pendulum testing (modified design of crush package)

5.3.3 Results of LS-DYNA Simulation of Pendulum Testing using Modified Design for Crush Package

In Figure 5.12 is shown the acceleration-time curve for the LS-DYNA simulation of the laboratory pendulum test using the modified design of the crush package. The LS-DYNA curve shows a peak acceleration of 35 g, which corresponds to a peak force of 292 kN (65.7 kips) with a pendulum mass of 851 kg and a duration of about 0.05 sec. Unlike the initial simulations using the

preliminary design of the crush package, the LS-DYNA simulations of laboratory pendulum testing with the modified crush package do exhibit a significant delay in reaching the peak acceleration value. Although the impact duration of the LS-DYNA simulations is somewhat less than that of the experimental pendulum tests, the impulse of 7200 N-sec and the experimental value of 5700 N-sec, are within tolerances of TL-3 of NCHRP *Report 350*.

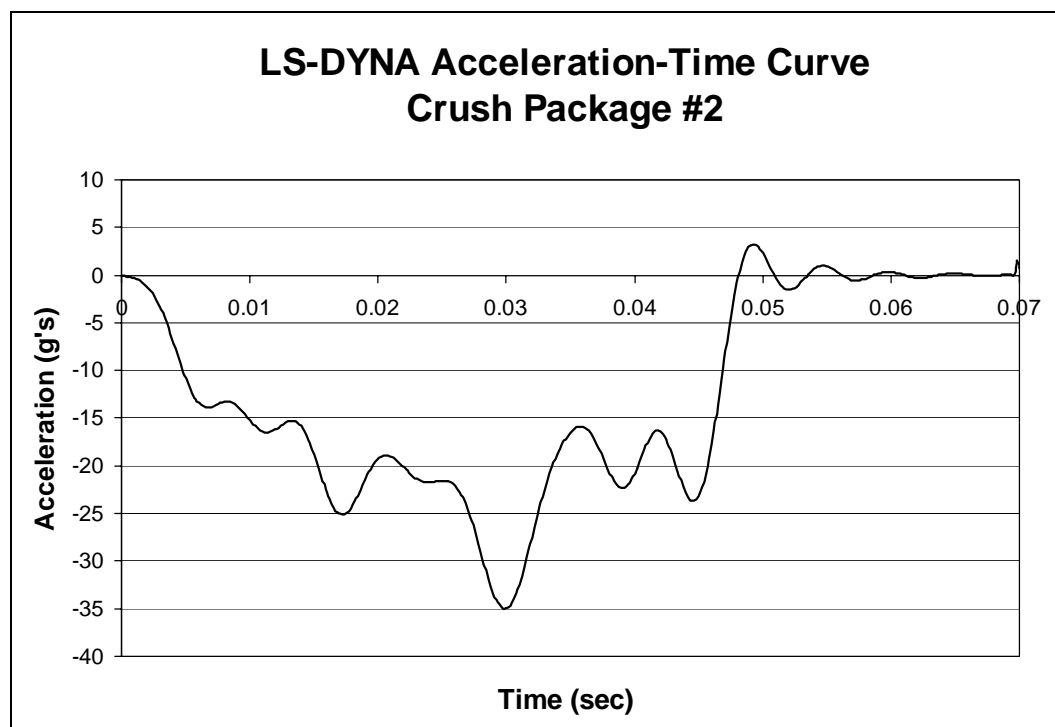


Figure 5.12 – Acceleration-time curve from LS-DYNA simulation of (laboratory test pendulum with modified design of crush package)

5.3.4 Recommendations for Refined Design of Pendulum Crush Package

In Figure 5.13, acceleration-time curves for laboratory pendulum testing with the modified crush package and for LS-DYNA simulation of that pendulum testing are compared with the curve for a real Geo Metro crash test. Although the impact durations differ slightly between the experimental pendulum test and its analytical simulation, the curves are again quite similar in shape to that of the real Geo Metro test. Also, as shown in Figure 5.14, the impulses for the pendulum test and its LS-DYNA simulation differ by only 18% and 6%, respectively, from the Geo Metro impulse, indicating that the modified design of the crush package meets the criteria for TL-3. Design of the crush package could be further refined, if desired, by changing the number of layers in each cross-section, and the cross-sectional areas of each layer to more closely match the vehicle crash curve. For stability under centrifugal accelerations, the length of the crush package should not exceed 610 mm (24 in.). To maintain the correct peak force, the cross-sectional dimensions should not exceed 152 mm (6 in.) on each side. Using several layers of gradually increasing cross-sectional area at the front of the crush package will extend the rise time of the force-time curve to its peak force; using more layers of the 152-mm (6-in.) square cross-section will maintain the desired impulse.

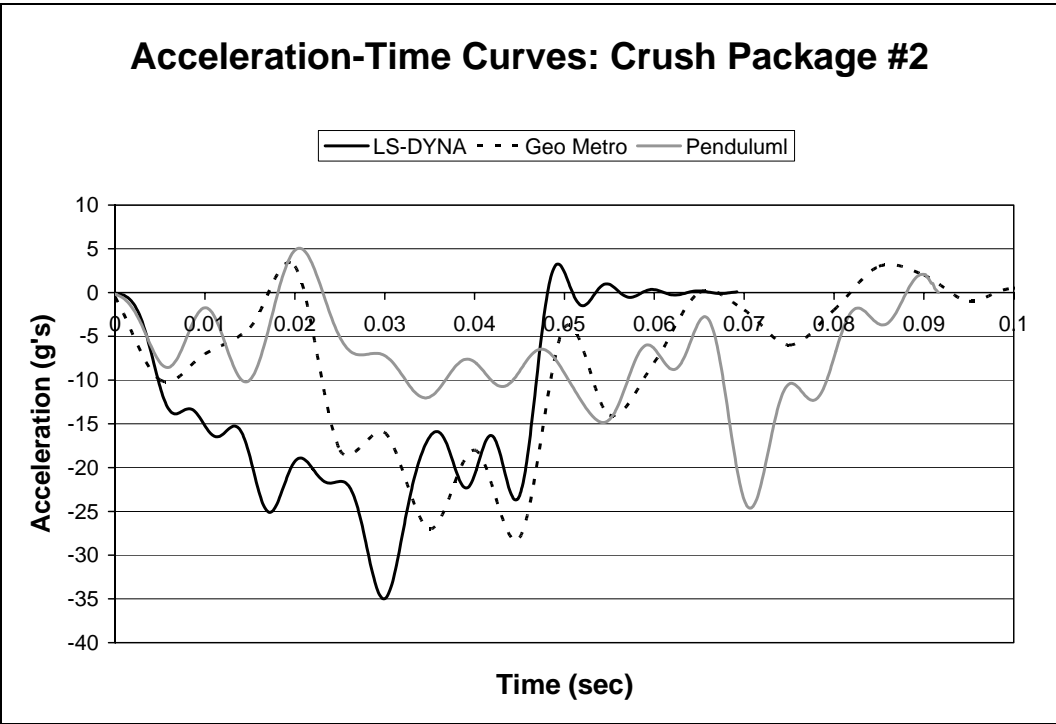


Figure 5.13 – Comparison of acceleration-time curves (laboratory pendulum testing with modified design of crush package; LS-DYNA simulation of that testing; and Geo Metro test)

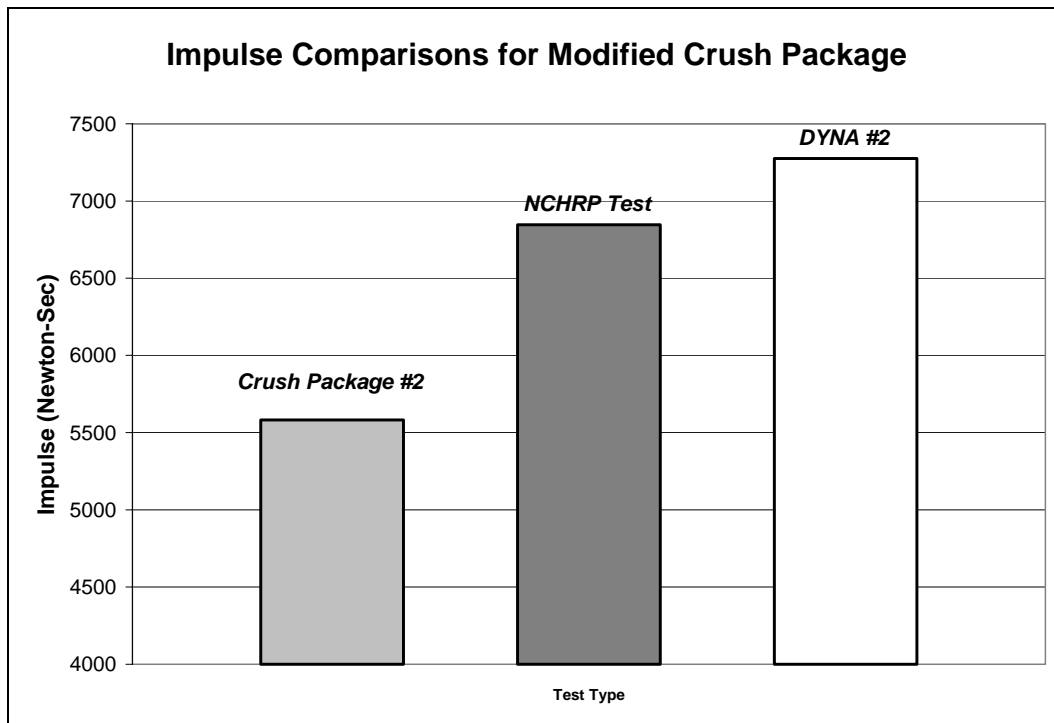


Figure 5.14 – Comparison of impulses (laboratory pendulum testing with modified design of crush package; Geo Metro test; and LS-DYNA simulation of pendulum test)

5.4 VALIDITY OF TESTING METHODS AND SIGNIFICANCE OF RESULTS

As shown in the preceding sections of this chapter, laboratory pendulum testing can be qualified under TL-3 of NCHRP *Report 350* by appropriately modifying the mass and drop height of the pendulum to deliver the correct amount of energy to the barrier, and by appropriately modifying the load-deformation properties of the crush package to match the impulse and acceleration-time history to those obtained from real impacts of vehicles against rigid barriers.

The impulse of the actual vehicle crash test is about 6800 N-sec, which is shown in the *NCHRP Test* column of Figure 5.15. Used with the laboratory pendulum, the preliminary design and the modified design for the crush package have impulses of about 6500 N-sec and 5500 N-sec respectively, as shown in the *Crush Package #1* and *Crush Package #2* columns of Figure 5.15. The impulses for the LS-DYNA simulations of pendulum tests with each crush package design are also shown in Figure 5.15, in the columns labeled *DYNA #1*, with a value of about 7600 N-sec, and *DYNA #2*, with a value of about of 7200 N-sec. Finally, the theoretical impulse of about 8000 N-sec for a TL-3 crash test, calculated using impulse-momentum theory, is shown in the *Theoretical* column of Figure 5.15 for purposes of comparison. The theoretical impulse was calculated using Eq. 5.1, where I is the impulse, m is the mass, and v_i and v_f are the initial and final velocities, respectively. The mass was assumed to be 850 kg and the final velocity was assumed to be zero.

$$I = F \cdot \Delta t = m \cdot v_i - m \cdot v_f \quad (5.1)$$

Although the impulses for each surrogate differ from that of the real test, each impulse qualifies the corresponding test as acceptable under NCHRP *Report 350*, because each impulse is similar to that of an actual vehicle crash test. Therefore, the testing plan developed for this research project, including the laboratory pendulum testing and LS-DYNA simulations of that testing, is acceptable for testing concrete barriers to TL-3 of NCHRP *Report 350*.

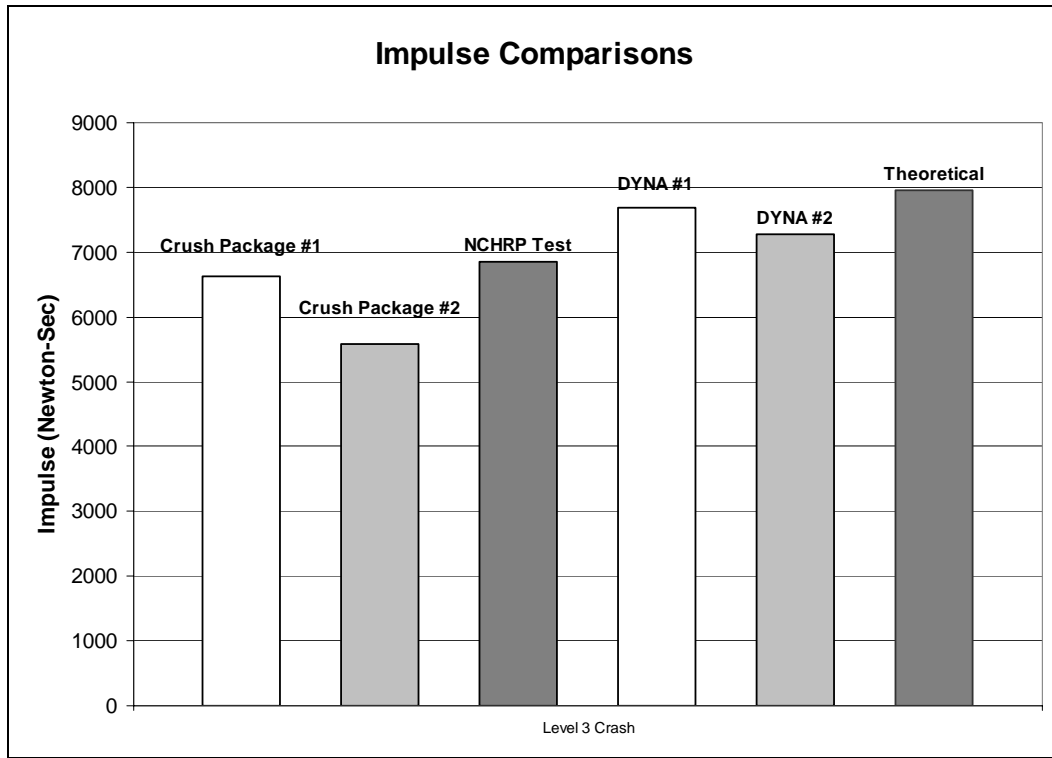


Figure 5.15 Comparison of impulses from different tests and simulations to TL- 3 of NCHRP 350

5.5 RECOMMENDED REFINEMENTS TO CURRENT LS-DYNA MODELS

Though basic LS-DYNA models have been developed for the cast-in-place barrier, for current designs of the retrofit barrier, and also for the laboratory pendulum and crush package, several aspects of the modeling either have not yet been considered, or should be evaluated further. These aspects include evaluation of different material models, evaluation of the discrete and continuous barrier boundary conditions, and development of a model for the bridge deck.

5.5.1 Evaluation of Material Models

The cast-in-place barrier model was developed based on the assumption that the concrete and reinforcing bar within the parapet itself behave compatibly. This assumption, in effect, resulted in a single material model with smeared properties. Once laboratory tests have been completed using the cast-in-place specimens, the results may indicate that the cast-in-place barrier may be better represented by distinct concrete and steel materials. In addition, even if the assumption of compatibility between concrete and steel is verified, distinct material models could be used for those materials to better represent actual observed behavior.

5.5.2 Evaluate Boundary Conditions for Barrier Segments and Infinitely Long Barriers

Previous sections of this thesis have treated barriers as though they were segments of finite length, like the laboratory test specimens. In reality, their length could be anywhere from that finite length to the infinite length of an ideal continuous barrier. To address the expected difference in behavior between those limiting cases, it is useful to idealize the effect of adjacent barrier segments on a particular barrier segment. To do so, the adjacent segments are idealized as translational springs attached to the ends of the barrier segment in question. Further testing should indicate useful ways to model the stiffnesses of adjacent barrier segments.

5.5.3 Develop Analytical Models for the Bridge Deck

Though the retrofit design for the concrete barrier is based primarily upon the behavior of the cast-in-place barrier itself, the behavior of the bridge deck also

affects overall barrier response. The current model for the bridge deck overhang is a rigid base. For use in the barrier models, a more realistic model for the bridge deck should be developed, incorporating a material model addressing deformation and also erosion of elements, to permit the LS-DYNA model to include flexural yielding of the deck, and concrete breakout around the anchors attaching the barrier to the slab.

5.6 RECOMMENDATIONS FOR OVERALL PROJECT PLAN

In addition to the recommendations for the analytical models, several other aspects of the project testing plan could be refined. These refinements are discussed below:

5.6.1 Finish Design of the Crush Package

As indicated previously, the modified design for the crush package (variable cross-section) is acceptable for TL-3 of NCHRP *Report 350*. If a more accurate acceleration-time profile with respect to the Geo Metro test is desired, however, lengths and cross-sectional areas of each tube layer could be refined further to more closely match crash duration, total impulse and maximum force compared with the results from the real Geo Metro test.

5.6.2 Test Cast-in-Place and Retrofit Barrier Designs

Once a final crush package is designed, cast-in-place and retrofit deformable barriers should be tested. Depending on the behavior exhibited by the cast-in-place barrier specimens, preliminary designs of the retrofit barriers may need to be refined further.

5.6.3 Modify Crash Characteristics using LS-DYNA Simulations

One advantage of finite element simulations is that they permit a wider variety of impact conditions than can realistically be tested using real vehicular impact. For instance, the retrofit barrier design that passes a TL-3 test may also be tested under other test levels using different finite element vehicle models. A wide range of crash characteristics can be hypothesized, including vehicle braking, and different velocities and impact angles. Other useful information, such as vehicle snagging and rollover, but can be provided by finite element simulations of those same crashes.

CHAPTER 6

Summary, Conclusions, and Recommendations

6.1 SUMMARY

This thesis is one of two addressing the first phase of TxDOT Study 4823. Its goal is to develop a retrofit design for existing cast-in-place vehicular impact barriers, based on testing according to NCHRP guidelines. In the first phase, a preliminary retrofit design is proposed, based on the current knowledge of anchorage to concrete. A testing procedure was developed for crash-testing discrete barrier sections using a laboratory pendulum with an attached crush package. The same barrier sections are also evaluated analytically under pendulum impact using LS-DYNA models developed for the purpose. Finally, the barriers are evaluated analytically using finite element models of actual vehicles.

6.2 CONCLUSIONS

Working in conjunction with the experimental tests and NCHRP guidelines, detailed finite element models have been developed for studying vehicular impact and designing retrofit barriers. These models address rigid barriers, cast-in-place barriers, and deformable retrofit barriers. Finite-element models for the laboratory pendulum and associated crush package have been developed for use in conjunction with the experimental pendulum tests. In addition, existing vehicle models from the FHWA Crash Analysis Center have been reasonably verified for use in vehicle crash simulations.

Those finite element models were then used to develop a coherent analytical framework for the remainder of Project 4823. Experimental tests using a real laboratory pendulum impacting a rigid barrier, and analytical verifications of those pendulum tests, show that the laboratory pendulum satisfies NCHRP standards based upon the area under the force-time curves of the impact tests and associated energy. Similar analytical evaluations with the previously developed vehicle models and a rigid barrier demonstrate that these vehicles reasonably satisfy NCHRP when used in crash simulations. Because the laboratory pendulum and analytical vehicle models satisfy NCHRP standards, the laboratory pendulum is an acceptable testing alternative to real vehicle crash tests. Finally, the similarities between the experimental and analytical tests of the crush packages tested thus far for the pendulum indicate that LS-DYNA offers useful guidance in designing the crush package.

6.3 RECOMMENDATIONS

The proposed testing procedure is valid, conforms to NCHRP *Report 350*, and should be implemented for crash tests of the preliminary retrofit barrier design. In addition, an acceptable crush package has been developed, and more advanced tests can be performed. The future goals of the research project, in terms of both analytical and experimental testing, are presented in the following sections.

6.3.1 Recommendations for Analytical Simulation

Several aspects of the analytical models should be considered in future research. The preliminary choice of material model for the cast-in-place and retrofit barriers should be confirmed using experimental test data. In addition, a

model for the bridge deck slab should be created, as the behavior of the bridge barrier is partially dependent on the behavior of the bridge deck under impact conditions. Finally, modeling of discrete versus continuous barriers should be explored further.

6.3.2 Recommendations for Future Testing for Project 4823

Before testing the cast-in-place and retrofit barrier designs, the crush package design should be further refined. Once a final design is selected, the response of the cast-in-place and the retrofit barriers to pendulum impact should be tested experimentally and simulated analytically. The retrofit design should be modified appropriately based on those test results. Finally, more advanced crash simulations can be created for the selected retrofit design to explore various initial impact conditions and vehicle responses such as snagging and rollover.

6.3.3 Recommendations for Future Implementation for Project 4823

After suitable retrofit bridge rail designs are developed as recommended above, they should be presented to TxDOT for implementation.

APPENDIX A

Example of a .dyn file

```

$-----1-----2-----3-----4-----5-----6-----7-----8
$ LS-DYNA(970) DECK WRITTEN BY : eta/FEMB-PC version 28.0
$ TEMPLATE #: 20040406
$ ENGINEER :
$ PROJECT :
$   UNITS : MM, TON, SEC, N
$   TIME  : 04:17:47 PM
$   DATE  : Saturday, April 30, 2005
$-----1-----2-----3-----4-----5-----6-----7-----8
*KEYWORD
$-----1-----2-----3-----4-----5-----6-----7-----8
*TITLE
LS-DYNA USER INPUT
$-----1-----2-----3-----4-----5-----6-----7-----8
$
$                               CONTROL CARD
$
$-----1-----2-----3-----4-----5-----6-----7-----8
*CONTROL_TERMINATION
$  ENDTIM  ENDCYC  DTMIN  ENDENG  ENDMAS
    0.15    0      0.0    0.0    0.0
*CONTROL_HOURLASS
$   IHQ    QH
    2     0.050
*CONTROL_OUTPUT
$  NPOPT  NEECHO  NREFUP  IACCP  OPIFS  IPNINT  IKEDIT  IFLUSH
    1     3      0      0      0.0    0      100     5000
$   IPRTF
    0
$-----1-----2-----3-----4-----5-----6-----7-----8
$
$                               DATABASE CONTROL FOR ASCII
$
$-----1-----2-----3-----4-----5-----6-----7-----8
*DATABASE_RCFORC
$   DT  BINARY
    0.000050  1

```

```

*DATABASE_NODOUT
$      DT      BI NARY
    0.00020      1
$-----1-----2-----3-----4-----5-----6-----7-----8
$
$                      DATABASE CONTROL FOR BI NARY
$
$-----1-----2-----3-----4-----5-----6-----7-----8
*DATABASE_BINARY_D3PLOT
$ DT/CYCL      LCDT      BEAM      NPLTC
    0.0010      0      0      0
$-----1-----2-----3-----4-----5-----6-----7-----8
$
$                      DATABASE HI STORY CARDS
$
$-----1-----2-----3-----4-----5-----6-----7-----8
*DATABASE_HI STORY_NODE
$^HI STORY_1
$      NI D1      NI D2      NI D3      NI D4      NI D5      NI D6      NI D7      NI D8
    103505
$-----1-----2-----3-----4-----5-----6-----7-----8
$
$                      PART CARDS
$
$-----1-----2-----3-----4-----5-----6-----7-----8
*PART
$HEADI NG
PendFrame
$      PI D      SECI D      MI D      EOSI D      HGI D      GRAV      ADPOPT      TMI D
    1      1      1      0      0      0      0      0
*PART
$HEADI NG
Ri gi dWal l
$      PI D      SECI D      MI D      EOSI D      HGI D      GRAV      ADPOPT      TMI D
    2      2      2      0      0      0      0      0
*PART
$HEADI NG
l ayer18
$      PI D      SECI D      MI D      EOSI D      HGI D      GRAV      ADPOPT      TMI D
    3      6      6      0      0      0      0      0
*PART
$HEADI NG
l ayer17
$      PI D      SECI D      MI D      EOSI D      HGI D      GRAV      ADPOPT      TMI D
    4      6      6      0      0      0      0      0

```

```

*PART
$HEADING
layer16
$      PID      SECID      MID      EOSID      HGID      GRAV      ADPOPT      TMID
          5          6          6          0          0          0          0          0

*PART
$HEADING
layer15
$      PID      SECID      MID      EOSID      HGID      GRAV      ADPOPT      TMID
          6          6          6          0          0          0          0          0

*PART
$HEADING
layer14
$      PID      SECID      MID      EOSID      HGID      GRAV      ADPOPT      TMID
          7          6          6          0          0          0          0          0

*PART
$HEADING
layer13
$      PID      SECID      MID      EOSID      HGID      GRAV      ADPOPT      TMID
          8          6          6          0          0          0          0          0

*PART
$HEADING
layer12
$      PID      SECID      MID      EOSID      HGID      GRAV      ADPOPT      TMID
          9          6          6          0          0          0          0          0

*PART
$HEADING
layer11
$      PID      SECID      MID      EOSID      HGID      GRAV      ADPOPT      TMID
         10          6          6          0          0          0          0          0

*PART
$HEADING
layer10
$      PID      SECID      MID      EOSID      HGID      GRAV      ADPOPT      TMID
         11          6          6          0          0          0          0          0

*PART
$HEADING
layer9
$      PID      SECID      MID      EOSID      HGID      GRAV      ADPOPT      TMID
         12          6          6          0          0          0          0          0

*PART
$HEADING
layer8
$      PID      SECID      MID      EOSID      HGID      GRAV      ADPOPT      TMID
         13          6          6          0          0          0          0          0

```

```

*PART
$HEADING
layer7
$      PID      SECID      MID      EOSID      HGID      GRAV      ADPOPT      TMID
      14         6         6         0         0         0         0         0

*PART
$HEADING
layer6
$      PID      SECID      MID      EOSID      HGID      GRAV      ADPOPT      TMID
      15         6         6         0         0         0         0         0

*PART
$HEADING
layer5
$      PID      SECID      MID      EOSID      HGID      GRAV      ADPOPT      TMID
      16         6         6         0         0         0         0         0

*PART
$HEADING
layer4
$      PID      SECID      MID      EOSID      HGID      GRAV      ADPOPT      TMID
      17         6         6         0         0         0         0         0

*PART
$HEADING
layer3
$      PID      SECID      MID      EOSID      HGID      GRAV      ADPOPT      TMID
      18         6         6         0         0         0         0         0

*PART
$HEADING
layer2
$      PID      SECID      MID      EOSID      HGID      GRAV      ADPOPT      TMID
      19         6         6         0         0         0         0         0

*PART
$HEADING
layer1
$      PID      SECID      MID      EOSID      HGID      GRAV      ADPOPT      TMID
      20         6         6         0         0         0         0         0

*PART
$HEADING
layer19
$      PID      SECID      MID      EOSID      HGID      GRAV      ADPOPT      TMID
      21         6         6         0         0         0         0         0

*PART
$HEADING
layer20
$      PID      SECID      MID      EOSID      HGID      GRAV      ADPOPT      TMID
      22         6         6         0         0         0         0         0

```

```

*PART
$HEADING
layer23
$      PID      SECID      MID      EOSID      HGID      GRAV      ADPOPT      TMID
          25          6          6          0          0          0          0          0

*PART
$HEADING
layer24
$      PID      SECID      MID      EOSID      HGID      GRAV      ADPOPT      TMID
          26          6          6          0          0          0          0          0

*PART
$HEADING
rigidplates
$      PID      SECID      MID      EOSID      HGID      GRAV      ADPOPT      TMID
          27          1          1          0          0          0          0          0
$-----1-----2-----3-----4-----5-----6-----7-----8
$
$                               SECTION CARDS                               $
$
$-----1-----2-----3-----4-----5-----6-----7-----8
*SECTION_SOLID
$^P-1
$      SECID      ELFORM      AET
          1          1          0

*SECTION_SOLID
$^P-2
$      SECID      ELFORM      AET
          2          1          0

*SECTION_SOLID
$^P-6
$      SECID      ELFORM      AET
          6          1          0
$-----1-----2-----3-----4-----5-----6-----7-----8
$
$                               MATERIAL CARDS                               $
$
$-----1-----2-----3-----4-----5-----6-----7-----8
*MAT_ISOTROPIC_ELASTIC_PLASTIC
$^STEEL
$      MID      RO      G      SIGY      ETAN      BULK
          17.9278E-09      79903.0      413.69      2757.9      166620.0

```

```

*MAT_RIGID
$^RIGID
$      MID      RO      E      PR      N      COUPLE      M      ALIAS
      22.3114E-07 24855.6 0.15 0.0 0.0 0.0
$      CMO      CON1     CON2
      0.0
$LCO_OR_A1      A2      A3      V1      V2      V3
      0.0 0.0 0.0 0.0 0.0 0.0
*MAT_HONEYCOMB
$^6X6
$      MID      RO      E      PR      SIGY      VF      MU      BULK
      61.1654E-09 199950.0 0.30 413.69 0.38 0.050 0.0
$      LCA      LCB      LCC      LCS      LCAB      LCBC      LCCA      LCSR
      4.0 4.0 4.0 4.0
$      EAAU      EBBU      ECCU      GABU      GBCU      GCAU      AOPT
      62.58 62.58 62.58 22.1 46.423 22.1
$      XP      YP      ZP      A1      A2      A3
$      D1      D2      D3      TSEF      SSEF

*MAT_HONEYCOMB
$^3X3
$      MID      RO      E      PR      SIGY      VF      MU      BULK
      71.1654E-09 199948.0 0.30 413.69 0.38 0.050 0.0
$      LCA      LCB      LCC      LCS      LCAB      LCBC      LCCA      LCSR
      5.0 5.0 5.0 5.0
$      EAAU      EBBU      ECCU      GABU      GBCU      GCAU      AOPT
      62.58 62.58 62.58 22.1 46.423 22.1
$      XP      YP      ZP      A1      A2      A3
$      D1      D2      D3      TSEF      SSEF

*MAT_HONEYCOMB
$^4X4
$      MID      RO      E      PR      SIGY      VF      MU      BULK
      81.1654E-09 199948.0 0.30 413.69 0.38 0.050 0.0
$      LCA      LCB      LCC      LCS      LCAB      LCBC      LCCA      LCSR
      6.0 6.0 6.0 6.0
$      EAAU      EBBU      ECCU      GABU      GBCU      GCAU      AOPT
      62.58 62.58 62.58 22.1 46.423 22.1
$      XP      YP      ZP      A1      A2      A3
$      D1      D2      D3      TSEF      SSEF

```


*MAT_HONEYCOMB

\$^5X5

\$	MI D	RO	E	PR	SIGY	VF	MU	BULK
	91.1654E-09	199948.0	0.30	413.69	0.38	0.050	0.0	
\$	LCA	LCB	LCC	LCS	LCAB	LCBC	LCCA	LCSR
	7.0	7.0	7.0	7.0				
\$	EAAU	EBBU	ECCU	GABU	GBCU	GCAU	AOPT	
	62.58	62.58	62.58	22.1	46.423	22.1		
\$	XP	YP	ZP	A1	A2	A3		
\$	D1	D2	D3	TSEF	SSEF			

*MAT_RIGID

\$^M-10

\$	MI D	RO	E	PR	N	COUPLE	M	ALIAS
	107.9728E-09	199950.0	0.30	0.0	0.0	0.0	0.0	
\$	CMO	CON1	CON2					
	0.0							
\$LCO_OR_A1	A2	A3	V1	V2	V3			
	0.0	0.0	0.0	0.0	0.0			

\$-----1-----2-----3-----4-----5-----6-----7-----8

\$

\$

DAMPING CARDS

\$

\$

\$-----1-----2-----3-----4-----5-----6-----7-----8

*DAMPING_GLOBAL

\$^DAMP_1

\$	LCID	VALDMP	STX	STY	STZ	SRX	SRY	SRZ
	0	3.0	0.0	0.0	0.0	0.0	0.0	0.0

\$-----1-----2-----3-----4-----5-----6-----7-----8

\$

\$

BOUNDARY SPC CARDS

\$

\$

\$-----1-----2-----3-----4-----5-----6-----7-----8

*BOUNDARY_SPC_NODE_ID

\$	ID							
	1							
\$	NI D	CID	DOFX	DOFY	DOFZ	DOFRX	DOFRY	DOFRZ
	100714	0	1	1	1	1	1	1
	2							
	100715	0	1	1	1	1	1	1
	3							

CONTINUED FOR ALL NODES IN RIGID BARRIER

```

$-----1-----2-----3-----4-----5-----6-----7-----8
$
$                               I N I T I A L  V E L O C I T Y  C A R D S
$
$
$-----1-----2-----3-----4-----5-----6-----7-----8

```

*I N I T I A L _ V E L O C I T Y _ N O D E

\$	NI D	VX	VY	VZ	VXR	VYR	VZR
	102836	9500.0	0.0	0.0	0.0	0.0	0.0
	102837	9500.0	0.0	0.0	0.0	0.0	0.0
	102838	9500.0	0.0	0.0	0.0	0.0	0.0
	102839	9500.0	0.0	0.0	0.0	0.0	0.0
	102840	9500.0	0.0	0.0	0.0	0.0	0.0
	102841	9500.0	0.0	0.0	0.0	0.0	0.0
	102842	9500.0	0.0	0.0	0.0	0.0	0.0
	102843	9500.0	0.0	0.0	0.0	0.0	0.0
	102844	9500.0	0.0	0.0	0.0	0.0	0.0

CONTINUED FOR ALL NODES IN PENDULUM

```

$-----1-----2-----3-----4-----5-----6-----7-----8
$
$                               C O N T A C T  C A R D S
$
$
$-----1-----2-----3-----4-----5-----6-----7-----8

```

*C O N T A C T _ A U T O M A T I C _ S U R F A C E _ T O _ S U R F A C E

\$^CONTACT1

\$	SSI D	MSI D	SSTYP	MSTYP	SBOXI D	MBOXI D	SPR	MPR
	26	2	3	3			0	0
\$	FS	FD	DC	VC	VDC	PENCHK	BT	DT
	0.20	0.10	0.0	0.0	0.0	0	0.01.0000E+20	
\$	SFS	SFM	SST	MST	SFST	SFMT	FSF	VSF
	1.0	1.0	0.0	0.0	1.0	1.0	1.0	1.0

*C O N T A C T _ A U T O M A T I C _ S U R F A C E _ T O _ S U R F A C E

\$^CONTACT2

\$	SSI D	MSI D	SSTYP	MSTYP	SBOXI D	MBOXI D	SPR	MPR
	25	26	3	3			0	0
\$	FS	FD	DC	VC	VDC	PENCHK	BT	DT
	0.0	0.0	0.0	0.0	0.0	0	0.01.0000E+20	
\$	SFS	SFM	SST	MST	SFST	SFMT	FSF	VSF
	1.0	1.0	0.0	0.0	1.0	1.0	1.0	1.0

```

*CONTACT_AUTOMATI C_SURFACE_TO_SURFACE
$^CONTACT5
$   SSI D      MSI D      SSTYP      MSTYP      SBOX I D      MBOX I D      SPR      MPR
      22        25         3         3
$   FS         FD         DC         VC         VDC         PENCHK         BT         DT
      0.0       0.0       0.0       0.0       0.0         0         0.01.0000E+20
$   SFS        SFM        SST        MST        SFST        SFMT         FSF        VSF
      1.0       1.0       0.0       0.0       1.0         1.0       1.0         1.0

*CONTACT_AUTOMATI C_SURFACE_TO_SURFACE
$^CONTACT6
$   SSI D      MSI D      SSTYP      MSTYP      SBOX I D      MBOX I D      SPR      MPR
      21        22         3         3
$   FS         FD         DC         VC         VDC         PENCHK         BT         DT
      0.0       0.0       0.0       0.0       0.0         0         0.01.0000E+20
$   SFS        SFM        SST        MST        SFST        SFMT         FSF        VSF
      1.0       1.0       0.0       0.0       1.0         1.0       1.0         1.0

*CONTACT_AUTOMATI C_SURFACE_TO_SURFACE
$^CONTACT7
$   SSI D      MSI D      SSTYP      MSTYP      SBOX I D      MBOX I D      SPR      MPR
      3         27         3         3
$   FS         FD         DC         VC         VDC         PENCHK         BT         DT
      0.0       0.0       0.0       0.0       0.0         0         0.01.0000E+20
$   SFS        SFM        SST        MST        SFST        SFMT         FSF        VSF
      1.0       1.0       0.0       0.0       1.0         1.0       1.0         1.0

*CONTACT_AUTOMATI C_SURFACE_TO_SURFACE
$^CONTACT8
$   SSI D      MSI D      SSTYP      MSTYP      SBOX I D      MBOX I D      SPR      MPR
      4         3         3         3
$   FS         FD         DC         VC         VDC         PENCHK         BT         DT
      0.0       0.0       0.0       0.0       0.0         0         0.01.0000E+20
$   SFS        SFM        SST        MST        SFST        SFMT         FSF        VSF
      1.0       1.0       0.0       0.0       1.0         1.0       1.0         1.0

*CONTACT_AUTOMATI C_SURFACE_TO_SURFACE
$^CONTACT9
$   SSI D      MSI D      SSTYP      MSTYP      SBOX I D      MBOX I D      SPR      MPR
      5         4         3         3
$   FS         FD         DC         VC         VDC         PENCHK         BT         DT
      0.0       0.0       0.0       0.0       0.0         0         0.01.0000E+20
$   SFS        SFM        SST        MST        SFST        SFMT         FSF        VSF
      1.0       1.0       0.0       0.0       1.0         1.0       1.0         1.0

```

```

*CONTACT_AUTOMATI C_SURFACE_TO_SURFACE
$^CONTACT10
$   SSI D      MSI D      SSTYP      MSTYP      SBOX I D      MBOX I D      SPR      MPR
      6         5         3         3
$   FS         FD         DC         VC         VDC         PENCHK         BT         DT
      0.0       0.0       0.0       0.0       0.0         0         0.01.0000E+20
$   SFS        SFM        SST        MST        SFST        SFMT         FSF        VSF
      1.0       1.0       0.0       0.0       1.0         1.0       1.0         1.0

*CONTACT_AUTOMATI C_SURFACE_TO_SURFACE
$^CONTACT11
$   SSI D      MSI D      SSTYP      MSTYP      SBOX I D      MBOX I D      SPR      MPR
      7         6         3         3
$   FS         FD         DC         VC         VDC         PENCHK         BT         DT
      0.0       0.0       0.0       0.0       0.0         0         0.01.0000E+20
$   SFS        SFM        SST        MST        SFST        SFMT         FSF        VSF
      1.0       1.0       0.0       0.0       1.0         1.0       1.0         1.0

*CONTACT_AUTOMATI C_SURFACE_TO_SURFACE
$^CONTACT12
$   SSI D      MSI D      SSTYP      MSTYP      SBOX I D      MBOX I D      SPR      MPR
      8         7         3         3
$   FS         FD         DC         VC         VDC         PENCHK         BT         DT
      0.0       0.0       0.0       0.0       0.0         0         0.01.0000E+20
$   SFS        SFM        SST        MST        SFST        SFMT         FSF        VSF
      1.0       1.0       0.0       0.0       1.0         1.0       1.0         1.0

*CONTACT_AUTOMATI C_SURFACE_TO_SURFACE
$^CONTACT13
$   SSI D      MSI D      SSTYP      MSTYP      SBOX I D      MBOX I D      SPR      MPR
      9         27        3         3
$   FS         FD         DC         VC         VDC         PENCHK         BT         DT
      0.0       0.0       0.0       0.0       0.0         0         0.01.0000E+20
$   SFS        SFM        SST        MST        SFST        SFMT         FSF        VSF
      1.0       1.0       0.0       0.0       1.0         1.0       1.0         1.0

*CONTACT_AUTOMATI C_SURFACE_TO_SURFACE
$^CONTACT14
$   SSI D      MSI D      SSTYP      MSTYP      SBOX I D      MBOX I D      SPR      MPR
     10         9         3         3
$   FS         FD         DC         VC         VDC         PENCHK         BT         DT
      0.0       0.0       0.0       0.0       0.0         0         0.01.0000E+20
$   SFS        SFM        SST        MST        SFST        SFMT         FSF        VSF
      1.0       1.0       0.0       0.0       1.0         1.0       1.0         1.0

```

```

*CONTACT_AUTOMATI C_SURFACE_TO_SURFACE
$^CONTACT15
$   SSI D      MSI D      SSTYP      MSTYP      SBOX I D      MBOX I D      SPR      MPR
      11        10         3         3
$   FS         FD         DC         VC         VDC         PENCHK         BT         DT
      0.0       0.0       0.0       0.0       0.0         0         0.01.0000E+20
$   SFS        SFM        SST        MST        SFST        SFMT         FSF        VSF
      1.0       1.0       0.0       0.0       1.0         1.0       1.0         1.0

*CONTACT_AUTOMATI C_SURFACE_TO_SURFACE
$^CONTACT16
$   SSI D      MSI D      SSTYP      MSTYP      SBOX I D      MBOX I D      SPR      MPR
      12        11         3         3
$   FS         FD         DC         VC         VDC         PENCHK         BT         DT
      0.0       0.0       0.0       0.0       0.0         0         0.01.0000E+20
$   SFS        SFM        SST        MST        SFST        SFMT         FSF        VSF
      1.0       1.0       0.0       0.0       1.0         1.0       1.0         1.0

*CONTACT_AUTOMATI C_SURFACE_TO_SURFACE
$^CONTACT17
$   SSI D      MSI D      SSTYP      MSTYP      SBOX I D      MBOX I D      SPR      MPR
      13        12         3         3
$   FS         FD         DC         VC         VDC         PENCHK         BT         DT
      0.0       0.0       0.0       0.0       0.0         0         0.01.0000E+20
$   SFS        SFM        SST        MST        SFST        SFMT         FSF        VSF
      1.0       1.0       0.0       0.0       1.0         1.0       1.0         1.0

*CONTACT_AUTOMATI C_SURFACE_TO_SURFACE
$^CONTACT18
$   SSI D      MSI D      SSTYP      MSTYP      SBOX I D      MBOX I D      SPR      MPR
      14        13         3         3
$   FS         FD         DC         VC         VDC         PENCHK         BT         DT
      0.0       0.0       0.0       0.0       0.0         0         0.01.0000E+20
$   SFS        SFM        SST        MST        SFST        SFMT         FSF        VSF
      1.0       1.0       0.0       0.0       1.0         1.0       1.0         1.0

*CONTACT_AUTOMATI C_SURFACE_TO_SURFACE
$^CONTACT19
$   SSI D      MSI D      SSTYP      MSTYP      SBOX I D      MBOX I D      SPR      MPR
      15        14         3         3
$   FS         FD         DC         VC         VDC         PENCHK         BT         DT
      0.0       0.0       0.0       0.0       0.0         0         0.01.0000E+20
$   SFS        SFM        SST        MST        SFST        SFMT         FSF        VSF
      1.0       1.0       0.0       0.0       1.0         1.0       1.0         1.0

```

```

*CONTACT_AUTOMATI C_SURFACE_TO_SURFACE
$^CONTACT20
$   SSI D      MSI D      SSTYP      MSTYP      SBOX I D      MBOX I D      SPR      MPR
      16        15         3         3
$   FS         FD         DC         VC         VDC         PENCHK         BT         DT
      0.0       0.0       0.0       0.0       0.0         0         0.01.0000E+20
$   SFS        SFM        SST        MST        SFST        SFMT         FSF        VSF
      1.0       1.0       0.0       0.0       1.0         1.0       1.0         1.0

*CONTACT_AUTOMATI C_SURFACE_TO_SURFACE
$^CONTACT21
$   SSI D      MSI D      SSTYP      MSTYP      SBOX I D      MBOX I D      SPR      MPR
      17        16         3         3
$   FS         FD         DC         VC         VDC         PENCHK         BT         DT
      0.0       0.0       0.0       0.0       0.0         0         0.01.0000E+20
$   SFS        SFM        SST        MST        SFST        SFMT         FSF        VSF
      1.0       1.0       0.0       0.0       1.0         1.0       1.0         1.0

*CONTACT_AUTOMATI C_SURFACE_TO_SURFACE
$^CONTACT22
$   SSI D      MSI D      SSTYP      MSTYP      SBOX I D      MBOX I D      SPR      MPR
      18        17         3         3
$   FS         FD         DC         VC         VDC         PENCHK         BT         DT
      0.0       0.0       0.0       0.0       0.0         0         0.01.0000E+20
$   SFS        SFM        SST        MST        SFST        SFMT         FSF        VSF
      1.0       1.0       0.0       0.0       1.0         1.0       1.0         1.0

*CONTACT_AUTOMATI C_SURFACE_TO_SURFACE
$^CONTACT23
$   SSI D      MSI D      SSTYP      MSTYP      SBOX I D      MBOX I D      SPR      MPR
      19        18         3         3
$   FS         FD         DC         VC         VDC         PENCHK         BT         DT
      0.0       0.0       0.0       0.0       0.0         0         0.01.0000E+20
$   SFS        SFM        SST        MST        SFST        SFMT         FSF        VSF
      1.0       1.0       0.0       0.0       1.0         1.0       1.0         1.0

*CONTACT_AUTOMATI C_SURFACE_TO_SURFACE
$^CONTACT24
$   SSI D      MSI D      SSTYP      MSTYP      SBOX I D      MBOX I D      SPR      MPR
      20        19         3         3
$   FS         FD         DC         VC         VDC         PENCHK         BT         DT
      0.0       0.0       0.0       0.0       0.0         0         0.01.0000E+20
$   SFS        SFM        SST        MST        SFST        SFMT         FSF        VSF
      1.0       1.0       0.0       0.0       1.0         1.0       1.0         1.0

```

*CONTACT_AUTOMATI C_SURFACE_TO_SURFACE

\$^CONTACT25

\$	SSI D	MSI D	SSTYP	MSTYP	SBOXI D	MBOXI D	SPR	MPR
	20	1	3	3			0	0
\$	FS	FD	DC	VC	VDC	PENCHK	BT	DT
	0.0	0.0	0.0	0.0	0.0	0	0.01	.0000E+20
\$	SFS	SFM	SST	MST	SFST	SFMT	FSF	VSF
	1.0	1.0	0.0	0.0	1.0	1.0	1.0	1.0

*CONTACT_AUTOMATI C_SURFACE_TO_SURFACE

\$^CONTACT26

\$	SSI D	MSI D	SSTYP	MSTYP	SBOXI D	MBOXI D	SPR	MPR
	21	27	3	3			0	0
\$	FS	FD	DC	VC	VDC	PENCHK	BT	DT
	0.0	0.0	0.0	0.0	0.0	0	0.01	.0000E+20
\$	SFS	SFM	SST	MST	SFST	SFMT	FSF	VSF
	1.0	1.0	0.0	0.0	1.0	1.0	1.0	1.0

*CONTACT_AUTOMATI C_SURFACE_TO_SURFACE

\$^CONTACT27

\$	SSI D	MSI D	SSTYP	MSTYP	SBOXI D	MBOXI D	SPR	MPR
	8	27	3	3			0	0
\$	FS	FD	DC	VC	VDC	PENCHK	BT	DT
	0.0	0.0	0.0	0.0	0.0	0	0.01	.0000E+20
\$	SFS	SFM	SST	MST	SFST	SFMT	FSF	VSF
	1.0	1.0	0.0	0.0	1.0	1.0	1.0	1.0

\$-----1-----2-----3-----4-----5-----6-----7-----8

\$

LOAD CURVE CARDS

\$

\$-----1-----2-----3-----4-----5-----6-----7-----8

*DEFINE_CURVE

\$^6X6

\$	LCI D	SIDR	SFA	SFO	OFFA	OFFO	DATTYP
	4	0	1.0	1.2	0.0	0.0	0
\$		A1		01			
		0.111		2.522			
		0.16		2.393			
		0.389		2.682			
		0.569		3.684			
		0.687		5.286			
		0.732		6.808			
		0.765		9.563			
		0.807		8.244			
		0.853		5.028			
		0.949		0.117			
		1.0		0.0			

```

*DEFINE_CURVE
$^3X3
$   LCI D      SIDR      SFA      SF0      OFFA      OFF0      DATTYP
      5          0        1.0        1.2        0.0        0.0         0
$
      A1          01
      0.284        2.429
      0.477        2.968
      0.641        3.936
      0.731        5.732
      0.769        7.733
      0.80         10.2
      0.816       10.175
      0.837        8.596
      0.895        3.351
      0.946        1.308
      1.0          0.0

```

```

*DEFINE_CURVE
$^4X4
$   LCI D      SIDR      SFA      SF0      OFFA      OFF0      DATTYP
      6          0        1.0        1.2        0.0        0.0         0
$
      A1          01
      0.216        2.431
      0.369        2.782
      0.547        3.668
      0.638        4.943
      0.687        6.721
      0.72         9.243
      0.739        9.584
      0.797        7.237
      0.849        2.735
      0.927        0.394
      0.956        0.137
      1.0          0.0

```

```

*DEFINE_CURVE
$^5X5
$   LCI D      SIDR      SFA      SF0      OFFA      OFF0      DATTYP
      7          0        1.0        1.2        0.0        0.0         0
$
      A1          01
      0.272        2.459
      0.444        2.906
      0.569        3.393
      0.666        5.521
      0.704        7.983
      0.727       10.667
      0.801        7.641
      0.89         1.516
      1.0          0.0

```


\$-----1-----2-----3-----4-----5-----6-----7-----8
 \$
 \$
 \$
 \$
 \$-----1-----2-----3-----4-----5-----6-----7-----8

NODE INFORMATION

*NODE

\$ NID	X	Y	Z	TC	RC
100714	612.8	299.9995	888.9999	0.0	0.0
100715	612.8	299.9995	856.0739	0.0	0.0
100716	612.8	299.9995	823.1479	0.0	0.0
100717	612.8	299.9996	790.2219	0.0	0.0
100718	612.8	299.9996	757.296	0.0	0.0
100719	612.8	299.9996	724.3702	0.0	0.0

CONTINUED FOR ALL NODES IN MODEL

\$-----1-----2-----3-----4-----5-----6-----7-----8
 \$
 \$
 \$
 \$
 \$-----1-----2-----3-----4-----5-----6-----7-----8

ELEMENTS INFORMATION

\$-----1-----2-----3-----4-----5-----6-----7-----8
 \$
 \$
 \$
 \$
 \$-----1-----2-----3-----4-----5-----6-----7-----8

SOLID ELEMENTS

*ELEMENT_SOLID

\$ EID	PID	NID1	NID2	NID3	NID4	NID5	NID6	NID7	NID8
76603	2	100714	100742	100743	100715	101414	101442	101443	101415
76604	2	100715	100743	100744	100716	101415	101443	101444	101416
76605	2	100716	100744	100745	100717	101416	101444	101445	101417
76606	2	100717	100745	100746	100718	101417	101445	101446	101418
76607	2	100718	100746	100747	100719	101418	101446	101447	101419
76608	2	100719	100747	100748	100720	101419	101447	101448	101420
76609	2	100720	100748	100749	100721	101420	101448	101449	101421
76610	2	100721	100749	100750	100722	101421	101449	101450	101422

CONTINUED FOR ALL ELEMENTS IN MODEL

*END

REFERENCES

(AC Engineering, Inc. 1996): *A Special Topic Seminar: ABAQUS Contact Problems Made Easy*. West Lafayette, Indiana.

(Bank, *et al.* 1998): Bank, Lawrence C.; Jiansheng Yin; and T. Russell Gentry, "Pendulum Impact Tests on Steel W-Beam Guardrails." *Journal of Transportation Engineering*, Vol. 124, July/August 1998.

(Eskandarian, *et al.* 1998): Eskandarian, Azim; Dhafer Marzougui; and Nabih E. Bedewi, "Finite element model and validation of a surrogate crash test vehicle for impacts with roadside objects." *International Journal of Crashworthiness*.

(FHWA 2005): FHWA/NHTSA National Crash Analysis Center, <http://www.ncac.gwu.edu/>.

(Livermore Software Technology Corporation 2003): *LS-DYNA Keyword User's Manual: April 2003, Version 970*.

(Livermore Software Technology Corporation 2005): <http://www.lstc.com>.

(Logan 1993): Logan, Daryl L., *A First Course in the Finite Element Method, second edition*. Rose-Hulman Institute of Technology. PWS Publishing Company, Boston.

(Marzougui, *et al.* 1996): Marzougui, Dhafer; Cing-Dao Kan; and Nabih E. Bedewi "Development and Validation of an NCAP Simulation using LS-DYNA3D." *4th International LS-DYNA3D Conference*.

(Mitchell 2005): Mitchell, Geoffrey T., 2005, *Masters Thesis*, The University of Texas at Austin.

(Reid, *et al.* 1996): Reid, John D.; Dean L. Sicking; and Gene W. Paulsen, "Design and Analysis of Approach Terminal Sections Using Simulation." *Journal of Transportation Engineering*, Vol. 122, September/October 1996.

(Sicking 1998): Sicking, Dean, "Alternative Techniques for Evaluating Roadside Safety Systems." *Transportation Research Circular*, Number E-C002, Issue No. 0097-8515, July 1998.

(NCHRP Report 350 1993): Transportation Research Board National Research Council, National Cooperative Highway Research Program. *NCHRP Report 350: Recommended Procedures for the Safety Performance Evaluation of Highway Features*. National Academy Press, Washington, D.C.

VITA

Megan A. Tolnai was born on October 1, 1979 in Bethlehem, PA. She is the daughter of Stephen and Wanda Tolnai. She received her Bachelor of Science Degree from The Pennsylvania State University in University Park, PA in May of 2003, where she graduated with honors and high distinction in civil engineering. She will receive her Master of Science in civil engineering, with an emphasis in structures, at the University of Texas at Austin in May 2005.

Permanent Address:

3186 Gloucester Dr.

Bethlehem, PA 18020

This thesis was typed by Megan A. Tolnai.